# Three Dimensional Aero-Structural Shape Optimization of Turbomachinery Blades

Vadivel Kumaran Sivashanmugam

A Thesis

in

The Department

of

Mechanical and Industrial Engineering

Presented in Partial Fulfillment of the Requirements

for the Degree of Master of Applied Science (Mechanical Engineering) at

Concordia University

Montréal, Québec, Canada

January 2011

**CONCORDIA UNIVERSITY**

**School of Graduate Studies**

This is to certify that the thesis prepared

By: **Vadivel Kumaran Sivashanmugam**

Entitled: **Three Dimensional Aero-Structural Shape Optimization of Turbomachinery Blades**

and submitted in partial fulfilment of the requirements for the degree of

**Master of Applied Science (Mechanical Engineering)**

complies with the regulations of the University and meets the accepted standards with respect to originality and quality.

Signed by the final examining committee:

_____ Dr. Gerard J. Gouw (Chair)

_____ Dr. Fariborz Haghighat (Ext. to Program)

_____ Dr. Ramin Sedaghati (Examiner)

_____ Dr. Wahid S. Ghaly (Supervisor)

Approved by _____

MIE Department Chair or Graduate Program Director

_____ 2011 _____

Dean, Faculty of Engineering and Computer Science

# ABSTRACT

Three Dimensional Aero-Structural Shape Optimization of Turbomachinery Blades

Vadivel Kumaran Sivashanmugam

Aero-structural optimization of gas turbine blades is a very challenging task, given e.g. three dimensional nature of the flow, stringent performance requirements, structural and manufacturing considerations, etc. The current research work addresses this challenge by development and implementation of structural shape optimization module and integrating it with an aerodynamic shape optimization module to form an automated aero-structural optimization procedure. The optimizer combines a Multi-Objective Genetic Algorithm (MOGA), with a Response Surface Approximation (RSA) of the Artificial Neural Network (ANN) type. During the optimization process, each objective function and constraint is approximated by an individual ANN, which is trained and tested using an aerodynamic as well as a structure database composed of a few high fidelity flow simulations (CFD) and structure analysis (CSD) that are obtained using ANSYS Workbench 11.0. Addition of this multiple ANN technique to the optimizer greatly improves the accuracy of the RSA, provides control over handling different design variables and disciplines. The described methodology is then applied to the aero-structural optimization of the E/TU-3 turbine blade row and stage at design conditions to improve the aerodynamic and structural performance of the turbomachinery blades by optimizing the stacking curve. The proposed methodology proved quite successful, flexible and practical with significant increase in stage efficiency and decrease in equivalent stress.

# ACKNOWLEDGEMENTS

I am heartily thankful to my supervisor, Dr. Wahid Ghaly, whose encouragement, guidance and excellent support from the initial to the final level enabled me to develop an understanding of the subject and given me an unforgettable journey.

It is a pleasure to thank my parents who were backbone for me throughout the life and having faith on me. They were always a great moral support in number of ways during the hardest period of my life.

I am thankful to Ms. Leslie Hosein and Ms. Charlene Wald for their timely administrative help, suggestion and kindness.

I offer my regards and blessings to my colleagues Raja, Mohammad Arabnia, Benedikt Roidl, Alfin and many others in the CFD lab who supported me in any respect during the completion of the project.

I owe my deepest gratitude to my friends in India, Dr. Ganesh Anavardhan, Vasanth, Sriram, Jey, Rajesh, Kamalesh, Rajini, Senthil and many other well-wishers for their timely support, advice and having confidence on me.

Finally, I would like to thank my wife Nithya for her continued enthusiasm, support and love. Without her support I may not followed my dream of pursuing a career in aerospace. She is the backbone of my success.

# TABLE OF CONTENTS

# LIST OF FIGURES

# LIST OF TABLES

# LIST OF SYMBOLS

| | |
|---|---|
| $C_{p_r}$ | Pressure coefficient in rotor=$\frac{P-P_2}{\frac{1}{2}\rho_2.V_{2,r}^2}$ |
| $P$ | Pressure |
| $T$ | Temperature |
| $Y_r$ | Rotor total pressure loss coefficient=$\frac{P_{02,r}-P_{03,r}}{P_{03,r}-P_3}$ |
| $\eta_{tt}$ | Total to total efficiency= $\frac{1-\left(\frac{T_{03}}{T_{01}}\right)}{1-\left(\frac{P_{03}}{P_{01}}\right)^{\frac{\gamma-1}{\gamma}}}$ |
| $\Omega^*$ | Dimensionless streamwise component of vorticity= $\frac{\vec{\Omega}.\frac{\vec{V}}{\lvert\vec{V}\rvert}}{2\omega}$ |
| $\alpha$ | Lean Angle (degree) |
| $\beta$ | Sweep Angle (degree) |
| $\gamma$ | Specific heat ratio, Span location of $P_1$ in QRBC parameterization |
| $\omega_1, \omega_2, \omega_3$ | Fundamental frequencies |
| $\theta$ | $\widehat{P_1P_0B}$ angle controlling circumferential location of $P_1$ in QRBC(degree) |
| $\sigma$ | Stress (MPa) |

**Subscripts**

| | |
|---|---|
| $1, 2, 3$ | Stator inlet, stator outlet and rotor outlet |
| $0$ | Total (or stagnation) quantity |
| $r$ | Relative to the rotor |
| $vm$ | Von Mises |

**Acronyms**

| | |
|---|---|
| CFD | Computational Fluid Dynamics |
| FEM | Finite Element Methods |
| BPANN | Back Propagation based Artificial Neural Networks |
| ANN | Artificial Neural Networks |
| GA | Genetic Algorithm |
| RSM | Response Surface Methodology |
| RSA | Response Surface Approximation |
| ORG | Original geometry |

| | |
|---|---|
| OPT | Optimum geometry |
| MDO | Multidisciplinary optimization |
| RBF | Radial Basis Function |
| SQP | Sequential Quadratic Programming |
| QRBC | Quadratic Rational Bezier Curve |
| MISO | Multi Input Single Output |
| MIMO | Multi Input Multi Output |
| ARE | Average Relative Error |
| RMS | Root Mean Squared Error |
| RAAE | Relative Average Absolute Error |
| RMAE | Relative Maximum Absolute Error |
| LRIH | Input to hidden node learning rate |
| LRHO | Hidden to output node learning rate |

# Chapter 1

# Introduction

Optimization of physical systems for better performance has always been a quest, mainly fueled by competitive aerospace environments. This undying quest gives the necessary impetus for aerospace design and development. These developments are amply supported by the enormous progress made in the computational technology in recent years and the use of computer-based simulations of complex physical models to design the engineering systems. In the face of highly competitive economic and design environments, reducing the operating and maintenance cost of the gas turbine engines are the primary focus of the designers apart from other design considerations such as developing newer materials for high temperature applications, environmental factors etc. These needs and technology advancements pushes the designers to venture into highly unconventional design methodologies which results better overall performance at all operating conditions. Further, the developments in computational fluid dynamics (CFD) and finite element methods (FEM) reached to a certain level of maturity, were the industries have integrated these high fidelity tools in their design cycle to understand the intricate physical performance behaviors of the systems such as compressors and turbines.

Continuous improvements in efficiency, safety, reliability, manufacturing

processes of gas turbine engines have been made in the past decade but the need for improvements in the areas such as noise, cost, power, efficiency and weight still exists; such are essential for companies to maintain the competitive edge in the aerospace market. Design requirements are also constantly evolving with time in addition to the constant motivation to decrease the design cycle time. For example, design requirements such as higher efficiency and longer life for the turbine blades requires, higher turbine inlet temperature and lower operating stress during normal operating conditions, which are contradictory in nature. Each new requirements are specific to a particular design condition and during the design process, improvements in one discipline reduces the effectiveness of the other. Moreover the design of turbomachinery blades are inherently highly multi-disciplinary, which involves multiple objectives and constraints related to different disciplines. Trade offs among the design parameters of different disciplines always considered depending on their relative merits and demerits and also based on the design requirements. Therefore development of multi-disciplinary optimization tools which involve of different disciplines and corresponding design variables is an effective way to address complex design problems such as turbomachinery shape optimization. Aerospace systems are highly complex in nature and always there exists a need to reduce the weight and improve the performance of at least one system. Application of evolutionary optimization techniques for the aerospace systems design are discussed by Kroo [8] and recent developments in the multidisciplinary optimization are summarized by Sobieszczanski-Sobieski *et al.* [9].

## 1.1. Turbomachinery optimization

In the case of gas turbine engines, the operating conditions of a the turbine stage varies with respect to their positioning from the combustion chamber and the type of engine etc. Usually turbine blades are designed to operate at a specific design

condition which is known as the design point.

Traditionally, the design of turbine blades begins with aerodynamic design of the blade shape, primarily focused to get higher efficiency and lower aerodynamic losses. Then the mechanical analysis is done on the same geometry to check whether the blades withstand the stress levels during its operating life and the natural frequency levels without interfering with other component frequencies. If the mechanical conditions are not satisfied then the blade is redesigned with additional constraints. Inclusion of aerodynamic, structural and thermal disciplines in the conventional design cycle makes the iterative process more costly in terms of time and computational resources. Hence, an umpteen number of researchers are working in developing the tools for multidisciplinary optimization(MDO) of turbomachinery blades and reducing the design cycle time. Following are some of the notable research areas in this regard:

1. Effective and accurate representation of blade profiles with less number of design variables (or Blade parameterization)

2. Faster and more accurate high fidelity analysis tool for CFD and FEM (Ex. ANSYS CFX, FLUENT, Mechanical, in-house tools (mainly in industries) etc)

3. Robust global, local or combination of both optimization methods (Examples of global algorithms are Genetic Algorithm (GA), Simulated Annealing (SA) etc)

4. Developing or modifying the metamodels to approximate the objective function and constraints with lesser prediction errors (Ex. Artificial Neural Networks (ANN), Radial Basis Function (RBF) etc)

5. Integration and variable handling of various disciplines during the optimization cycle

6. Increasing the robustness and accuracy of the tools without sacrificing the optimization cycle time (e.g. using data mining techniques, etc)

**Need for Response surface models (RSM) in turbomachinery optimization**

Use of high fidelity computational analysis tools (CFD and FEM) in the optimization process increases the design cycle time to a prohibitively large extent, mainly due to the time taken to solve the Navier Stokes equations in the complete flow domain and finite element models to solve the solid models. In this case, low fidelity response surface models (RSM) come handy and are used as a low cost (but also low fidelity) substitute for the high fidelity models in the optimization process because of their advantage in reducing the design cycle time and exploring the complete design space with minimal computational cost. ANN, RBF, Kriging are some examples of RSMs.

Selection of RSM is highly problem-dependent. It varies depending on the number of input design variables, dimensionality of the given problem, output variables, availability of high fidelity database, model accuracy or order of the prediction error, integration with other disciplines, variable handling etc.

### 1.1.1 Previous investigations

Coupling multiple disciplines with optimization algorithms to create new designs or to redesign existing geometries for increased performance is a complex and involved design process. Different optimization techniques like gradient based methods (such as sequential Quadratic programming (SQP)), Global optimization techniques (GA, SA etc) or the combination of both are used depending on the problem at hand. Right choice of optimization algorithm is an important pre-requisite to achieve a true optimum shape at the end of the optimization process.

However, the inherent nonlinearities, multimodalities (or presence of many

local minima in the design space) that exist in the aero-structural shape optimization can be effectively handled by global optimizers such as GA rather than gradient based methods (although these algorithms are computationally more expensive than gradient methods). Many researchers have applied this type of methodology in turbomachinery optimization, see [5, 10, 11, 12, 13, 14, 15, 16, 17, 18, 19].

Structural optimization is not a new topic in the field of aerospace due to its integral nature in the design of aircraft, gas turbine engines and in other important systems. Finite element based structural shape optimization survey was done by Haftka *et al.* [20] and Ding [21]. Structural optimization of turbomachinery blades mainly focused on maximizing or minimizing the blade fundamental frequencies of a low pressure compressor blade and hollow turbine blade was done by Frischbier [22]. Finite element software SAMCEF used to minimize the first bending mode frequency by sizing the thickness with constraints on the mass, second bending mode and first torsional mode frequencies. The blade was modeled using plate elements and thickness of the plate elements are considered as design variables (51 design variables in total) to represent the blade configuration [22]. Finite element tools SAMCEF and RASNA/MECHANICA were employed to maximize the frequency of the hollow turbine blade modeled with solid elements. A 7.4% increase in fundamental mode was achieved at the end of optimization.

Doorly *et al.* [23] proposed an optimization methodology which combines parallel GA, aerodynamic and structural analysis tools to maximize the performance of 2D airfoil, and aircraft wing. A simple beam model was used to represent the wing of an aircraft for structural analysis. Martin *et al.* [24] developed an efficient constrained hybrid aero-structural optimization methodology to optimize the turbine blade 2D profiles. Improvements in aerodynamic and thermal performance of the airfoil were taken as the objectives. Complete profile of an airfoil, thickness of the

thermal coatings, coolant flow passages, internal strut shapes and locations are optimized during the process. Combination of David - Fletcher - Powell (DFP), Gradient search, GA, Nelder Mead (NM) simplex method and SA forms a hybrid algorithm in this case [24].

Tappeta *et al.* [25] studied the applicability of Concurrent SubSpace Optimization (CSSO) (which is a type of MDO methodology) for high temperature aircraft engine components. The cooled turbine blade was approximately modeled as a stepped cantilever box in the commercial multi physics software NASTRAN. Uniform external pressure load with equal magnitude applied on all the sides, and the optimization of the blade was carried out using the iSIGHT optimization software with weight minimization as the objective while constraining the stress and frequencies.

Talya *et al.* [26] and Rajadas *et al.* [27] applied multidisciplinary optimization (MDO) to optimize the shape of a generic 3D turbine blade by considering aerodynamic, heat transfer, structural and modal objectives. The blade surface was represented by Bezier-Bernstein polynomials and the constrained multi-objective optimization problem was solved with Kreisselmeier-Steinhauser (K-S) method. A combination of 3D Navier-Stokes equations and finite element software (ANSYS) was used to solve the blade aerodynamic and thermal performance. The maximum blade temperature, average blade temperature and blade weight were considered as the objectives with constraints imposed from aerodynamic, modal, structural and geometric domains.

Optimization of steam turbine stage was done by Rolf Dornberger *et al.* [28] using multi-objective Pareto optimization and 3D CFD solver. Main objective of the work was to minimize the stage aerodynamic losses by varying the rotor and stator lean and sweep. From turbine stage parameterization 8 controlling parameters were used as design variables to represent the blades. For multi disciplinary optimization, other disciplines like mechanical integrity and cost analysis were calculated in parallel

or after the CFD solver process.

An aerodynamic optimization of axial turbines and compressors were done by Pierret *et al.* [29] using FINE/Design3D (Commercial CFD package developed and marketed by NUMECA). Optimization process incorporates blade modeler tool (Autoblade), NUMECA CFD and a mesh generator, GA, ANN etc, the interconnection of multiple tools is handled by FINE/Design3D. A single objective aerodynamic shape optimization was also done by the same author to minimize the loss coefficient with several mechanical, aerodynamic and manufacturing constraints. To maximize the high pressure turbine blade efficiency, stacking and lean were considered as design variables and in the case of transonic compressor blade (NASA rotor 37), maximizing the adiabatic efficiency was achieved by decreasing the shock strength. Strong mechanical constraints were imposed on the compressor due to their critical nature in lean (due to thinner construction leaning of the blade induces large stresses).

Dirk Buc̆he *et al.* [30] coupled evolutionary strategy based optimization algorithm with simplified beam model (mechanical integrity analysis), Q3D flow analysis and a Bezier curve based blade parameterization scheme to optimize a subsonic industrial gas turbine compressor. 2D sections of the blade are stacked in the third direction (spanwise) and each section was defined by a Bezier curve. A total of 27 design variables were selected to optimize the compressor blade. The objective function aggregates the aerodynamic and structural discipline objectives including the constraints into a single merit function. Improvements in aerodynamic performance were observed in terms of reduction in aerodynamic losses and increased operating range.

Choon Man Jang *et al.* [31, 32, 33] proposed a methodology which combines polynomial based RSMs and 3D thin layer Navier-Stokes equations to optimize the transonic axial compressor blade. Geometric parameters that controls the lean, sweep and skewness of the blade were considered as the design variables. The main objective

of the optimization was to maximize the adiabatic efficiency by decreasing the shock strength at the design point.

Pierret *et al.* [14, 16] applied GA and Radial Basis Function (RBF) based aero-structural optimization framework to optimize Rotor 67 compressor blades. Finite element structural mechanics software SAMCEF was used to predict the static stresses and modal frequencies. A Navier-Stokes solver was used to calculate the aerodynamic performance. A RBF-based RSM was integrated with FEM and CFD solvers to get an automated optimization tool. Maximizing the efficiency at multiple operating points was considered as an optimization objective with constraints imposed on von Mises stress, modal frequencies, mass flow rates and pressure ratios. The overall improvement in aerodynamic efficiency was achieved with an increased operating range.

A harmonic perturbation-based blade optimization was proposed by Li *et al.*[34], and the methodology was employed to optimize the aero-thermal performance of the Rotor 67 simultaneously by applying mechanical and aero-mechanical constraints. Aerodynamic efficiency at the design mass flow rate were used as an objective with blade displacement, mass flow rate, pressure ratio, maximum static stress and flutter safe aerodynamic damping were imposed as constraints. An improvement of 0.4% in thermal efficiency was noted but a notable 33% increase in static stress were achieved at the end of optimization process.

A GA based multi-objective optimization was applied to minimize the manufacturing cost and volume of the 2D high pressure turbine disk by Rao *et al.* [35]. Disk stress and fatigue life (number of cycles) were considered as constraints and the parameters controlling the shape of the disk were considered as design variables. A generic manufacturing cost modeling tool DECISIONPRO along with Finite element structural solver SC03 (Rolls Royce PLC) were used to estimate the objectives and constraints during the optimization process.

An automated GA and neural network-based structural optimization algorithm was proposed by Dominique *et al.* [36] for preliminary design of gas turbine rotor disc. The main objective of this method is to minimize the weight of the rotor disc with aerodynamic and stresses are constrained. The goal of the proposed method was to provide the best possible starting solution to the designer to start the new designs in a shorter time. Geometric parameters which control the disc shape, are used as design variables and a sensitivity analysis of the design variables is used to decide on the design variables that should be kept.

Frederic *et al.* [37] developed a fully automated aero-mechanical MDO tool box, which was then applied to optimize the high pressure compressor (HPC) stage so as to improve the aerodynamic performance by applying mechanical and geometric constraints. The optimization tool contains a Non Uniform Rational B-Splines (NURBS) parametrization scheme and an ANN response surface approximation model to create more efficient models and to approximate the error functions better.

Ashakiran *et al.* [38] proposed a GA and ANN based multi-disciplinary optimization methodology to improve the performance of an axial turbine stage. Commercial CFD tool NUMECA was used to analyze the complete flow domain and ANSYS Mechanical was used to analyze the blisk and rotor stresses during the optimization. Parameters like blade stagger angle, rotor tip clearance along with blisk geometric variables were taken as optimization design variables.

A differential evolution based optimization algorithm in combination with a NURBS parameterization scheme were developed and applied to optimize Rotor 37 by Luo *et al.* [18]. Panchenko *et al.* [39] presented an optimization tool box for the design of small aircraft engines during the preliminary design stage. Interactions between the disciplines and influential geometry tools which control the engine cross sections were also explained.

Arabnia *et al.* [5, 19] presented an optimization process which combines GA, ANN with CFD flow solver to improve the E/TU-3 turbine stage aerodynamic performance. The blade stacking line is parameterized using a QRBC and the parameters which control the blade shape like lean, sweep and bowing intensity are taken as the optimization design variables. Single- and multi-objective aerodynamic optimization was carried out to maximize the aerodynamic efficiency and simultaneously minimize the secondary losses.

### 1.1.2 Current work

The current work is an extension of the work done by Arabnia *et al.* [5, 19] to include the structure discipline into the optimization. In Arabnia's work, the blade geometry is divided into several two dimensional sections at different radial locations and joined with the stacking curve in the third direction. The stacking curve is parameterized using a quadratic rational Bezier curve (QRBC), whose parameters are related to the blade design variables used in the optimization such as the blade lean, sweep and bow. The QRBC representation of the stacking curve results in a smooth curve with continuous second order derivative, it can generate wide range of shapes without violating any geometric constraints. The current optimization method combines a genetic algorithm (GA) with Artificial Neural Networks (ANN). The main objectives of the current work are,

1. Improving the approximation capability of the response surface model (RSM).
2. Developing a structural optimization methodology for turbine blades.
3. Integrating aerodynamic and structural disciplines in order to develop a three dimensional aero-structural shape optimization algorithm for turbomachinery blades.

## 1.2. Thesis outline

The work done on this particular topic detailed in the following manner. $Chapter-1$ gives the introduction to the topic, motivation, previous work done, scope and organization of the thesis. The numerical optimization and computational design tools used in this thesis i.e Artificial Neural Networks, Genetic Algorithm, ANSYS Fluent and ANSYS Simulation are discussed in $Chapter-2$. Optimization methodology followed in the current work in addition to the blade parametrization scheme are presented in $Chapter-3$. In $Chapter-4$, the current methodology applied to optimize an existing turbine stage and turbine blade row, namely single point aero-structural optimization of the E/TU-3 turbine stage and turbine blade row are presented in detail. The last chapter summarizes the findings and concludes the thesis, it presents also some of the challenges that need to be addressed, and some recommendations for future work.

# Chapter 2

# Numerical Implementation

## 2.1. Introduction

The main components of any shape optimization procedure are:

1. Blade shape parameterization
2. Numerical optimization algorithm and
3. Objective function computation

These components can be applied manually or they can be integrated into an automated shape optimization methodology by providing proper coupling between them.

The use of high fidelity simulation tools (Navier-Stokes and Finite elements methods) to compute the aerodynamic and structural objectives always comes with a prohibitively large computing time. For this reason, Response Surface Approximation (RSA) is an important element in the design process so as to reduce the optimization cycle time by providing a good approximation of objectives and constraints.

This chapter focuses mainly on presenting the numerical optimization methods that were used namely GA and RSA to approximate the output variables. It also outlines the high fidelity tools that were used to predict the flow field properties and

stress contours so as to compute an accurate value of the objective function and the constraints.

## 2.2. Numerical Optimization

Numerical optimization schemes are categorized into two broad classes:

- Gradient based and
- Non-gradient based or Stochastic schemes or Evolutionary based

### 2.2.1 Gradient Optimization

Gradient based optimization schemes are fast and needs relatively small number of function evaluations when compared with non-gradient based schemes. However they are local optimizers and will probably stop at the first optimum obtained during the search process. This method will outperform almost all other numerical optimization schemes while solving continuous, unimodal problems but it is not suitable when searching for global optimum in a multi-modal optimization problem [40].

The most popular and common gradient based algorithm is the sequential quadratic programming (SQP). The SQP method works very well and relatively fast for the problems that do not have multi modal extrema. This issue could be addressed to a certain extent by starting the optimization process from different points however the final optimum may not be the global optimum; this ultimately increases the optimization cycle time.

Coupling of the gradient method with global stochastic search schemes is an idea found to perform well in many cases [41, 42]. Gradient and non-gradient schemes were tested for different cases of multi-modal problems and for the aero-structural optimization.

### 2.2.2 Non-Gradient or Direct Optimization Methods

Global optimizers such as GA and SA are found to perform best in most cases due to their robust and random nature of search but with a relatively high computing cost. The high computing cost involved in calculating the objectives can be greatly reduced by approximating the objective functions using RSA, hence taking advantage of their global optimization behavior.

For the current work, combination of GA and ANN used as an optimizer and back propagation based neural networks (BPNN) used to build the response surface model. The basic GA and ANN tools which are used in this work, were originally implemented by Mengistu [43]. Extensive work has been done on the basic ANN improve the robustness, multi discipline and variable handling capability of the ANN; this will be presented in detail in Sec. 3.4.

#### Genetic Algorithm

Genetic algorithms are increasingly used to handle aerodynamic, structural and multidisciplinary optimization problems [14, 16, 31, 32, 44, 45] in turbomachinery blade designs. They provide a robust search mechanism to find the near global minimum in a problem that contains many local minima.

Genetic algorithms are general purpose random search algorithms based on the principles of evolution observed in nature. Genetic algorithms combine selection, crossover, mutation and elitism operators with the goal of finding the best solution to a particular problem. It searches for the optimal solution until a specified termination criterion is met [46].

The representation of variables in the GA (the genes or chromosomes) can be either binary coded or real coded. If the variable is continuous (i.e floating-point number), it is more tedious to represent the variable with $0's$ and $1's$ and to get the accurate results. A real coded genetic algorithm is used in this work and has the

capability to handle floating point numbers with ease. Following are some advantages of real coded GA over binary GA [46]

1. Less storage required due its use of single floating-point number to represent the variable and

2. Faster because chromosomes need not be decoded prior to the evaluation of the cost function.

These advantages plus the need to have more accurate results make the real coded GA an ideal candidate for highly complex optimization problems like multidisciplinary optimization of turbomachinery blades.

The basic operations that make up the genetic algorithm are selection, crossover, mutation and elitism. Figure 2.1 gives the overview of the GA operation.

**Population**

The population size is the number of candidate solutions in one generation. The larger the population size the more diverse it is but the search becomes computationally more intensive. In nature, the bigger the gene pool the more diverse the genetic makeup of the population with many individuals each with its own set of characteristics that enable it to survive. One advantage of this diversity is that there will be no dominant gene that may be susceptible to a particular disease and may result in the elimination of the whole species in certain circumstances.

If the population size is small, then a strong individual quickly becomes dominant and the diversity of the gene pool is reduced. The result is that good individuals (local optima) are quickly created but the dominance of particular genes restricts the search space.

GA is a global search technique, it is usually set to explore a given region of the design space to maintain the balance between computing cost and effective

optimization. This is effectively done by imposing constraints on the objectives and specifying upper and lower bounds for the design variables. It should be noted that enough diversity in the initial population should be given if the promising search region (where the optimum solution lies) is not known a priori to the optimization (most of the optimization problems fall in this category) [46]. Moreover the size of the population should always be even.

For all new generations, the population size is kept constant by replacing the old individuals with new ones. During each generation the candidates could be completely replaced by their offspring, or as a new offspring is created, it could be accepted or rejected depending on its fitness, which is based on the value of the objective function. The use of computers helped to retain the good individuals for indefinite reproduction without dying though which is not possible in nature. The retention of certain fit individuals is known as elitism.

**Selection**

It is one of the critical parts in the GA operation and plays a major role in creating new offsprings. This operation basically selects candidates (parents) on which crossover is performed later to create new offspring. The offspring created from the parents will have the favorable qualities of each parent and preferably better than the parents.

There are two commonly used selection procedures which are mainly driven by fitness value:

1. Roulette wheel

2. Tournament selection

In roulette wheel, each individual is assigned a slice of a wheel. The size of the slice is proportional to the fitness of the candidate. The wheel is then spun and the individual having better fitness has a better chance of being selected.

Tournament selection approach closely mimics the mating competition in nature. From the main population, subset of individuals are selected in a random manner and the best candidate is selected as a first parent, the second parent also selected in the same approach. A large value for the subset indicates more elitist selection and a small value corresponds to less fit parents. This makes the population more diverse. Complete optimization strategy depends on retaining the best of the two individuals selected. Harinck *et al.* [47] proposed two elite individuals, which is more effective. Both tournament selection and roulette wheel are common for most GA. Some of the facts regarding both methods are:

- In some cases roulette wheel selection method is slower than slower than the tournament selection in reaching to the optimum
- Less fit individuals are given a chance to reproduce in the tournament selection which provides more diversity to the population
- In the roulette wheel selection, elite individuals are always given more preference. This makes the population less diverse

**Crossover**

Crossover is the main operator that is responsible in creating new candidate solutions, even though mutation operator is also used for the same purpose sparingly [40]. The main idea behind crossover is that the new chromosome may be better than both of the parents if it takes the best traits from each of the parents and sometimes it could even be better. Crossover occurs during the evolution process based on a user definable crossover probability $P_c$. The typical range for $P_c$ varies from 0.1 to 0.9 and in this work, $P_c$ was maintained as 0.7. Two kinds of crossover operations are available in the real coded GA, arithmetic and heuristic crossover operators.

Arithmetic crossover is a linear combination of two parent chromosome vectors to produce two new offspring's given as:

$$Child1 = a * Parent1 + (1 - a) * Parent2$$

$$Child2 = (1 - a) * Parent1 + a * Parent2$$

Where $'a'$ is the random number between 0 and 1.

Heuristic crossover operator uses fitness values of the best parent chromosome and the worst parent chromosome to determine the search direction and to create the new offspring. The following formulae are used create the offsprings:

$$Child1 = Bestparent1 + a * (Bestparent - Worstparent)$$

$$Child2 = Bestparent$$

Where $'a'$ is the random number between 0 and 1.

**Mutation**

Mutation is a generic operator that alters one or more gene values in a chromosome from its initial state after the crossover operation. This can result in entirely new chromosome values being added to the population and may result in a better solution than was not previously possible. Mutation is important in the convergence process to avoid GA being trapped in local minima and also prevents the chromosomes from becoming too similar to each other, which ultimately slow down the evolution process. It is controlled through a user defined mutation probability $P_m$ and typically the value of mutation should be kept as low as possible, in this case 0.15 used. Uniform type mutation is used for the algorithms used in this work; it replaces the value of the

chosen gene with a uniform random value selected between the user-specified upper and lower bounds for that gene.

**Elitism**

During the evolutionary process, the best individuals may be lost due to crossover and mutation operations. To prevent this loss of valuable candidates, elitism operator is introduced in many genetic algorithms. Generally elitism makes few identical copies (e.g two) of the best performer in the old pool and places them in the new pool, thus ensuring the survival of the fittest. It simply ensures that the fit solutions found during the evolutionary process would remain within the population. In the current work two (constant) elite candidates are moved to the next generation.

Following are the three stopping criteria for GA, if any one of them is reached during the evolutionary process it will automatically stop.

1. If the best fitness in the current population becomes less than the specified fitness threshold for the minimization problem
2. After reaching a predetermined maximum number of generations or
3. When the elapsed evolution time exceeds the specified maximum computing time.

In summary, GA is an evolutionary optimization method. It does not use gradient information during the process instead it uses function value, which makes GA more computationally intensive than SQP (i.e it requires a larger number of iterations). GA cannot be easily trapped in local minima or maxima due to crossover and mutation operations, which makes it an ideal method to effectively handle multi-modal optimization problems with several extrema multidisciplinary optimization of turbomachinery blades.

## 2.3. Response Surface Approximations (RSA)

Response surface function approximates the output of a given system as a function of some input variables (design variables). This method is widely employed as an inexpensive low order approximation of the objectives and constraints instead of the more time consuming but accurate calculations using CFD and FEM simulations. The initial approximations are achieved by fitting the system response for a number of chosen combinations of the control variables (design points). The approximation model can then be used inside the optimization loop to compute the objective function in place of the original expensive high fidelity model; hence eliminating the associated prohibitive computing time. In addition to the above mentioned advantages, the approximation models can eliminate the computational noise which has a strong adverse effect on numerical optimization techniques by creating some non-physical local optima, see Lai and Yuan [48]. Some of the most commonly used approximation methods are polynomial approximations and artificial neural networks (ANN). RSA are more accurate when the number of design variables is small. However as the number of design variables increases, these methods need more number of evaluations to find a solution with reasonably acceptable accuracy levels. In the polynomial approximation method, the response surface model is a polynomial of $n^{th}$ degree whose coefficients are determined from a linear system of equations. The linear system is set using least square minimization of the error between the polynomial and the actual method.

### 2.3.1 Design of Experiments (DOE)

The selection of the sampling points for building an approximation model is crucial and challenging. The prediction capabilities of the approximation function is

highly influenced by the sampling points in the given design space. The latin hypercube based Design of experiments (DOE) techniques is so as to ensure that the sampling points are evenly distributed over the design space. This method gives a systematic and efficient means of analyzing the complete design space. It explores the high-dimensional design space and screens the most influential design points corresponding to the set of design variables. Quadratic model is widely used in polynomial approximation scheme due to its flexibility and ease of use.

### 2.3.2 Artificial Neural Networks (ANN)

ANN is a very powerful interpolator that can be used to map functions with multiple inputs/outputs. The concept of ANN has been widely used in most of the engineering and scientific fields due to its proven efficiency in capturing the physics of complex design analysis problems. Following are some of the notable applications of ANN

- Image processing
- Pattern recognition
- Medicine
- Military and aerospace system deign
- Artificial intelligence(in expert systems)
- Financial market forecasting and market analysis etc.

Researchers have used ANN-based approximation successfully for turbomachinery blade design optimization [5, 16, 19, 37, 45, 49]. Performance of ANN and polynomial approximations were compared by Papilla *et al.* [50, 49] from aspects like computational effort, noise and handling of complex functions. Compare to

polynomial based approximations, ANNs were found more suitable in handling multi-dimensional interpolation of data that lacks structure, because of their flexibility in functional form [51].

In the current work ANN is used as a low order RSA model to predict the objective function and constraints at relatively low computing cost. ANN is a mathematical model of a human brain. It is a network of multiple layers of simple processing elements called neurons. Each neuron is linked to some of its neighbors with varying coefficients of connectivity that represent the strengths of these connections. Learning is accomplished by adjusting these strengths to cause the overall network to output results for a certain set of inputs [52].

The most basic element of the human brain is a neuron (specific type of cell), which provides us with the abilities to remember, think, and apply previous experiences to each of our every actions. Each of these cells can connect with up to $2 \times 10^5$ other neurons. Brain capacity to work effectively is a function of the number of these basic components (neurons) and the interconnectivity between them [53].

General functionality of a biological neuron is to receive inputs from other sources, combines them in some way, performs a generally nonlinear operation on the result, and then provides its own output as the final result. Fig. 2.2 shows a simplified biological neuron and the relationship of its four components.

The basis of ANN is to emulate the basic functions of natural neurons; however it is much simpler than the biological neuron. Fig. 2.3 shows the basic operation of each artificial neuron in ANN.

The basic building blocks of ANN are the artificial neurons which is analogous to the natural ones. The various inputs to each neuron are multiplied by its connection weights and then their products are summed up. It is then fed to a transfer function which could linear or non-linear (most of the times) to generate the output.

The following equation mimics the action of neuron network:

$$Y = f(I)$$

$$I = \Sigma(W_i * X_i)$$

Where the neuron output $Y$ is a function of the weighted sum $I$ of inputs / or the input layer from the previous layer of neurons. $W_i$ and $X_i$ are the connection weights and input variables respectively.

As the brain basically learns from its previous experiences, ANN also learns from the given training data. It is sometimes called machine learning algorithms. Change in connection weights (training) helps the network to approximate the design space and to learn the solution for the particular problem. By adjusting its connection weights $W_i$, the neural net acquires new knowledge using an optimization algorithm which minimizes its error of prediction.

The ability of a neural network to learn the data set is determined by its architecture and the algorithmic method chosen for training. These are generally two kinds of training schemes [52]:

1. Unsupervised learning
2. Supervised learning

In unsupervised learning, the sample output is not provided and the network learns from the given input data only. It will automatically find a way to organize or cluster the data without seeing the outputs by capturing the patterns of the inputs [52].

In supervised learning, the network provided with the input and output sample data and it learns from that. This is method widely used and computationally more effective compare to unsupervised learning. For current work supervised learning

is employed.

Back propagation algorithm (BP) is a gradient based method that is proven highly successful in training of multilayered neural nets using supervised learning. It is believed based on a semi-theoretical proof that a feed-forward neural net (FFNN) with at least one hidden layer can approximate any continuous nonlinear function arbitrarily well, provided that sufficient numbers of hidden neurons are available [54].

A typical back propagation neural network (BPNN) has an input layer with several neurons (depends on the number of design variables), one or more hidden layers and an output layer. Each one of them are connected by adjustable weights with values closer to $'0'$ which enable the network to capture complex associations between the input and output variables. Fig. 2.4 shows a typical neural net with one input layer having four neurons or nodes, one hidden layer with several nodes and one output layer with two nodes. The design of ANN involves two steps: a training step followed by a testing step.

### 2.3.3 ANN training

ANN is response surface approximation method that is based on the notion of Artificial Intelligence (AI). The data set obtained from the DOE analysis is divided into a training set and a testing set. ANN approximation model is obtained by training it with some representative data (training set) and testing it with data that was not a part of training set.

The ANN training involves finding an appropriate ANN model for a given problem, i.e. determining the type of ANN network, its architecture, transfer functions, learning rates and choosing a right training strategy. These choices depend on the function being approximated, like the presence of local minima, high dimensionality, disparity in input scales, etc. ANN model and its results are highly dependent on the training data set provided, it is necessary to ensure that the training data is

not clustered around one part of the design domain. The diversity of the training set should always be maintained to get a good prediction model.

The training algorithm in this work is a mainly gradient based back propagation neural network but in some cases GA used to explore the design space for optimum weights. The weights are initialized randomly at the start of each run and gradient of error (different between ANN predicted and real outputs value) is added with the weights for the epoch. During the ANN training process, the approximation model first trained using the training set and then a validation set (testing set) is given to gauge its effectiveness for the unknown data. The final approximation model and corresponding weights are saved and are used for future experimentation and in the optimizer.

The error is measured based on the maximum relative error or average error or percentage of the exact prediction out of the total cases under consideration at certain predefined accuracy. The error measures used in this work are explained in Appendix A.

The steps in designing ANN model are:

- *Choosing an appropriate structure*: The multi-layer feed forward network is the most popular, it is the hierarchy of processing units, organized in a series of two or more mutually exclusive set of neurons or layers [52]. The first is the input layer which accepts input from the external. The last layer is the output layer which returns the output of the neural net. One or more hidden layers placed in between the input and output layers, where the computational process of the network is concentrated. The inter connectivity between layers are established by weights which connect each unit in one layer to those in the next layer.

- *Training strategy*: The complete training strategy is problem dependent. The following factors must be given importance to get a right training strategy:

  - Order of training set
  - Training algorithm convergence and divergence
  - Trap at local minimum error
  - Measure of error

- *Setting and updating initial conditions for the weights*: The weights are initialized in a random manner and this is mainly depends on the characteristics of the error surface. If the error surface changes rapidly, the gradient calculated based on local information alone will give a poor indication of the right path [55]. Learning rate value depends on the smoothness of the surface; a smaller learning rate is a preferred for a surface which is not smooth. If the surface is relatively smooth, a larger learning rate will speed convergence and it sometimes causes oscillation. However the shape of the error surface is rarely available at the beginning, thus a general rule might be to use a larger learning rate that works and does not cause any oscillations. Learning rates are problem dependent and basically fixed by trial and error method by varying the values from its lower bound to upper bound. It also depends on the transfer function and training data sets. Proper initialization of the weights overcomes local minimum and make the training more efficient [56] but the weights are initialized in a random manner when using the BPNN so it is mandatory to run the BPNN multiple times to get the right weight combinations at the end.

- *Choosing the number of hidden layers and units*: The choice of the number of hidden layers and units requires experience and engineering judgment. The number of hidden nodes should be as low as possible for a good generalization. When the number of hidden nodes increases larger then certain limit, it over fits the function which makes the network brittle with less generalization capability. The number of hidden nodes is a function of number of inputs, transfer

functions, number of hidden layers, and number of samples in the training set etc. Trade-offs between training time and network accuracy lead to iterative adjustment of the network using simulations. It is highly problem dependent. It is vital to have right number of hidden nodes to get a good approximation model which predicts the true optimum results.

### 2.3.4 ANN testing

The accuracy and generalization capability of the neural network is measured by ANN testing. Generalization is the ability of the trained neural network model to predict the outputs for an input data which is not a part of training set. Practically, there is always been a trade off involved between a model which generalizes well and robust, and the one which is more accurate but brittle. The main aim of the ANN training and testing is to get a model which generalizes the new and unforseen inputs well with some degree of accuracy.

During the training process, a decreasing trend in error is not an indication of the better model because the ANN units could memorize the I/O data of the train set without any generalization capability. Due to this reason, the optimum stopping point of the training is determined by the test set which is not a part of train data set. The training of the neural network has to be stopped at the point where the training and testing error is minimum and within acceptable error limits, sample graph is shown in Fig. 2.5. When the neural network is overtrained, it results more accurate and brittle model with fitting more points in the training set but the generalization capability of the network vanishes [57]. Overtrained (or overfitted) model also captures the noise in the training set which reflects in the subsequent outputs as shown in the Fig. 2.6.

BPNN is most commonly used ANN method in many practical applications. In this method, supervised learning strategy is coupled with the ANN topology.

During the ANN training, the difference (or error) between the neural network output and actual output is estimated and propagated back through the neural network. ANN training process shown as a flowchart in Fig. 2.7. This algorithm basically works on the 'Delta rule' principle, which is basically reducing the difference between the actual and neural output by continuously varying the strength of the connection weights from input towards output. This rule changes the connection weights in such a way that the errors measures like, average relative error, root mean square, correlation, R square etc to decrease. The back propagation of errors starts from the last layer and progresses towards the input layer, updating each layer at a time until it reaches the first layer. The name of the method feed forward back propagation neural networks basically derived from the way in which error term is computed.

Data for the training set given in the following formats, input/target data

$$[X, T] = \{(x_1, t_1), (x_2, t_2), ...., (x_n, t_n)\} \tag{2.1}$$

n denotes the number of training set provided.

The basic steps in designing a back propagation based ANN described as follows:

1. Number of input and output variables of the neural network decided based on the problem at hand.

2. Number of hidden layers (most of the problems could be solved with a single hidden layer-universal model) required to solve the problem.

3. Number of hidden nodes required to generalize the design space and transfer function.

4. Connection weights are randomly generated.

5. Input vector (set of design variables) is fed forward.

6. The output of the given vector is calculated based on the Eq. 2.1 that mimics the actual neuron behavior by provide weights for each input, summing up and passing it through the specific transfer function.

7. The error of the network is estimated by calculating the difference between the actual and neural net outputs.

8. Then the network minimizes the error by a methodological training process based on gradient based back propagation method.

**ANN Error Estimation**

Many practical optimization problems could be effectively modeled using a three layer neural network. The first layer is an input layer, last being the output layer between the two lies the hidden layer. The input to each layer (except first layer) given by the weighted sum of outputs coming from the previous layers.

$$net_j = \sum_i w_{ij} x_i \tag{2.2}$$

$i$ denotes the index for the node in the previous layer while $j$ is the current layer.

The total output is obtained by applying the transfer function for the Eq. 2.2

$$Y_j = \varphi(net_j) = \varphi(\sum_i W_{ij} X_i) \tag{2.3}$$

$\varphi$ is called transfer or activation function. It could be any function that is used to covert the activation input into an output. It should be continuously differentiable and an analytic function. There are different type of transfer functions available

- Step function (to simulate binary decisions)

- Sigmoid function (for non linear, continuous and differentiable replacement for step function)

- Tan hyperbolic (same as above)

**Sigmoid Function**

This is one of the most used transfer function in the ANN training,

$$\varphi(x) = \frac{1}{1 + e^{-x}} \tag{2.4}$$

This is one of the robust activation function, due to its non-symmetric nature (Fig. 2.8), may take slightly longer time while training.

**Tanh Function**

$$\varphi(x) = \tanh(x) = \frac{e^{x} - e^{-x}}{e^{x} + e^{-x}} \tag{2.5}$$

The asymmetric nature of the function (Fig. 2.9) aides to improve the learning speed [57]. This function is highly sensitive to the initial ANN weights.

The difference or error between the output of the neural net and target output given by the equation 2.1 calculated as follows:

$$E = \frac{1}{2} \sum_{i} (t_i - o_i)^2 \tag{2.6}$$

$E$ = Sum of squared errors

$t$ = Target output

$o$ = Neural net predicted output

The network weights are adjusted to minimize the error according to the learning rule imposed in the algorithm which looks as follows:

$$W_i \longleftarrow W_i + \triangle W_i, \triangle W_i = -\eta \frac{\partial E}{\partial W_i} \tag{2.7}$$

$\frac{\partial E}{\partial W_i}$ is the gradient of error function with respect to the given connection weights $W_i$, and $\triangle W$ is the change in connection weight with $\eta$ as learning rate (takes the values between 0 and 1). The learning rate value varies based on the nature of the error surface (or problem dependent). The larger value for the learning rate speed up the convergence but in most of the cases the information about the error surface in not known prior so it is always better to start the training process with lower learning rate.

Performance of the ANN model is measured from different aspects such as accuracy, robustness, efficiency, transparency and conceptual simplicity [58]. Goodness of fit obtained from the training data doesn't represent the accuracy of the model, because of this reason test data set which is not a part of training set used to evaluate the model. Appendix A explains in detail about the error measures used in this work to effectively judge the generalization availabilities of metamodel parameters.

## 2.4. Flow Field Analysis

The commercial CFD software ANSYS Fluent were used to simulate the flow in order to compute the aerodynamic forces acting on a given turbomachinery blade. An accurate evaluation of the flow field is necessary to calculate the aerodynamic performance parameters such as total pressure loss, aerodynamic efficiency, pressure ratio, mass flow rate which will help to build better prediction model and to sweep the complete design space for optimum configurations. If the flow simulation captures the flow physics accurately, it is reasonable to expect the optimizer to capture the flow physics and give the optimum solution. In other words, the optimum design is at best as good as flow simulation tool. ANSYS Fluent was used as a CFD tool in this work along with $K-\omega$ turbulence model and mixing plane interface between the stator and rotor passage. Geometry and mesh generated using GAMBIT GTurbo.

## 2.5. Structural Analysis

### 2.5.1 Finite element analysis

Structural analysis is carried out to determine the blade structural stress, displacement and integrity; to this end. ANSYS workbench 11.0 - Mechanical was used. The CAD geometry for different turbine blade configurations was generated using ANSYS GAMBIT and the CAD geometry is trimmed using ANSYS ICEMCFD. Mesh was generated inside ANSYS Mechanical, and three dimensional solid tetrahedral elements were used with midside nodes for the blade. Solid elements with midside nodes were chosen since they capture the highly complex and curved profiles better than many other elements. Changes in the stacking line result in highly complex blade shapes that are difficult to mesh with hexagonal elements. A fine mesh with approximately $100,000$ elements was used for structural analysis in ANSYS.

Pressure loads from CFD pressure loads on the blade are obtained from ANSYS Fluent which is one of the boundary conditions (loads) for structural analysis. Since the numerical mesh used in Fluent is different from ANSYS finite element mesh, the surface loads obtained from Fluent were automatically interpolated in ANSYS Workbench according to the structural mesh. All the nodes at the blade root are assumed as fixed and will have zero displacement. Normally this problem is solved in two steps, the first will solve the flow domain using ANSYS Fluent and the second will analyze the structure subject to pressure and centrifugal loads in ANSYS Workbench - Simulation. The von Mises stress are considered as the main output parameter from the structural analysis and the maximum is used as an objective in aero-structural optimization. In this particular problem structural optimization was carried out to reduce the maximum von Mises stress.

From structural consideration, the sharp corner at the hub represents a stress discontinuity where the stress would tend to be infinite. To minimize the

impact of such singularity on the computation of max. stress, the mesh density and topology near the corner was kept the same for all blade profiles that were tested. This ensured that the relative stress improvement is a genuine one.

### 2.5.2 Modal Analysis

It is important that the consecutive natural frequencies are not very close to other for good vibration characteristics which is done through modal analysis. ANSYS Workbench simulation is used to setup the modal and calculate the modal frequencies. The same blade geometry used for structural analysis used here also. Modal analysis doesn't require higher number of mesh elements to calculate the frequencies so less number of elements is used and only first five modes were calculated. Further, only centrifugal load is applied for modal analysis with root fixed boundary condition. The Block Lanczos method is used to extract the first five nodes. Static structural analysis results used as an initial condition for the modal analysis.

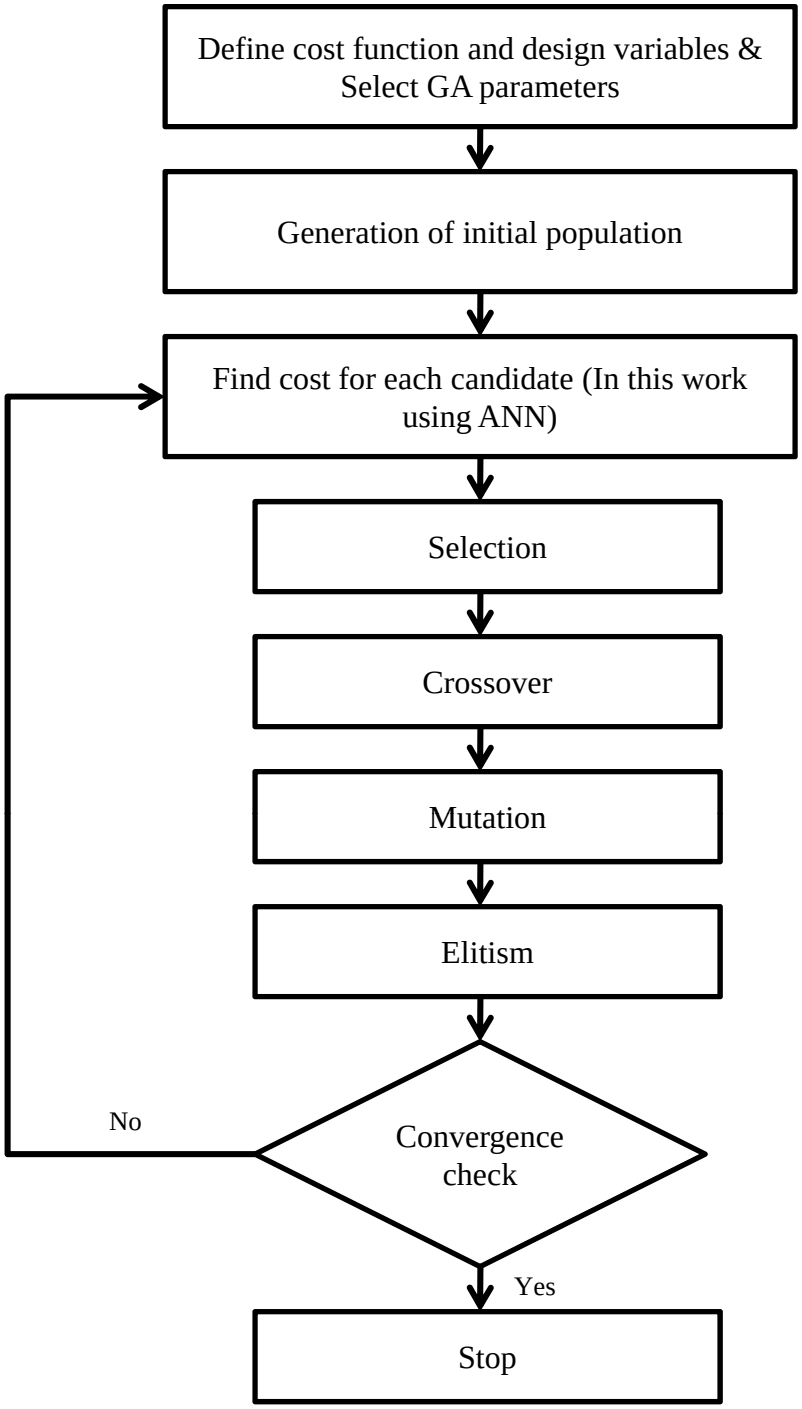


Figure 2.1: Typical flow of GA operation

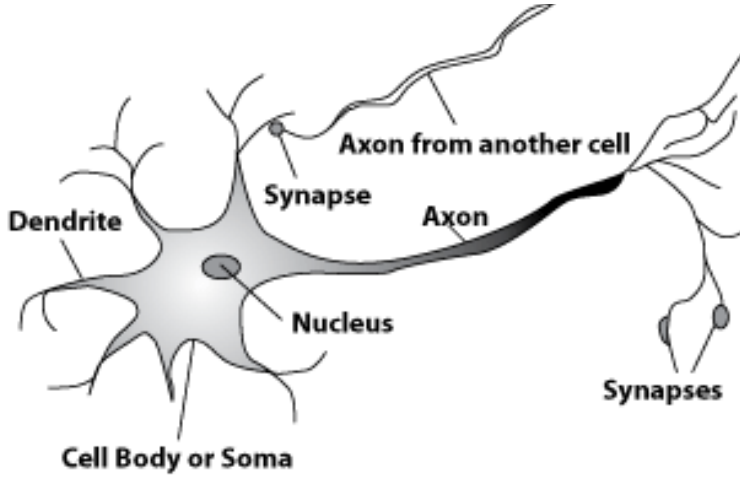


Figure 2.2: A sample bio-neuron [1]

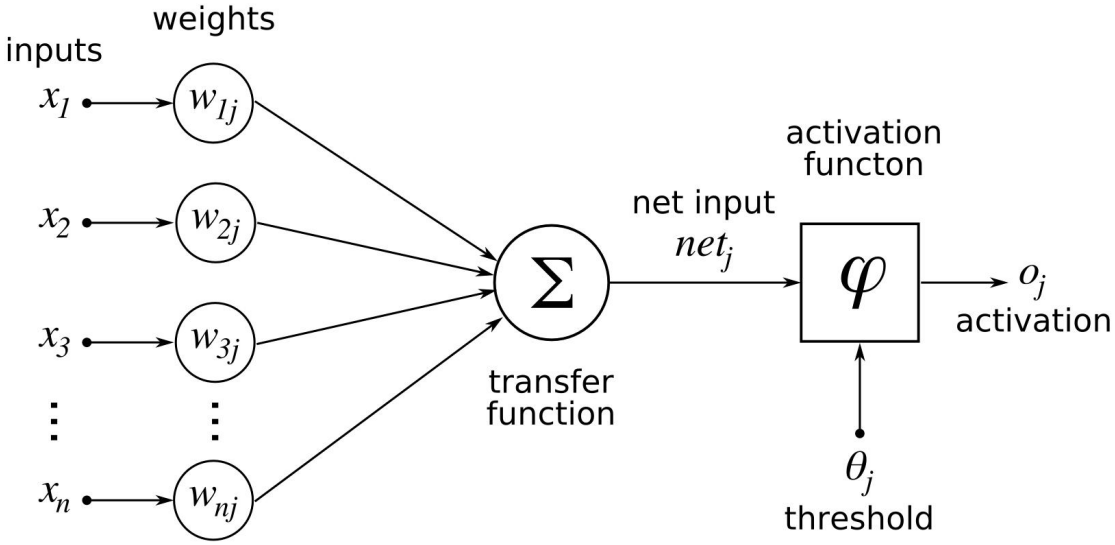


Figure 2.3: A sample artificial neuron [2]

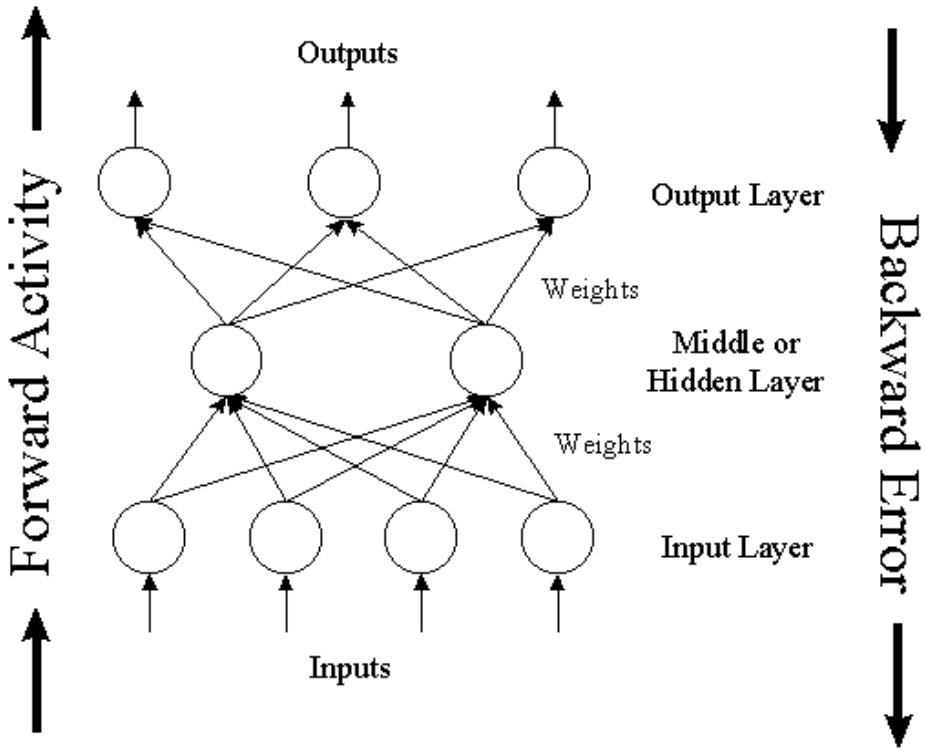


Figure 2.4: A sample artificial neuron [3]

stopping.png stopping.pdf stopping.jpg stopping.mps stopping.jpeg stopping.jbig2 stopping.jb2 stopping.PNG stopping.PDF stopping.JPG stopping.JPEG stopping.JBIG2 stopping.JB2

Figure 2.5: Typical training and testing trends with optimum stopping point

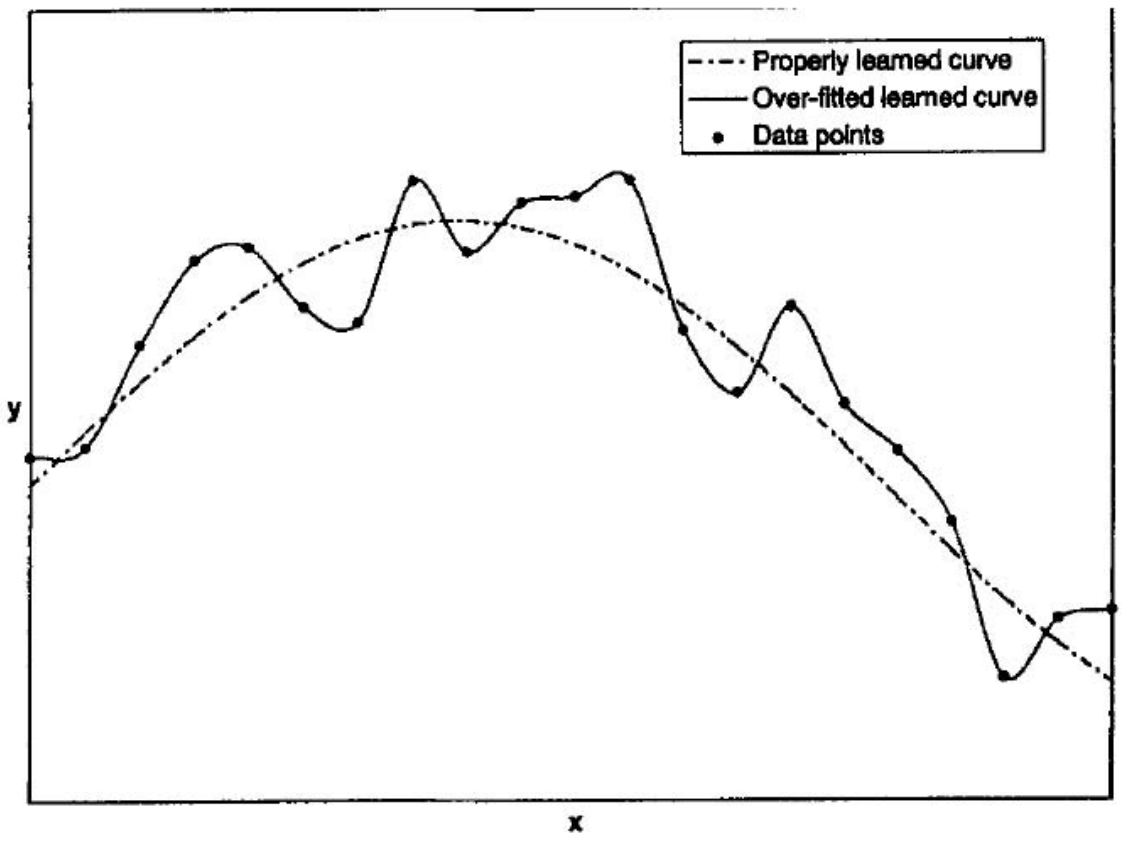


Figure 2.6: A typical example of over fitted and properly fitted curves [4]

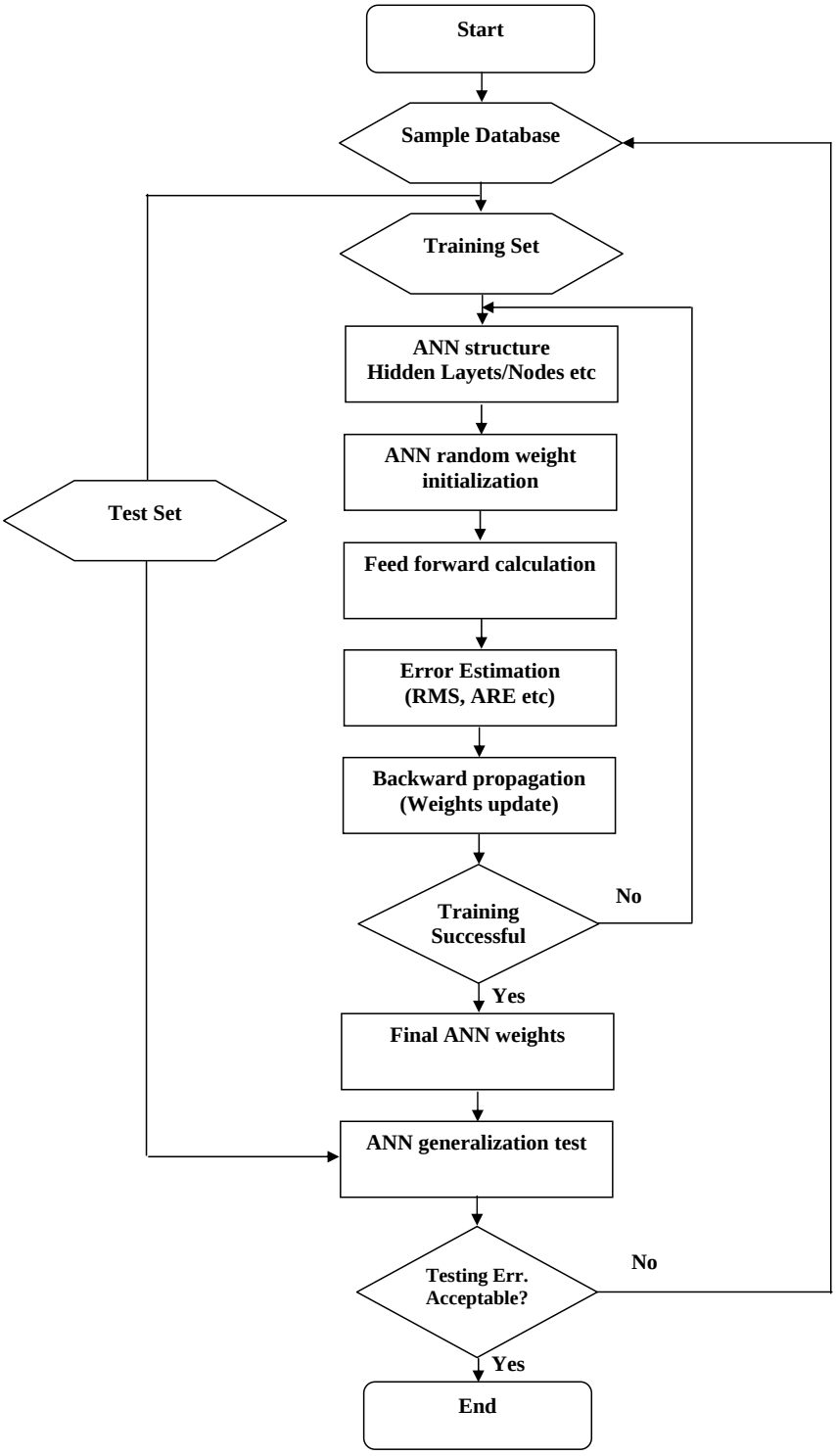


Figure 2.7: Flow of controls: Back Propagation Neural Network

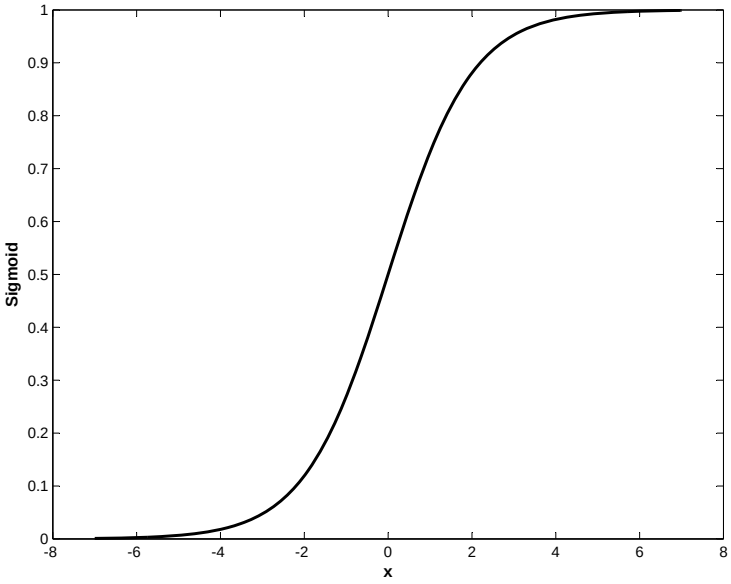


Figure 2.8: Sigmoid transfer function

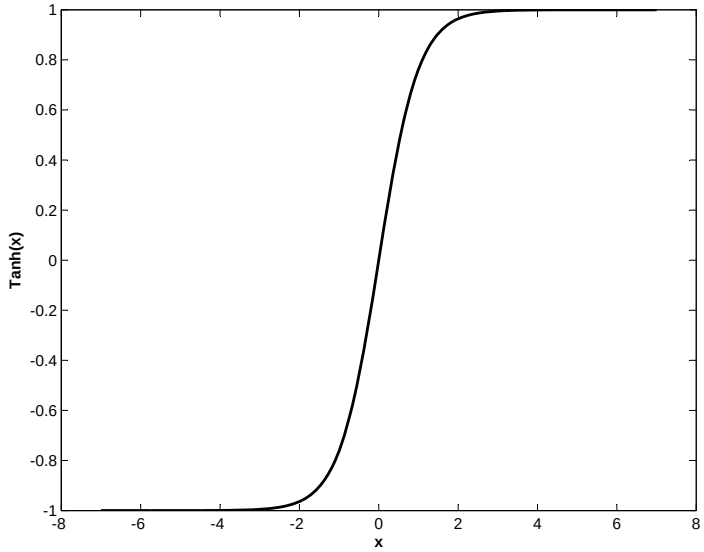


Figure 2.9: Hyperbolic tangent transfer function

# Chapter 3

# Optimization Methodology

## 3.1. Introduction

Selection of the optimization methodology is highly problem dependent. Arriving at the right optimization strategy based on the problem description and objectives are the main keys in achieving a successful optimum design at the end. This chapter focuses mainly on the optimization methodology selected for the current work. The optimization methodology is expected to have an ability to handle different response surface methodologies, design variables, outputs simultaneously and also to be modular and able to handle multiple disciplines without much change in the code. Finally, the methodology should be simple, effective and easy to use.

For the present work, an ANN based GA is used as optimizer. Individual ANNs are assigned to approximate each component of the objective function and constraints separately including the objectives and constraints. A Quadratic Rational Bezier Curve (QRBC) is used in the shape parametrization of the stacking curve [5, 19]. The overall optimization process is shown as a flowchart in Fig. 3.1.

## 3.2. Geometric representation

Blade parameterization and representation of the profile is a vital part of the shape optimization process. Selecting the least and right number of design variables to represent the geometry throughout the complete design space is one of the most challenging tasks. Three dimensional blade geometry is usually defined interms of several 2D airfoils at different spanwise locations, these airfoils are then stacked in the spanwise direction. Traditionally multidisciplinary optimization of turbine blades deal with blade lean, sweep, bow and the set of geometric parameters to represent the blade thickness, leading and trailing edge radius and the other parameters in the hub and tip section etc [16, 31, 32, 44, 37]. If all these parameters are included in the optimization, the number of design variables will increase significantly, it will also make the problem more complex by increasing its dimensionality. So it was decided to keep the 2D airfoil profiles unchanged and to allow only the lean, sweep, bowing in the radial direction, bowing in the circumferential direction and bowing intensity of the blade to vary so as to get a physical insight into the design space. For this reason and due to its flexibility and suitability, a quadratic rational Bezier curve (QRBC) was used to parameterize the stacking line. It also helps to define the design parameters directly in terms of QRBC parameters.

This work focuses on optimizing the stacking line so as to improve the aerodynamic and structural performance of the turbine blades mainly by translating the two dimensional sections but without altering the 2D profiles or their orientation with respect to the rotor axial direction.

### 3.2.1 Quadratic Rational Bezier Curve (QRBC)

A QRBC represents the conic curve in an oblique coordinate system, it can be expressed parametrically in terms of $u \in [0,1]$ as [59]:

$$\overrightarrow{C}(u) = \frac{(1-u)^2 w_0 \overrightarrow{P}_0 + 2u(1-u)w_1 \overrightarrow{P}_1 + u^2 w_2 \overrightarrow{P}_2}{(1-u)^2 w_0 + 2u(1-u)w_1 + u^2 w_2} \tag{3.1}$$

Where $\overrightarrow{C}(u)$ gives the cartesian or cylindrical coordinates of any point on the stacking curve in terms of the parameter $u$, $\overrightarrow{P}_i$ are the cartesian (or cylindrical) coordinates of control points $i$. QRBC is a smooth second order curve which could be used to represent any conic section e.g. an ellipse, a parabola, a circle or a hyperbola. The design variables are represented in terms of QRBC parameters namely $P_1$, $P_2$, and $w_1$, so that the design space is estimated and the optimum shape is interpreted in terms of design variables.

### 3.2.2 Design variables

Based on the QRBC representation given in Eq. 3.1, the QRBC parameters namely, $P_i$, and $w_i$ for $i = 0-2$, can be selected to parameterize the stacking curve. $P_0$ is fixed at some point on the hub surface in most of the cases, blade center of gravity or blade leading edge and $P_2$ moves on the tip surface as shown in Fig. 3.2 in other words, without loss of generality, the coordinates of $P_0$ and the radial coordinate of $P_2$ are fixed. Since $P_0$ and $P_2$ are end points, $w_0$ and $w_2$ are set to 1. The axial coordinate of $P_1$ was chosen to be equal to that of $P_0$, this poses a rather weak restriction on the flexibility of QRBC to generate a variety of geometries by modifying the stacking line.

According to Fig. 3.3.a, the sweep angle is defined as $\beta$ and is controlled by the axial coordinate of $P_2$. Fig. 3.3.b shows the lean angle $\alpha$, which is set by the circumferential coordinate of $P_2$. Fig. 3.3.c shows the blade bowing which can be

controlled by the circumferential and radial coordinates of $P_1$ as well as the weight $w_1$. The circumferential coordinate of $P_1$ is controlled by angle $\widehat{P_1P_0B}$ as shown in Fig. 3.3.c. The lean angle is positive in the direction of the rotation (or suction side) and the sweep angle is positive in the axial direction. The positive sign makes the pressure side concave as shown in Fig. 3.3.c and a negative value makes it convex. With this set up of the QRBC parameters, we end up with 5 design variables per blade row namely the lean angle, sweep angle, the percent span of $P_1$ which specifies this radial location, the angle - which specifies circumferential location of $P_1$ and the bowing intensity is measured by $w_1$.

The design variables and their range of variations are first chosen through a parametric study as explained by Arabnia *et al.* [5, 19]. An important design concern is to keep the design space within a feasible range from blade structural and manufacturing points of view and at the same time be large enough for an adequate exploration.

## 3.3. Sensitivity analysis

Selection and handling of the design variables for the turbine stage optimization is an involved process. Axial turbine stator design is based purely based on the aerodynamic and manufacturing considerations and assuming a non-cooled stator. This is possible further, since the stator is not a rotating part and the resulting stress due to pressure forces is considered negligible, this automatically eliminates the need for including the stator in structural optimization. This results in a change in number of design variables considered for the aerodynamic and structural metamodels. So for the stage optimization only rotor related design variables are considered for the structural discipline and for the aerodynamic discipline the design variables for both stator and rotor are considered.

In order to apply QRBC parametrization for stage optimization a sensitivity analysis has been carried out to select most important design variables affecting the aerodynamic and structural performances. It is a two stage process, in the first stage design variables affecting the aerodynamic performance are identified and in the second stage (based on the aerodynamic design variables) most effective structural design variables pertaining to rotor are identified.

Initially for the aerodynamic discipline five design variables are assumed for each of stator and rotor blade. Since a large number of design variables makes the optimization implementation not only time consuming but also makes the design space more complex, a sensitivity analysis of the objective function to all ten design variables is performed. The goal is to find the most influential parameters amongst the described ten design variables. First order variance-based method is used, it assumes no interaction between the different design variables, hence the effect of each one on the objective function is studied one at a time. The variance of the objective function around original geometry objective function can be calculated with changing one parameter within its specified range while fixing the rest. Then all the calculated variances are normalized by total variances and measure of importance of each parameter are calculated in terms of percentage as indicated in Fig. 3.4. This exercise was done for both stator and rotor. The results indicate that there are four important design variables which are lean and sweep angles for both stator and rotor. Bowing intensity for the stator is neglected because of its lower percentage contribution to the optimization objective. Sensitivity of total pressure loss coefficient to bowing intensity of rotor ($w_r$) and percent span of $P_1$ ($\gamma_r$) are relatively equal. Hence bowing intensity is chosen as fifth parameter (design variable) of the aerodynamic discipline because if there is no bowing ($w_1 = 0$) then radial location of $P_1$ will not change the stacking curve. This reduction of design variables is not very restrictive, at least for the rotor and for cooled vanes; but it results in a significant saving in terms of the

Table 3.1: Design variables used in the aerodynamic and structure optimization

| *Case* | *Aerodynamic design variables* | *Structure design variables* |
|---|---|---|
| Stator | $\alpha_s$, $\beta_s$ | Not included |
| Rotor | $\alpha_r$, $\beta_r$, $w_r$ | $\alpha_r$, $\beta_r$, $w_r$ |

number of CFD flow simulations required to build the ANN model.

For the rotor based structural sensitivity analysis, design variables $\alpha_r$, $\beta_r$, $w_r$ and percent span of $P_1$ ($\gamma_r$) are only considered. Sensitivity of von Mises stress and first natural frequency to design variables is analyzed and explained in the previous paragraph. Measure of importance of each design variable is calculated in terms of percentage as indicated in Fig. 3.5. Based on the aerodynamic and structural sensitivity analysis it was decided to keep three design variables ($\alpha_r$,$\beta_r$ and $w_r$) to represent the rotor shape. In fact the reduction of design variables is not only based on sensitivity analysis but also on the basis of earlier work [5]. In that work, the stator and rotor were separately optimized each with all 5 design variables and the results showed that, for aerodynamic stage optimization, the 5 design variables suggested by the sensitivity analysis were the ones that need to be kept. Final set of design variables for aerodynamic and structural optimization is shown in Table 3.1.

## 3.4. Optimizer

### Genetic Algorithm

A real coded MOGA is applied to multi-objective optimization by introducing a non-dominated sorting procedure [60]. The initial population is generated randomly within the design space and the fitness in each generation is based on the non-domination level and a niche count factor, which depends on the number and proximity of neighboring solutions. All sets in the first non-domination level are assigned

a maximum value of equal dummy fitness and this value may be reduced based on the factor called niche count if that solution is located in the dense region of the solution space, see [60] for details. The population in the second non-domination level is assigned a dummy fitness, which is smaller than the smallest fitness value of the previous front. The same kind of fitness reduction is carried out based on the niche count. These procedures are repeated until all the individuals are assigned a fitness value. The genetic algorithm operations like selection, crossover, mutation, elitism and reproduction are then carried out on the individuals to provide a search direction towards the Pareto-optimal region and the solution becomes well diversified due to the inclusion of a sharing strategy [60]. The main difference between single-objective and multiple-objective optimization is the fitness assignment. For multi objective optimization NSGA-II [60] is used. Basically having the same evolutionary operators as GA, it uses non-dominated solutions concept and Niche count factor to specify the fitness function.

**Artificial Neural Networks**

In the current work, ANN based RSA model is used to predict the objective function and constraints, which reduces the computing cost to a significant level [19, 37]. Multi-layer feed forward network is a universal approximation tool for any non linear and finite function [55] and is built with back propagation algorithm [52]. The ANN training and testing has already been discussed in Chapter 2.

The ANN training process is challenging and requires careful selection of parameters, architecture (number of hidden layers, number of hidden and output nodes), transfer functions and effective training strategy. These choices completely depend on the function being approximated, like the presence of local minima, high dimensionality, disparity in input scales, etc. ANN model and its results are highly dependent on the training data set provided, it is very important to ensure that the

training data are not clustered around one part of the design domain. The diversity of the training set should always be maintained to get a good prediction model.

Following are some contributions made to the ANN model to improve its generalization capability, accuracy of approximation, variable handling and training time:

1. Multiple ANNs: The capabilities of artificial neural networks to handle multi dimensional outputs are well known. However, it is preferred to use individual ANN models to predict each output. This method of multiple neural networks was employed by Norgaard *et al.* [61] to predict the lift, drag, moment of inertia and lift to drag ratio ($C_L, C_D, C_M$ and L/D) for different angles of attack and flap settings to improve the aerodynamic design. Optimization of a compressor for micro gas turbine was done by Verstraete [45] using multiple neural networks to predict efficiency, mass flow rate, Mach number distribution and maximum stress of the geometry. Use of multiple neural networks is like a divide and conquer policy, here are some of the practical advantages of using multiple ANNs,

   (a) Different number of sample points (or patterns) are used to prepare aero and structural database. To train both domains which contain different patterns is not feasible by using a single ANN (to predict all the output variables)

   (b) Continuous database enrichment is required to get a better prediction model in this case RSA, so during the enrichment process individual output variable databases could be updated based on the performance.

   (c) Enhances the prediction accuracy because of only one output

   (d) Improves the handling capability of the optimizer during the optimization process. Each metamodel can handle different number of hidden nodes,

inputs, outputs, transfer functions, bounds (upper and lower) etc, these characteristics makes them more attractive and ideal for complex problems like the current one.

(e) Handling of multiple disciplines becomes very effective and simple.

(f) The main disadvantage could be an increase in training time and it linearly varies depending on the total number of output variables considered for the problem at hand.

The difference between single ANN Fig. 3.6 to predict all the outputs and individual ANN to predict each output is shown in Fig. 3.7.

2. Database enrichment: Though the ANN is trained and tested with the right number of patterns in the database, enriching the database during the optimization process improves the capability of the metamodel to predict the better optimum. This process also reduces the difference between the ANN predicted objective and high fidelity solutions. Generally enrichment of database indicates the right path for the metamodel by means of correcting its mistakes. Care should be taken not to include multiple optimum candidates which have similar design variables closer to each other because it might dominate the optimization process and result in an untrue optimum.

3. Handling of design variables: Selection and handling of the design variables for the turbine stage optimization is a tricky process. Aero-structural optimization of turbine stage could be done with six design variables (2 for stator and remaining 4 for rotor) but optimizing the stage which contains stator and rotor needs more design variables and raises additional problems in terms of response surface modeling and variable handling. Selection of design variables corresponding to stator completely depends on the aerodynamics performance of the stage and manufacturing difficulties. So for the stage optimization there are only

two stator related design variables (lean and sweep) and both are included in the aerodynamic design variables set but not considered for structure analysis. Finally for the structural optimization only rotor related design variables are considered and aerodynamic optimization contains variables related to stator and rotor. Different number of design variables for aero and structural domains are effectively handled by the multiple ANNs and MOGA developed in this work. The results presented are only for the turbine blade row aero structural optimization and turbine stage optimization will be carried out subsequently as the continuation of the present results. In the current work, ANN based RSA model is used to predict the objective function and constraints, which reduces the computing cost significantly [19, 37]. Multi-layer feed forward network is a universal approximation tool for any non linear, finite function [55] and is built with back propogation algorithm [52]. Building an ANN based RSA model involves two steps: Training the ANN with the sample database followed by testing the ANN model.

## 3.5. Present optimization cycle

The flow chart in Fig. 3.8 describes the complete flow of optimization process used in the current work. All the modules can work individually as well as in groups which makes it easy to evaluate their performance whenever required. Moreover, due to modular approach followed in handling different disciplines, it is easy to customize for the problem at hand and add other disciplines such as heat transfer, blade life estimation, manufacturing cost estimation etc without any major modifications.

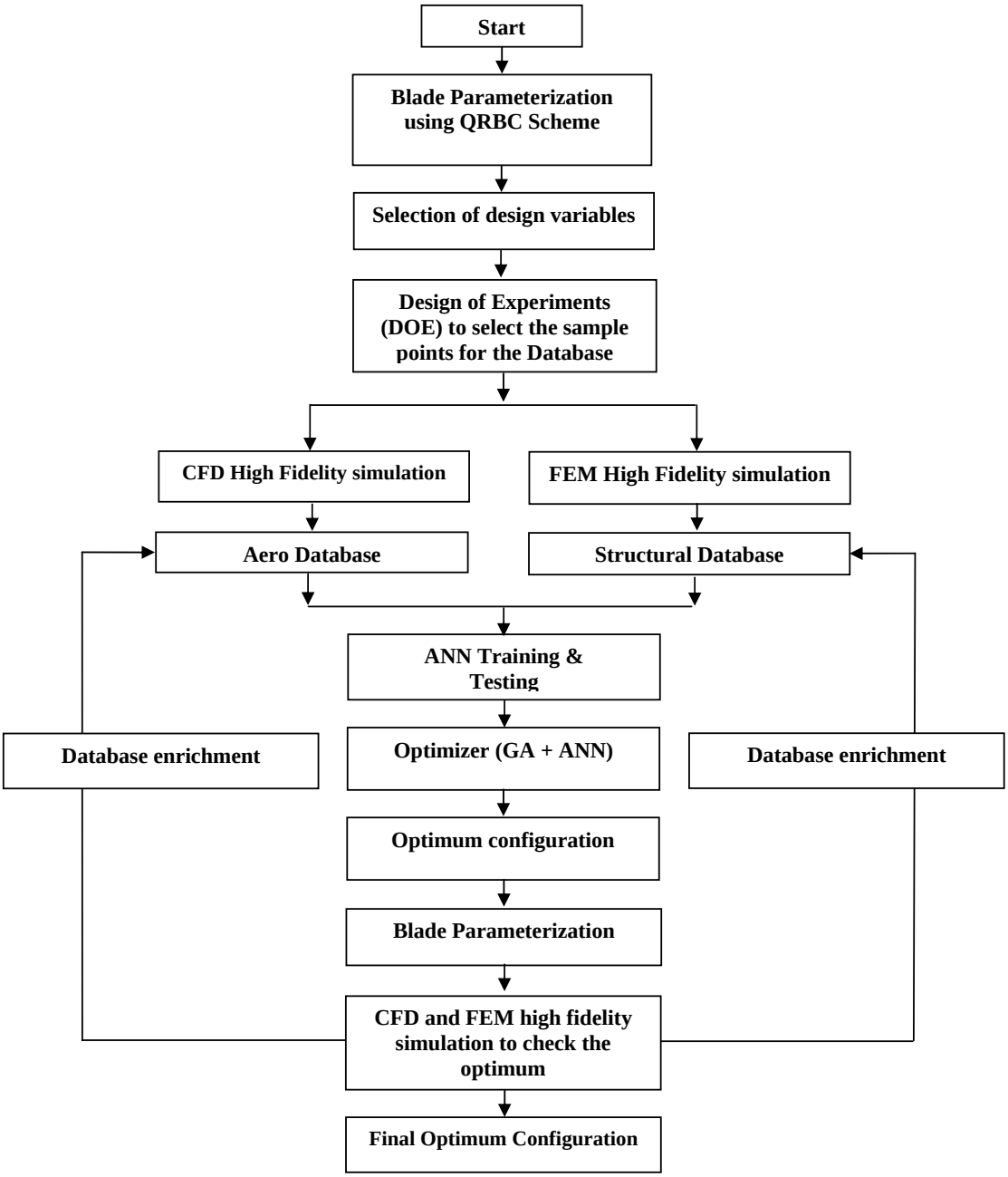


Figure 3.1: Aero-Structural Optimization Cycle.

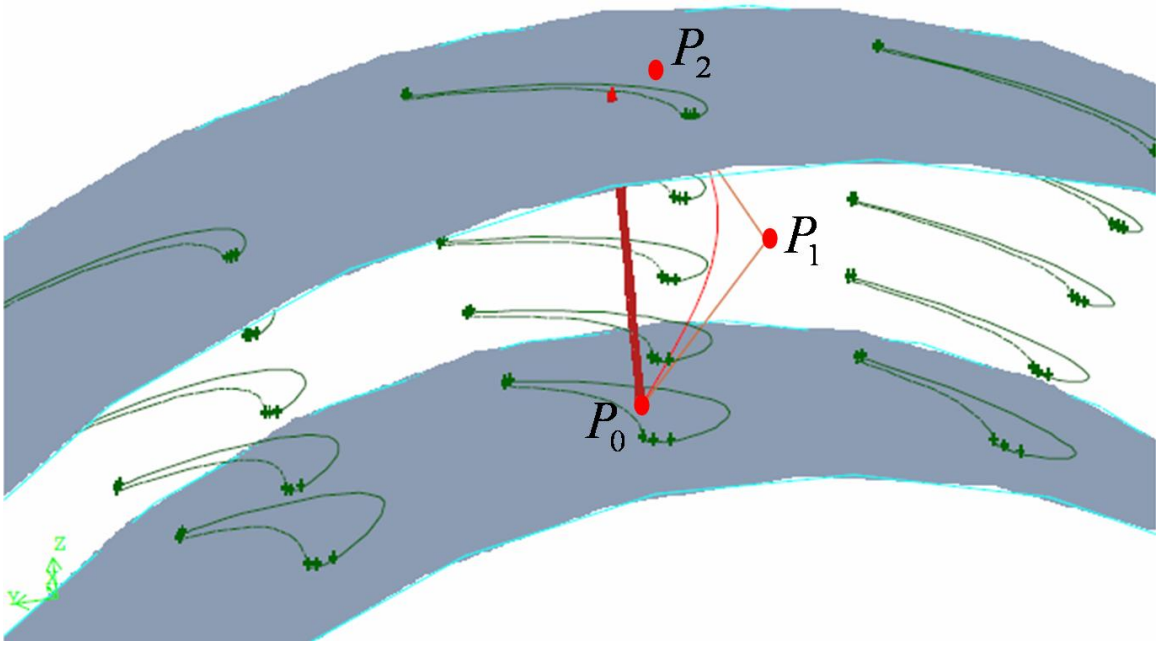


Figure 3.2: Quadratic Rational Bezier Curve (QRBC) representation [5]

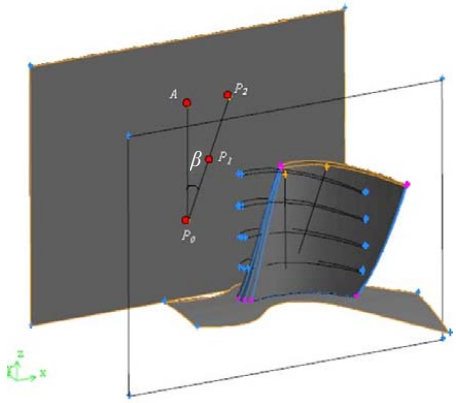


a. Blade sweep

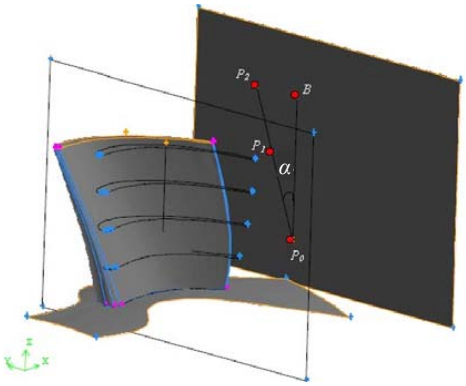


b. Blade lean

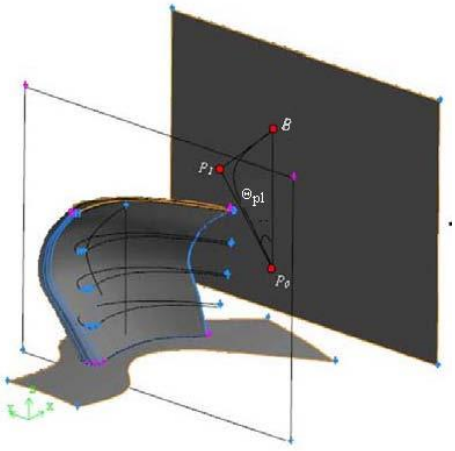


b. Blade bowing

Figure 3.3: Stacking curve parametrization using QRBC [5]

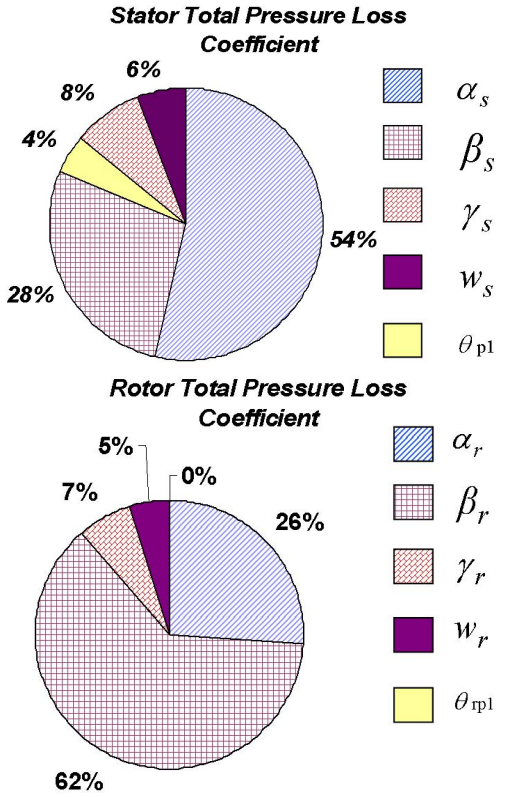


Figure 3.4: Aerodynamic sensitivity analysis of objective functions to design variables [5]

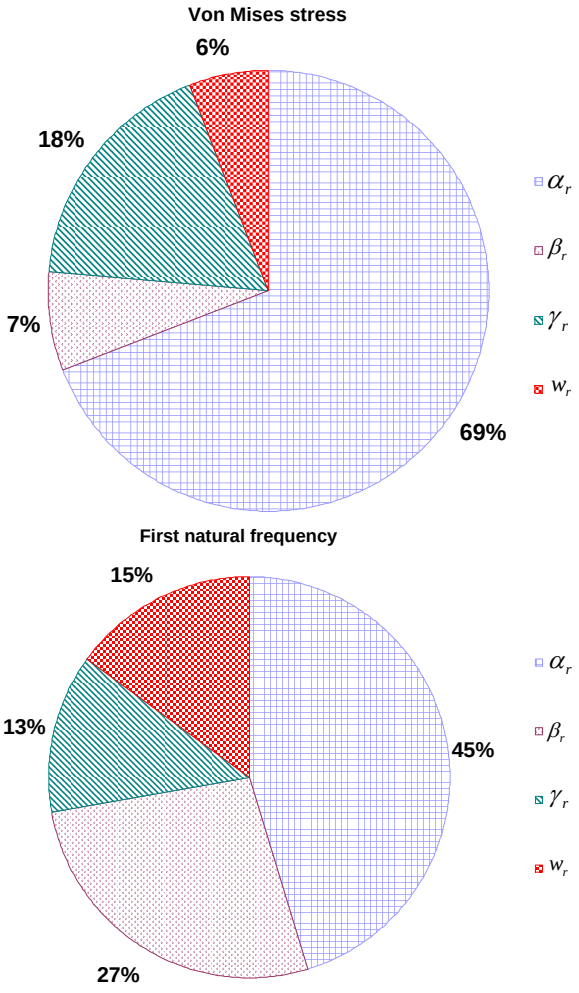


Figure 3.5: Structural sensitivity analysis of objective functions to design variables

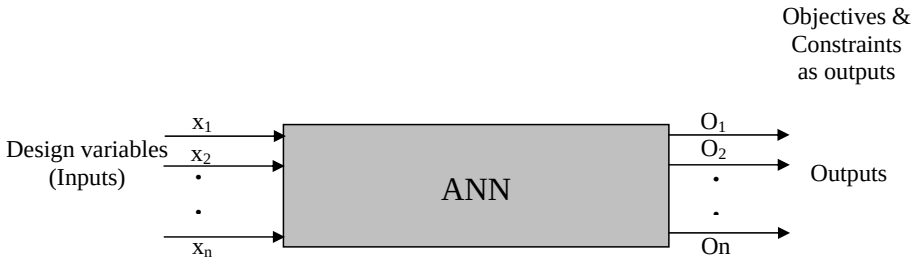


Figure 3.6: Single ANN for all the outputs

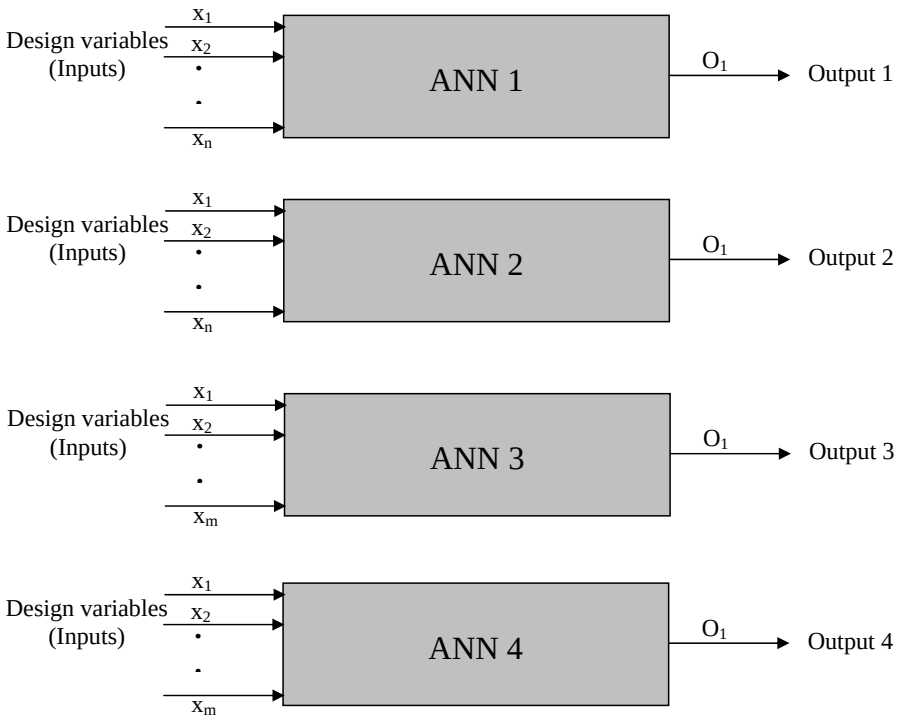


Figure 3.7: Single ANN for each output (Concept of multiple ANNs)

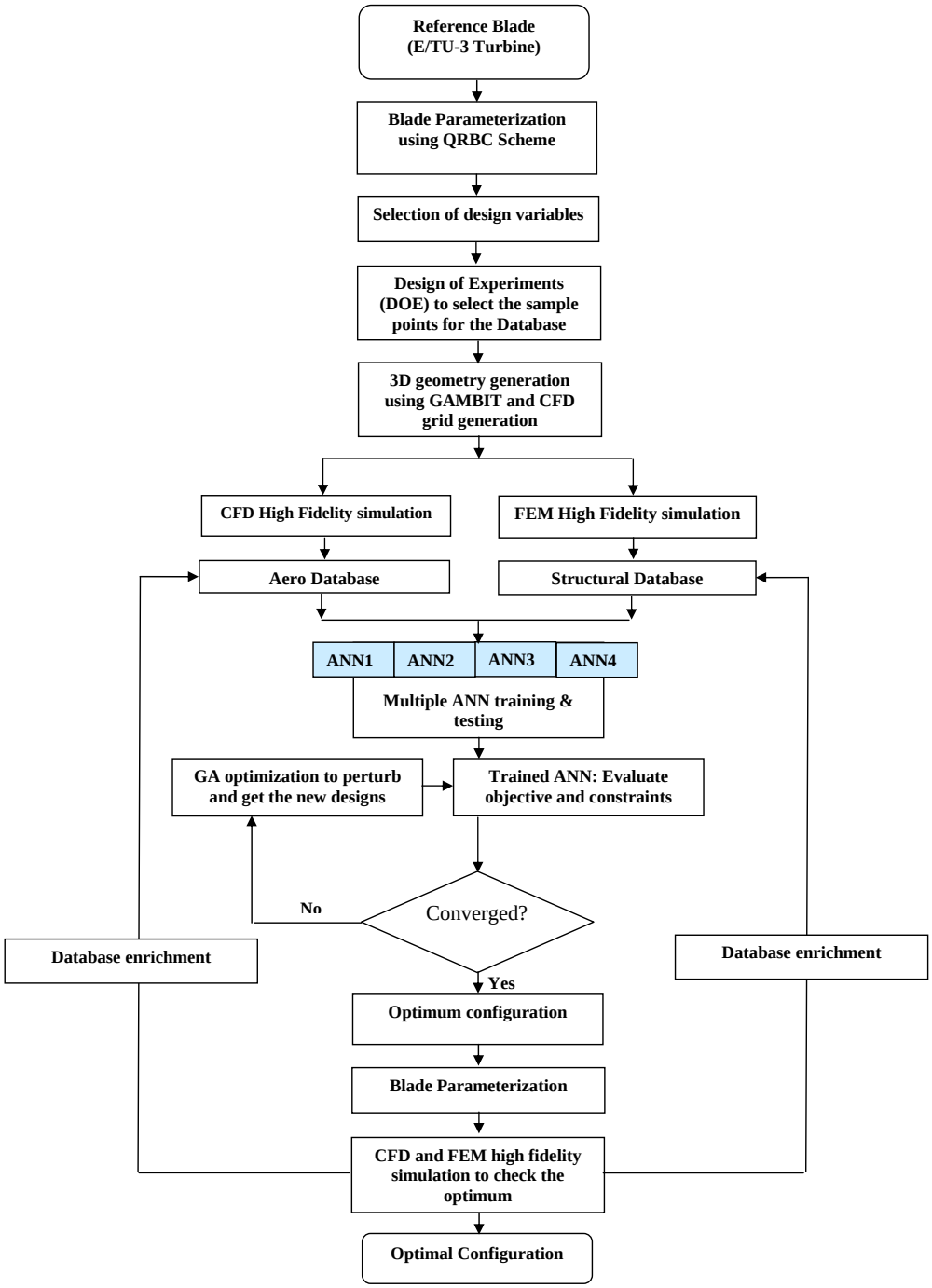


Figure 3.8: Optimization Process

# Chapter 4

# Redesign cases

## 4.1. Introduction

In this chapter, the optimization scheme described in the previous chapter is applied to a well documented, single stage low speed subsonic turbine, referred to as the E/TU-3 turbine. The work is divided into different sections as mentioned below:

- E/TU-3 turbine stage optimization
    1. Structural optimization of E/TU-3 turbine blade with three design variables
    2. Aero-Structural optimization of E/TU-3 turbine stage with five design variables
- E/TU-3 turbine blade row with four design variables
    1. Aero-Structural optimization of E/TU-3 turbine blade

The notable aerodynamic and structural performance improvements obtained from the redesigned cases reiterates the robustness and accuracy of the optimizer as well as the developed methodology. Results also underline the advantages of modularizing the ANN's while integrating multiple disciplines.

Table 4.1: E/TU-3 single stage turbine specifications

| Data | Stator | Rotor |
|---|---|---|
| Number of blades | 20 | 31 |
| Blade aspect ratio | 0.56 | 0.95 |
| Blade solidity | 1.56 | 1.51 |
| Flow deflection | 69° | 105° |

Table 4.2: E/TU-3 single stage turbine design point specifications

| | |
|---|---|
| Inlet total temperature (K) | 346 |
| Rotor speed (RPM) | 7800 |
| Stage pressure ratio | 0.51 |
| Reynold number | $1.5 \times 10^6$ |
| Mid-span flow coefficient | 0.74 |
| Mid-span stage loading | 1.93 |
| Average reaction (%) | 31 |

## 4.2. E/TU-3 Turbine Stage Redesign

E/TU-3 is a single stage low speed subsonic turbine, built and tested at DLR, Cologne [6], this turbine is used as a test case to prove the effectiveness of the proposed optimization methodology. The turbine stage geometry is given as a set of x and y coordinates describing the 2D airfoils profiles at five different radial locations from hub to tip. Several geometric and aerodynamic features of that stage are provided in Tables 4.1 and 4.2. The additional details on the geometry and aerodynamic features that are provided in Fottner [6] help in redesigning the turbine stage for performance improvements. The original stator and rotor blade profiles are sketched in Fig. 4.2.

The rotor tip clearance was ignored in simulating the flow in the turbine stage.

## 4.3. Geometry preparation and boundary conditions

Obtaining a CAD model for structural analysis is not a straightforward process, the steps involved in achieving the final CAD model is shown as a flow chart in Fig. 4.1. Blade geometry generated using GAMBIT preprocessor [62] and the geometry clean up was done using ANSYS ICEMCFD which is a part of ANSYS Workbench [63]. ANSYS workbench - Simulation option was used for mesh generation and finite element analysis. Three dimensional solid tetrahedral elements with midside nodes was selected to discretize the solid blade as it can capture highly complex and curved profiles. All the nodes at root of the blade are assumed as fixed (like a cantilever).

**Turbine materials**

The E/TU-3 turbine stage is basically an aerodynamic test case hence details of the structural tests and materials used for the blades are not available in the open literature. Different materials are used for turbine blades based on their proximity to the combustion chamber, rpm and loading, normally for turbine blades which are operating at high temperature and rpm require high strength materials like Inconel 718, etc [64]. For this work two different materials were used

- Stainless steel (Optimization of turbine blade row using four design variables)
  - Elastic modulus $1.93 \times 10^{11} Pa$
  - Poisson's ratio 0.31
  - Mass density $7750 Kg/m^3$
  - Tensile yield strength $2.07 \times 10^8 Pa$
  - Compressive yield strength $2.07 \times 10^8 Pa$
  - Tensile ultimate yield strength $5.86 \times 10^8 Pa$

- Inconel 718 (Optimization of turbine stage using three design variables)
  - Elastic modulus $2.00 \times 10^8 Pa$
  - Poisson's ratio 0.284 and
  - Mass density $8220 Kg/m^3$

**Other facts**

In reality turbine blade which is fitted on the turbine disk will have some definite amount of stiffness value but for the current work all the nodes at the blade root are assumed as fixed (like a cantilever) with zero displacement (worst case scenario). Turbine blades are normally thicker and heavier then compressor blades due to their operating conditions so the stresses due to pressure forces acting on the turbine blade are negligible compared with the centrifugal forces [65]. This is not the case for compressor blades which are much thinner resulting in aerodynamic and centrifugal forces to be comparable. For the current work, pressure forces are neglected when performing the stress analysis, only centrifugal forces are simulated by imposing the blade rotation. Von Mises stress considered as the main output parameter from the structural analysis and used as one of the objectives in structural optimization.

Large tensile stresses developed during rotation (due to the centrifugal forces) can be captured by carrying out a static structure analysis. This also causes significant stiffening of the blade. Performing a prestressed modal analysis would provide more realistic values for natural frequencies. Hence, static structure analysis results are taken as an initial solution for the modal analysis.

## 4.4. Effect of design variables on turbine blade stress

Design variables and their lower and upper bounds control the feasible optimum shapes and the amount of aero-structural performance improvements achieved at

the end of optimization. Understanding the effect of individual variables on the performance of the blade is essential to limit the allowable change in variables.

Optimizing the stacking line to improve the aerodynamic performance has been addressed by several researchers [5, 19, 34], where the optimization focuses on decreasing the three dimensional losses in turbine and compressor. The importance of stacking line optimization in improving the aerodynamic and structural performance of the blade were also emphasized by Moustapha *et al.* [66]. Basically stacking line optimization helps to improve the aerodynamic performance of the blade by unloading the tip and the root (loading more on the blade mid section) and reducing the three dimensional losses, on the structural side can redistribute the stresses on the suction side to decrease the maximum stresses.

Leaning the blade towards the pressure side considered as negative and leaning towards the suction side (direction of the rotation) is positive. The range for lean considered varied between $-5^o$ and $20^o$ in intervals of $5^o$. In general, negative lean increases the maximum stress and positive lean decreases the maximum stress up to $10^o$ lean and then the stress increases again. The applied negative lean, moves the blade center of mass closer to the axis of rotation compared to the original geometry, and addition of centrifugal forces creates larger tangential moments. When the leaned blade is rotating, the combination of blade mass and centrifugal forces, will try to straighten the blade which results in increasing the tangential moment. This increased moment results in higher stress at the root of the blade leading and trailing edges (minimum thickness area location) due to its highly cambered profile when the blade is rotating. However the application of positive lean decreases the maximum stress compared to the original geometry due to the blade camber and thickness distribution. Combination of positive lean and blade rotation tries to straighten the blade due to centrifugal forces, which increases the tangential moment but the increase in tangential moment is effectively handled by the available higher

blade thickness. Moreover the thickness distribution and shape of the turbine blade from hub to tip also helps to effectively handle the increase in the stress due to the tangential moment. Again the maximum stress starts increasing after $10^o$ lean and it occurs at the root of blade near the maximum camber location (on the suction side). The comparison of suction side stress contours for different lean angles is shown in Fig. 4.4 and pressure side stress contours are shown in Fig. 4.5.

Original E/TU-3 blade sections are stacked radially. Leaning the stacking line in the flow direction indicates a positive sweep and opposite to the flow direction is considered as negative sweep. Sweep angles $-10^o, 0, 5^o, 10^o, 15^o$ were considered in this analysis. A decrease in maximum stress value was observed compared to the original E/TU-3 blade when negative sweep is applied, this is due to an increase in tangential moment. This effect also relieves the stress at the root trailing edge and maximum stress occurs in the root leading edge region. Positive sweep increases the maximum stress because of the increase in tangential moment and change in center of mass, hence increases load in the root trailing edge region. The comparison of suction side stress contours for different sweep angles and pressure side stress contours are given in Fig. 4.6 and Fig. 4.7.

An increase in bowing intensity always raises the maximum stress values. The max. magnitude of bowing occurs at 50% span, which gives the blade a curved look from hub to tip from the front view. When the rotor is spinning the centrifugal forces, try to untwist the blade which causes more stress near the blade trailing edge at 50% span and near the maximum thickness distribution area at the root. The stress increase is also due to the increase in axial moment and change is center of mass relative to the original E/TU-3 turbine blade. Variation in stress with respect to different bowing intensities is shown in Fig. 4.8 and Fig. 4.9 for suction and pressure sides respectively.

Based on the above analysis discussion it can be concluded that the design

variables lean, sweep and bowing intensity have a great impact on the blade maximum stress. It could also be seen from the previous results that the combination of positive lean and small amount positive and negative sweep could decrease the maximum stress on the blade, but the bowing intensity always increases the stress.

## 4.5. Objectives and Constraints

Objective functions and constraints used for the current structural and aero-structural optimization problems are given in this section.

### 4.5.1 Single objective structural optimization

$$F_{Obj}(X) = Min(\sigma_{vm}) + PT \tag{4.1}$$

Where PT is the penalty term which is given by an inequality constraints that restricts the first three natural frequencies of the blade to be larger that the original blade frequencies.

$$\omega_1 > \omega_{etu3} \tag{4.2}$$

$$\omega_2 > \omega_{etu3} \tag{4.3}$$

$$\omega_3 > \omega_{etu3} \tag{4.4}$$

### 4.5.2 Multi objective aero-structural optimization

For the aero-structural optimization the objective takes the following form:

$$\begin{aligned} F_{obj}(X) = \{&Min(-\eta_{tt}{}' + PT_a), \\ &Min(\sigma_{vm}{}' + PT_s)\} \end{aligned} \tag{4.5}$$

Where X is the vector of design variables, which includes the stator and

rotor lean and sweep angles, and the rotor bowing intensity.

$$PT_a = 0.5 \quad when \quad \frac{|\dot{m} - \dot{m}_{org}|}{\dot{m}_{org}} > 0.005$$
$$= 0 \qquad otherwise$$

$$PT_s = 0.5 \quad when \quad f_1 < f_{1,org}$$
$$= 0 \qquad otherwise$$

where $f_{1,org} = 2294Hz$ is the first natural frequency of the original rotor. The first term on the right hand side of the objective function indicates the aerodynamic loss $-\eta$' and second term corresponds to von Mises stress $\sigma_{vm}$'. Reduction of loss increases the aerodynamic efficiency and at the same time reduction in von Mises stress reduces the maximum stress due to centrifugal forces. The penalty terms are given by the mass flow rate ($PT_a$) and the rotor first fundamental frequency ($PT_s$).

$$f' = \frac{f - f_{min}}{f_{max} - f_{min}} \tag{4.6}$$

The objectives, $-\eta$' and $\sigma_{vm}$', are normalized between 0 and 1 according to Eq. 4.6, so as to have an equal weight for all disciplines and eliminate the possibility of reaching a biased optimum.

## 4.6. E/TU-3 turbine stage optimization

### 4.6.1 Structural optimization of turbine blade with three design variables

#### Preparation of structural database

23 sample points were selected for the structural database including the initial E/TU-3 configuration. Latin hypercube model developed by Temesgen [43] was used as a DOE model to distribute the data samples in the design space. Only rotor related design variables were considered for structural optimization. It was decided to maintain the same range of design variables for structural and subsequent aero structural optimization due to structural and manufacturing reasons. The lean, sweep and bowing intensity were varied between $-5°$ to $20°$, $-10°$ to $15°$ and 0 to 3, respectively, during the optimization process. The upper and lower bound for output variables such as von Mises stress and fundamental frequencies were calculated from the database extremes by adding 15% to the upper bound and subtracting 30% from the lower bound. For minimization problems expanding the lower bound range helps the optimizer to improve its effective search region.

#### ANN Training and Error analysis

ANN was trained with the structural database which contains 23 candidates and the range for training is given in Table 4.3. ANN training is an involved process, and getting a right combination of ANN parameters such as hidden nodes, transfer functions, learning rates (input and output), number of epochs is a kind of optimization process by itself. Two approaches were followed in building the ANN metamodels; in the first approach each output variable is predicted by individual ANN trained to predict only one output variable, this method is called multi input single output ANN or MISO ANN. In the second approach all four outputs are predicted using single ANN, which

Table 4.3: E/TU-3 Turbine stage operating conditions

| Variables | Lower bound | Upper bound |
|---|---|---|
| $\alpha_r$ | -5 | 20 |
| $\beta_r$ | -10 | 15 |
| $w_r$ | 0 | 3 |
| $\sigma_{vm}$ MPa | 189 | 1231 |
| $\omega_1$ Hz | 945 | 2885 |
| $\omega_2$ Hz | 1820 | 5580 |
| $\omega_3$ Hz | 1981 | 6779 |

is called multi input multi output ANN or MIMO ANN. In both cases the number of input variables is kept the same. The flow chart for ANN training is give in Fig. 2.7 and the final ANN training parameters are given in Table 4.10. The accuracy of the ANN approximation could be verified from the ANN performance measures. MISO ANN performs or approximates the error function better than the MIMO ANN which can be seen from the main performance measures (Appendix A) such as ARE, RMS, Max error, R square and correlation are better than the RAAE, RMAE.

**Results and validation with high fidelity results**

GA was used as a global optimizer along with ANN metamodel and optimum results proposed by GA + ANN and corresponding high-fidelity evaluations are given in Table 4.4. From the design variables proposed by MIMO ANN and MISO ANN, it is evident that the optimum lean varies with respect to the metamodel and other two design variables remains almost same. The MISO ANN over predicts the objective by 25% and MIMO under predicts it by 33%, prediction of constraints are almost close but overall MISO ANN predicts better optimum designs (with lower maximum stress values) than MIMO ANN. The proposed MISO ANN produced (or resulted in) more accurate approximation of the stress when it was used in optimization, with maximum stress $177.33MPa$ which is 37.45% lower than the original E/TU-3. In turn MIMO ANN proposed optimum shape resulted in a maximum stress of $271MPa$ which is

Table 4.4: ANN proposed optimum values and its corresponding high fidelity solutions

| | | MISO | ANSYS | % change | MIMO | ANSYS | % change |
|---|---|---|---|---|---|---|---|
| Design variables | $\alpha_r$ | 7.38182 | 7.38182 | | 19.5422 | 19.5422 | |
| | $\beta_r$ | -9.73835 | -9.73835 | | -9.83017 | -9.83017 | |
| | $w_r$ | 1.75E-05 | 1.75E-05 | | 0.000452 | 0.000452 | |
| Objectives | $\sigma_{vm}$ | 235.79 | 177.33 | 25 | 203.391 | 271.1 | 33 |
| Constraints | $\omega_1$ | 2529.39 | 2584.7 | 2 | 2610.18 | 2841.7 | 8.8 |
| | $\omega_2$ | 4820.49 | 4914 | 2 | 4754.42 | 4758.4 | 0.08 |
| | $\omega_3$ | 6101.87 | 6024.5 | 1.3 | 6141.69 | 6239 | 1.6 |

just 4% less compared to original E/TU-3. Subsequent comparisons between the two approaches revealed that the MISO ANN performs consistently better than the MIMO ANN and due to their flexibility and better approximation capabilities, for subsequent optimization cases it was decided to use only MISO ANN. The selected approach also helps to effectively handle different number of design variables as input, apart from removing inter dependency among the outputs, however the time taken to train individual ANNs is relatively high compared with MIMO ANN.

**Need for more samples in the structural database**

**Need**

A larger no of samples in the design space automatically improves the approximation capability of the metamodel which helps in finding the real global minimum. Training ANN with more samples could also help in decreasing the difference between the proposed optimum values of ANN and its corresponding high fidelity solutions.

**Issues**

Building a database with a large number of samples increases the number of high fidelity simulation runs. High fidelity simulations always require more time due to geometry modeling, meshing, analysis and post processing the results. In case of

aerodynamic analysis, each simulation needs more than 24 hrs on a single CPU and structural analysis needs less than an hour from geometry generation till postprocessing the results. So it was decided to increase the number of samples from 23 cases to 100 cases only for the structural database due to its lower computational cost. The main purpose for this exercise is to build a more accurate metamodel to predict the von Mises stresses. Moreover the use of MISO ANN provides a greater flexibility in handling the individual outputs and their sample points, otherwise it could be very complex to handle them with the single MIMO ANN. It is not possible to increase number of sample points for one domain (like structures or aero) without considering the other domains.

**Structural database**

Need for better approximation of the design space and lower computational cost involved in getting the structural results prompted to develop a larger database. Latin hypercube model was used to discretize the design space with 100 sample points. A larger database generally requires more training time and a larger number of nodes in the hidden layer. To get an ANN which could generalize the complete design space, 70% of the samples in the database were used for training and the rest for testing. The ANN training/testing algorithm is given in Fig. 2.7. For this case the hyperbolic tangent transfer function is used with a range of $[-1, 1]$. It was found that the use of hyperbolic tan transfer function speeds up the ANN learning process and approximates the design space with less number of hidden nodes. The complete ANN training parameters are given in Table 4.11. The prediction capability of the trained ANN model was analyzed and tabulated from the train and test individual sample error measures. Complete distribution errors are plotted in Fig. 4.12.

Single objective structural optimization was carried out with an updated metamodel trained and tested with 100 sample points in order to reduce the von

Table 4.5: ANN proposed optimum values and its corresponding high fidelity solutions with updated database

| | | E/TU-3 | Case 1 | ANSYS | % change | Case 2 | ANSYS | % change |
|---|---|---|---|---|---|---|---|---|
| Design variables | $\alpha_r$ | 0 | 6.8524 | 6.8524 | | 7.10493 | 7.10493 | |
| | $\beta_r$ | 0 | -1.59525 | -1.59525 | | -1.08041 | -1.08041 | |
| | $w_r$ | 0 | 0.00253 | 0.00253 | | 0 | 0 | |
| Objectives | $\sigma_{vm}$ | 287 | 172.62 | 145.00 | 19.05 | 172.60 | 147.70 | 16.859 |
| Constraints | $\omega_1$ | 2273 | 2396.34 | 2427 | 1.263 | 2390.37 | 2424 | 1.387 |

Mises stress at design point conditions. Combination of GA + ANN was used as an optimizer, the convergence history of the GA is shown in Fig. 4.13. Metamodel built with 23 candidates reduced the von Mises stress to $177MPa$ from an original value of $287MPa$, see Table 4.4 around 38% reduction. The current updated metamodel trained with a new database with 100 sample points was found to reduce the von Mises stress by 48%. New optimum values proposed by optimizer and corresponding high fidelity solutions are given in Table 4.5. The stress contours along the SS, PS and along the hub of the original and redesigned E/TU-3 are compared in Fig. 4.14.

### 4.6.2 Database enrichment and optimization

The need and use of database enrichment in the optimization process is already discussed in Sec. 3.4. Care should be taken not to include multiple optimum candidates with design variables closer to each other because it might dominate the optimization process hence ending up with the same optimum solution. The enriched database was divided into training and testing sets with 73 and 30 samples respectively to approximate the objective function and new ANN training parameters were given in Table 4.15. The optimum configurations proposed by optimizer were better than all the previous optima in terms of objective function, there is a 52% reduction in von Mises stress achieved compare to the original E/TU-3 blade. The original E/TU-3

Table 4.6: ANN proposed optimum values and its corresponding high fidelity solutions with updated database

| | | E/TU-3 | Optimum | ANSYS | % change |
|---|---|---|---|---|---|
| Design variables | $\alpha_r$ | 0 | 7.46389 | 7.46389 | |
| | $\beta_r$ | 0 | -2.80523 | -2.80523 | |
| | $w_r$ | 0 | 0 | 0 | |
| Objectives | $\sigma_{vm}$ | 287 | 162.48 | 137.97 | 17 |
| Constraints | $\omega_1$ | 2273 | 2425.24 | 2465.32 | 1.6 |

and optimum shape design variables, objectives and constraints are given in Table 4.6. In the E/TU-3 configuration, the maximum stress was located at the hub trailing edge region (lowest thickness area). Leaning the blade in the rotational direction combined with forward sweep and zero bowing intensity redistributed the stresses in the maximum thickness region along the span direction. In the optimum configuration, on the pressure and hub surface average equivalent stress is decreased and on the suction side it got increased due to lean and sweep of the blade. So E/TU-3 turbine blade was structurally optimized for lower stress by optimizing the stacking line parameters. Stress contours of the optimum and original E/TU-3 shapes are given in Fig. 4.17.

Optimizing the turbomachinery blade with a structural objective will not improve the overall performance of the turbine stage instead it might act as a detrimental factor for aerodynamic efficiency. So combining aerodynamic and structural disciplines and performing multi objective optimization would be the right solution to address this issue. In the following section, the aero-structural optimization of the turbine stage is carried out to achieve an overall performance improvement in stator and rotor.

### 4.6.3 Single point aero-structural Multi objective optimization of E/TU-3 stage

The optimization of stacking line is the best way to obtain the better performance without modifying the two dimensional airfoil profiles since it is the main parameter affecting the 3D-related flow phenomena. Change in stacking line affects the aerodynamic performance by varying the three dimensional flow field around, and structural loadings on, the blade so it is essential to consider simultaneously both disciplines during the optimization process to get a better performance for both disciplines.

Turbine stage aerodynamic optimization of the rotor is highly dependent on the stator that is located upstream of it. Optimization of rotor or stator alone may not provide as much improvement in performance as the stage. So it is advantageous to include the stator in the aero-structural optimization to improve the stage performance and the overall effectiveness of the optimization process. The initial aerodynamic database was taken from the previous work of Arabnia *et al.* [5, 19].

The design parameters are given by the lean angle, sweep angle and bowing intensity (controlled by weight $w_1$). Individual output variables (objectives and constraints) are approximated by individual back propagation based ANNs (MISO ANN) with a single hidden layer between the input and output layers. It improves the approximation model accuracy and allows for a better control of the error surface for each particular output. To approximate the efficiency and mass flow rate, two ANN modules with 5 and 6 nodes in the hidden layers were used. A set of 23 cases selected through LHM were used to build the aerodynamic database and approximately 70% of the samples were selected for ANN training and the rest used to test the ANN model. Structural ANN model from Sec. 4.6.2 with 103 sample points were used with the aerodynamic model. Two ANN modules were used to approximate the von Mises stress and fundamental frequency with 10 and 7 nodes used at the hidden layers, respectively. GA or MOGA were employed as the optimizer to search the

Table 4.7: Comparison of initial E/TU-3 and optimum design variables and their range used in optimization

| Case | $\alpha_s$ | $\beta_s$ | $\alpha_r$ | $\beta_r$ | $w_r$ |
|---|---|---|---|---|---|
| E/TU-3 | -7.3 ° | 6.9 ° | 0 ° | 0 ° | 0 |
| Optimum | -14.26 ° | -7.99 ° | 5.55 ° | -1.17 ° | 0.012 |
| min | -36 ° | -8 ° | -5 ° | -10 ° | 0 |
| max | 0 ° | 12 ° | 20 ° | 15 ° | 3 |

design space, each generation consisted of 50 individuals, the mutation constant 0.15 and a crossover probability value of 0.7 were used. During each generation two elite individuals were selected for passing to the next generation. Totally 4 ANN modules were trained and tested to predict the 4 outputs. An aero-structural optimization is done based on the above mentioned ANN metamodel, the optimum proposed by the optimizer (GA+ANN) was analyzed with the high fidelity CFD and FEM simulations. The mathematical form of objective function and constraints are already explained in Sec. 4.5.2.

**Aero improvements**

On the aero-structural multi objective optimization, the aerodynamic objective is to increase the total to total efficiency and it is penalized by mass flow rate and first fundamental frequency (Eq.4.5). The optimization is carried out for the constant operating conditions i.e inlet and exit boundary conditions, rotor speed is fixed and mass flow rate is allowed to increase within 0.5%. Very few flow simulations were used to build the aero database. The lower and upper bounds of the design variables are given in Table 4.7.

The above mentioned methodology was applied to redesign the E/TU-3 turbine stage. The initial and optimum design variables are given in Table 4.7. The aero structural optimization cycle was carried out and the proposed optimum configuration was simulated in CFD to confirm the optimizer results. The efficiency

Table 4.8: Comparison of original and optimum objectives and constraints

| Case | $\eta_{tt}$ | change | $\dot{m}$ | $\sigma_{vm}$ | change | $\omega_1$ |
|---|---|---|---|---|---|---|
| E/TU-3 | 87.53 | 0.8 % | 0.3347 | 287.1 | 48.68 % | 2273 |
| Optimum | 88.20 | | 0.3357 | 147.4 | | 2390 |

increased from 87.5% to 88.2%, see Table 4.8. The redesigned rotor has a forward lean and sweep (in the direction of the rotation) Fig. 4.18. The stacking lines for the original and optimum configurations are shown in Fig. 4.19.a and Fig. 4.19.b, which clearly indicates the change in lean and sweep angles for the optimum shapes from the initial E/TU-3 rotor. As expected the magnitude of the bowing intensity is negligible. The increase in efficiency is mainly due to the decrease in secondary losses associated with the large flow turning and thick leading edges [67].

The blade lean and sweep change the blade spanwise loading. Leaning towards the direction of rotation (i.e suction side) will unload the tip and increase the loading at the hub and vice versa. The effect of this can be seen in Fig. 4.20 and Fig. 4.21 which basically explains the change in pressure coefficient at different radial locations. Hence the original separation region near the hub-SS corner was reduced in the redesigned stator, see Fig. 4.24.a. Moreover the Mach number level in the redesigned stator is reduced near the hub hence reducing the sonic region and associated total pressure loss and increasing the stage efficiency. Change in blade loading also modifies the velocity triangles. During the initial analysis it was assumed that the change in velocity triangles at the inlet and exit were not due to lean and sweep. But, it was observed that the combined lean and sweep can change the spanwise distribution of axial velocity and flow angles. The effect of lean and sweep on the exit flow angle distribution in the radial direction is shown in Fig. 4.22. Increasing the axial velocity indicates an increase in loading at the mid section because of the higher circumferential velocity at that section. This change in loading

is also reflected in the spanwise distribution of incidence angle, see Fig. 4.25.a. and axial velocity distribution in the radial direction at the rotor exit as shown in Fig. 4.23. The optimum rotor has a lower incidence near the hub and a higher incidence near the tip. Unloading the tip reduces the vortices intensity (loses) and directly increases the efficiency of the rotor.

Restacking of the profiles also redistributed the stage loading as shown in Fig. 4.26. The stage loading near hub and tip has not changed between the optimum and original stages. This is because the blade loading and mass flux balance each other at these regions, see Fig. 4.25.a and Fig. 4.25.b. Near the hub there is a lower incidence in the optimum case but higher mass flux at rotor inlet. This trend is reversed near the tip.

It should be noted that an increase in the rotor lean would further improve the aerodynamic performance [19], however such an increase would be in conflict with the structure objective. Further Arabnia *et al.* [19] also gives detailed physical interpretations of the effects of lean, sweep and bowing intensity on the blade efficiency.

**Structural improvements**

The E/TU-3 turbine blade is thicker at the root and tapered from hub to tip to reduce mass and hence the centrifugal stresses. The main component of stress in a turbine blade is due to blade rotation rather than aerodynamic forces but for a compressor the aerodynamic loads play an important role in the overall blade stress and blade rotation. Further, high blade stiffness in turbine blades helps to minimize the stress due to pressure forces. For the current work only centrifugal force is considered for stress analysis. The computational time required for ANSYS to simulate a single static stress simulation is less than 2 minutes on a single desktop PC, which is very cheap compare to the time taken to solve a single CFD simulation.

Table 4.9: Comparison of average von Mises stress at different surfaces of the original and optimum blades.

| Surface Type | E/TU-3(MPa) | Optimum(MPa) | % change |
|---|---|---|---|
| Hub | 9.982 | 9.1863 | -8 |
| Pressure | 10.646 | 6.7546 | -36 |
| Suction | 7.7614 | 8.6659 | +11.65 |

Figures 4.27, 4.28, and 4.29 compare the von Mises stress distribution of the initial and optimized configurations. On the initial configuration the maximum stress occurs at the root of the blade near the trailing edge because of the lowest thickness distribution and due to straightening of the blade because of centrifugal forces. The root is fixed which also results in a high stress concentration at the hub trailing edge. The optimum blade has a combined lean and sweep with a negligible bowing intensity, which basically changes the center for mass, as well as the tangential and axial moments. The increase in tangential moment due to lean is effectively handled by the blade spanwise thickness distribution. Due to the shift in center of mass and the change in moments, the trailing edge untwisting effect is reduced and the resulting maximum stress is 45% less compare to original von Mises stress. Location of the maximum stress (with less intensity) also shifts from hub trailing edge location to the suction side maximum thickness location Fig. 4.29, and no longer hub trailing edge (minimum thickness area) is considered critical from the stress point of view. To understand the overall effect of lean and sweep, von Mises stress was averaged on the pressure, suction and hub surfaces using ANSYS APDL programming and the averaged values are given in Table 4.9. Due to lean, the stress on the suction side of the blade increases up to 11% but this is effectively handled by the blade thickness distribution. The design speed of the turbine is $7800RPM$ which is lower compare to current high speed turbine stages, so the improvements achieved are highly problem dependent.

Table 4.10: Multi objective aero-structural optimization - Optimum design variables, objectives and constraints

| Case | $\alpha_r$ | $\beta_r$ | $\gamma$ | $w_1$ | $Y_r$ | $\sigma_{vm}$ | $\omega_1$ | $\dot{m}$ |
|---|---|---|---|---|---|---|---|---|
| Original | 0° | 0° | 0 | 0 | 0.1854 | 175.94 | 2292.9 | 0.3205 |
| Optimum | 11.8605° | 2.1461° | 0.0075 | 0.782 | 0.1671 | 111.3 | 2460 | 0.3206 |
| min | −5° | −10° | 0 | 0.2 | – | – | – | – |
| max | 20° | 15° | 3 | 0.8 | – | – | – | – |

## 4.7. E/TU-3 turbine blade row optimization

### 4.7.1 Single point multi objective aero-structural optimization of E/TU-3 turbine blade row

This case was mainly carried out to identify the effect of non uniform inlet conditions (aerodynamic) on the blade optimum shape and design variables. Optimization of turbine stage carried out in the previous Sec. 4.6.3 contains only five design variables in which three design variables (lean, sweep and bowing intensity) controls the turbine stacking line but inclusion of non uniform inlet conditions automatically necessitates the need for an additional design variable i.e location of the bowing in the radial direction. Section 3.3 explains in detail the sensitivity analysis carried out in finalizing the most effective design variables affecting the aerodynamic and structural objectives and constraints. The location of the bowing in the radial direction is one of the main parameter which controls the blade shape according to the non uniformity in the inlet conditions, moreover it also affects the structural stress and natural frequencies.

#### Aerodynamic improvements

The original and optimum rotor blade shapes are shown in Fig. 4.30. The pressure loss coefficient decreased from 0.1854 to 0.1670, a decrease of 9.8%; the blade has a lean of 11.8°, a sweep of 2.1° (backward sweep) and zero bowing, see Table 4.10. The bowing intensity is zero as a compromise between the selected aerodynamic and the structural

objective functions. This parameter is non zero when considering the aerodynamic optimization only. Further reduction of radial velocity component throughout the flow domain indicates the reduction in secondary velocity in the optimum blade hence more work is extracted from the flow. Also the level of non dimensional secondary vorticity is reduced from 0.9118 to 0.8299. Detailed physical interpretations of the aerodynamic results are given in Arabnia *et al.* [7].

**Structural improvements**

Modification of the stacking line profile changes the structural loading on the blade. The initial ANN database is prepared with 51 sampling points covering the design space. To improve the prediction capability of the ANN model, database enrichment was carried out as explained in Sec. 3.4. During the enrichment process, the optimum candidate obtained at the end of the optimization process is added to the database and the ANN model is retrained with the updated database, according to the optimization cycle shown in Fig. 3.1. The database is enriched until the objective predicted by ANN is better than the previous predictions and also the difference between ANN predicted and high fidelity simulation is getting reduced. Seven cycles of database enrichment were carried out and the reduction achieved in von Mises stress at the end of the enrichment process is 46.5% i.e 94.23 MPa compared to the original E/TU-3 blade stress level of 175.94 MPa. Figure 4.31 shows the convergence of the ANN-based prediction to the CSD-based predictions. For multi-objective optimization, the final ANN model obtained from the enrichment process is selected.

From a structural point, the increase in bowing intensity is always detrimental to the blade structure as it results in high stresses, and the current optimum results clearly confirm this fact. Figures 4.33, 4.34, and 4.32 compare the von Mises stress distribution of the initial and optimized rotor. The same contour range is maintained for all the stress contours to identify the relative stress levels. On the

initial configuration, the maximum stress occurs at the blade root near the trailing edge because of the lowest trailing edge thickness distribution. But on the optimum configuration, the maximum stress occurs on the suction side near the hub maximum thickness area location. Large tensile forces that are developed due to centrifugal forces, tend to straighten the blade and also result in an increased stress level at the blade root. The fixed-root boundary condition results in a high stress concentration at the hub.

The optimum blade has a combined lean and sweep with almost zero bowing intensity, which modifies the center for mass, tangential and axial moments. The change in lean and sweep increases the tangential moment and these changes in structural loading are effectively handled by the available blade thickness distribution along the span. The shift in center of mass and change in moments, the trailing edge untwisting effect is reduced and the resulting maximum stress is reduced by 36.73% compared with the original E/TU-3 blade von Mises stress. The initial and optimum stress values are compared in Table 4.11.

Location of the maximum stress (with less intensity) shifts from hub trailing edge location to the suction side maximum thickness location Fig. 4.32, and no longer hub trailing edge (minimum thickness area) is considered as critical from the stress point of view. To understand the overall effect of lean and sweep, von Mises stress was averaged on the pressure, suction and hub surfaces using ANSYS APDL programming and the averaged values are given in Table 4.12. Due to lean, the average von Mises stress on the suction side of the blade increases by 73% but this is effectively handled by the available spanwise thickness distribution of the blade. Hence the average stress on the hub and pressure surface were reduced by 12% and 3% respectively. This result would be more drastic if this was a high speed turbine stage. As a last comment, the improvements achieved are highly problem dependent, however the optimization methodology will remain the same.

Table 4.11: Original and Optimum output comparisons

| $Case$ | $\sigma_{vm}$ | $\%Change$ | $\omega_1$ | $\%Change$ |
|---|---|---|---|---|
| Original | 175.94 | | 2292.9 | |
| | | 36.7 | | 7.28 |
| Optimum | 111.3 | | 2460 | |

Table 4.12: Surface based comparison of von Mises stress at hub, pressure and suction sides for original and optimum configurations(single and multi objective

| $Surfacetype$ (Stress unit MPa) | $Original$ $(E/TU-3)$ | $Multiobjective$ $Optimum$ | $\%Change$ |
|---|---|---|---|
| Hub | 7.2849 | 6.426 | −11.79 |
| Pressure | 5.93 | 5.7413 | −3.1821 |
| Suction | 6.1425 | 10.652 | +73.4147 |

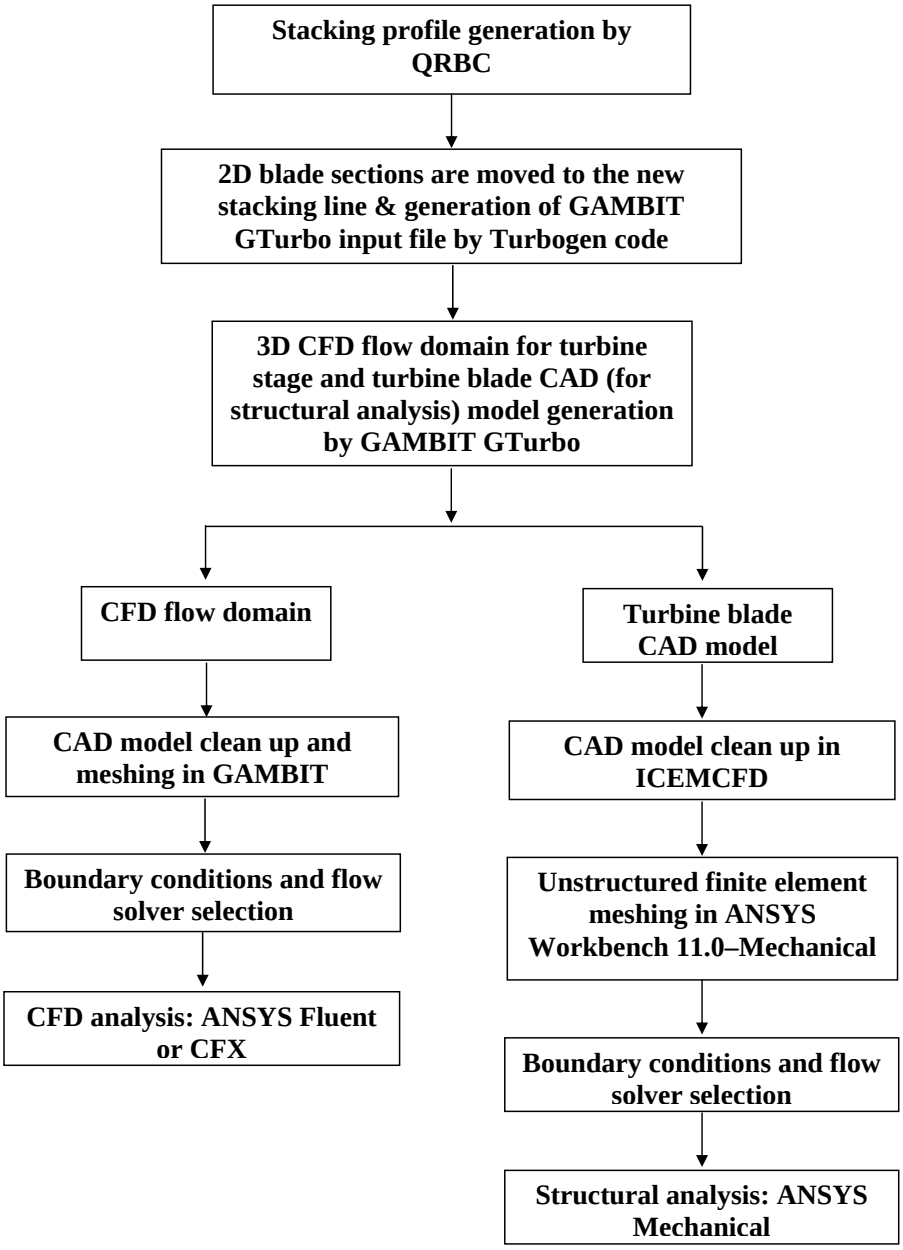


Figure 4.1: Steps in getting the geometry for CFD and FEA

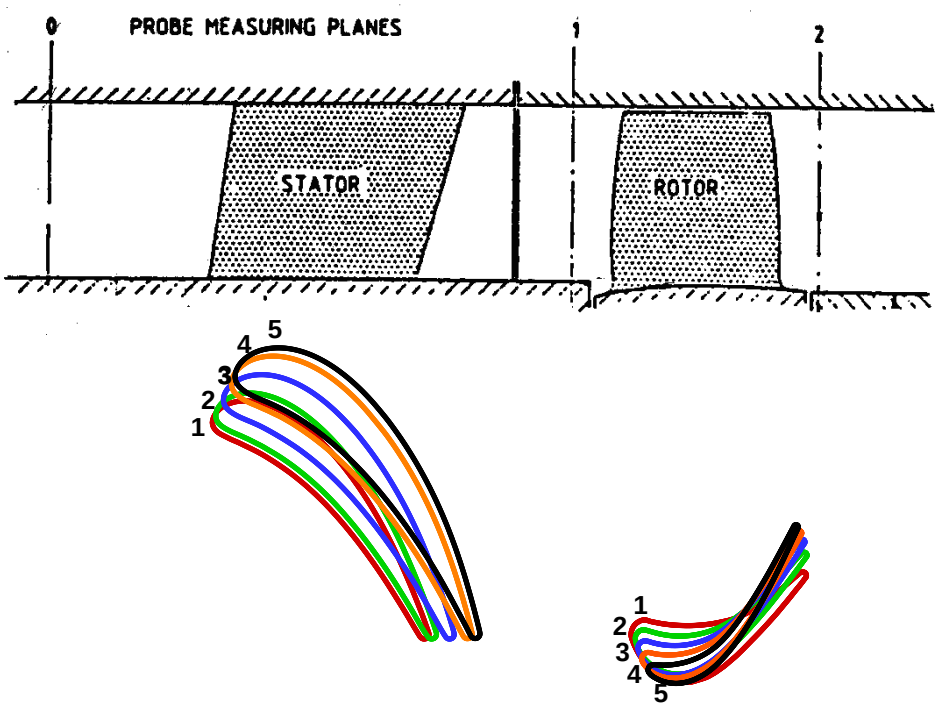


Figure 4.2: E/TU-3 Original geometry [6]

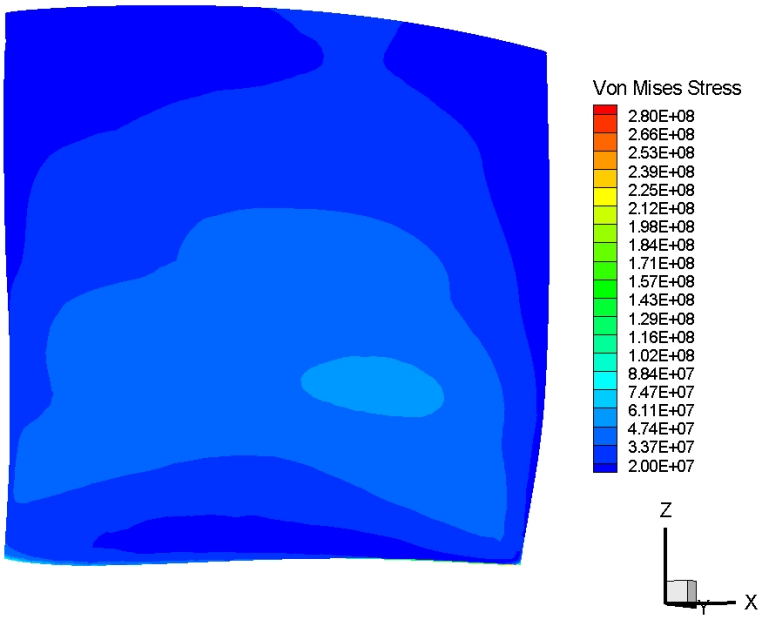


a.Suction side

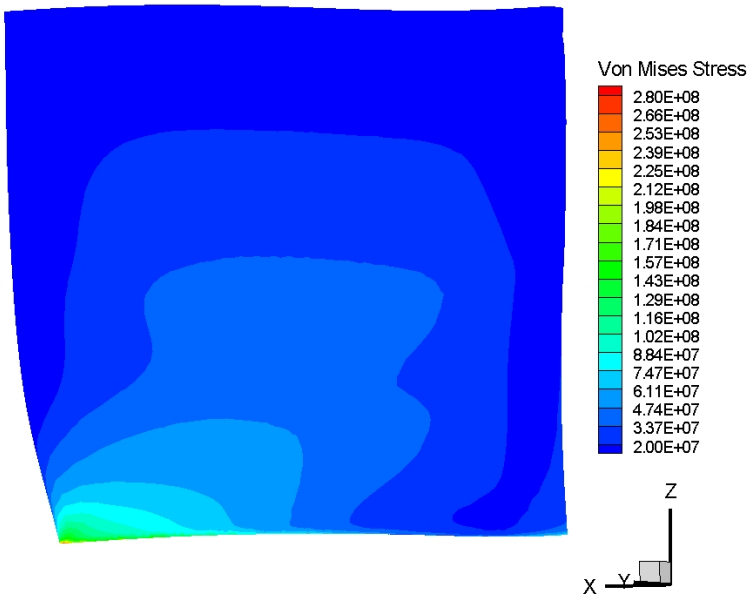


b.Pressure side

Figure 4.3: Stress contours: E/TU-3 Original turbine blade

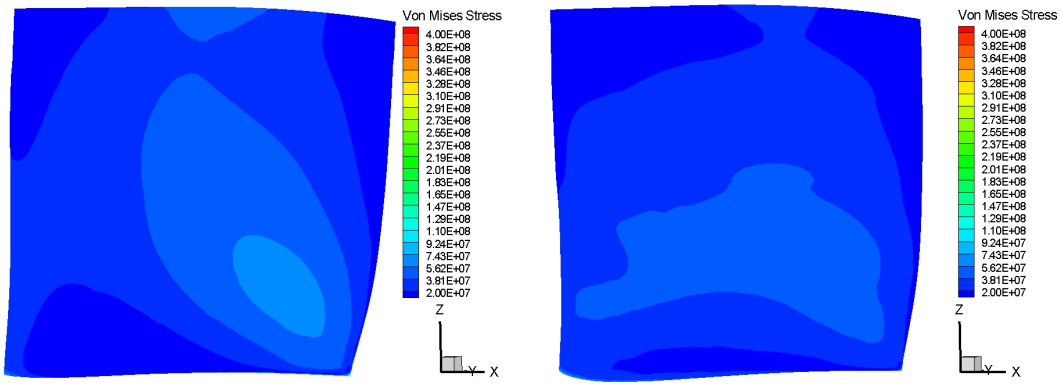


a.Lean $-5^o$b.Lean 0 (E/TU-3)

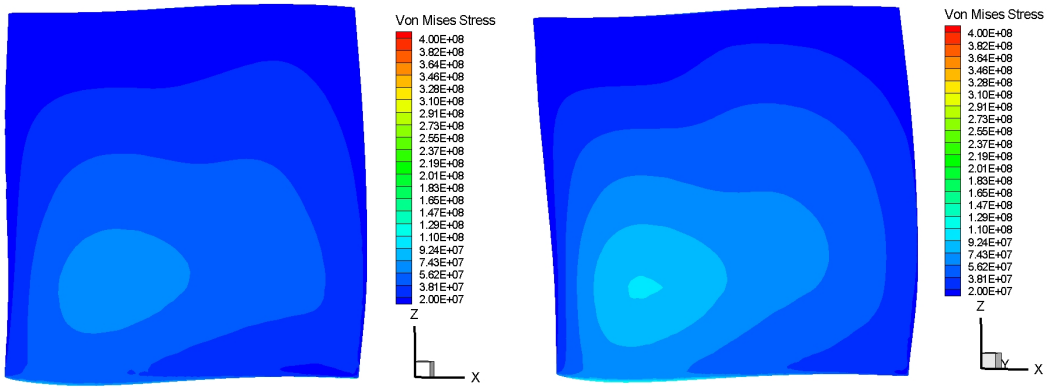


c.Lean $5^o$ d.Lean $10^o$

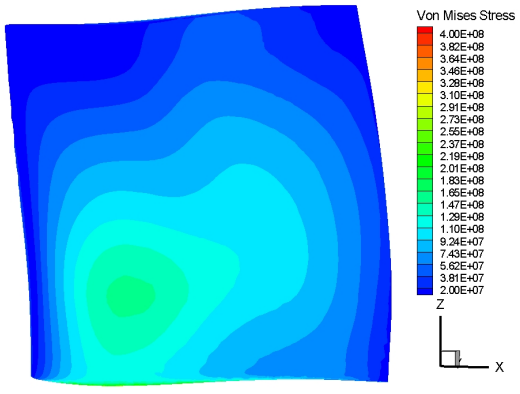


e.Lean $20^o$

Figure 4.4: Suction side stress contours for different lean angles

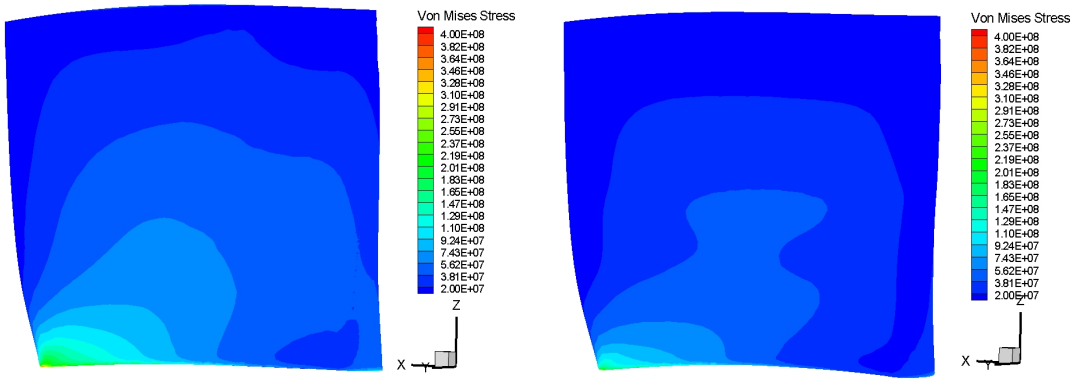


a.Lean $-5^o$b.Lean 0 (E/TU-3)

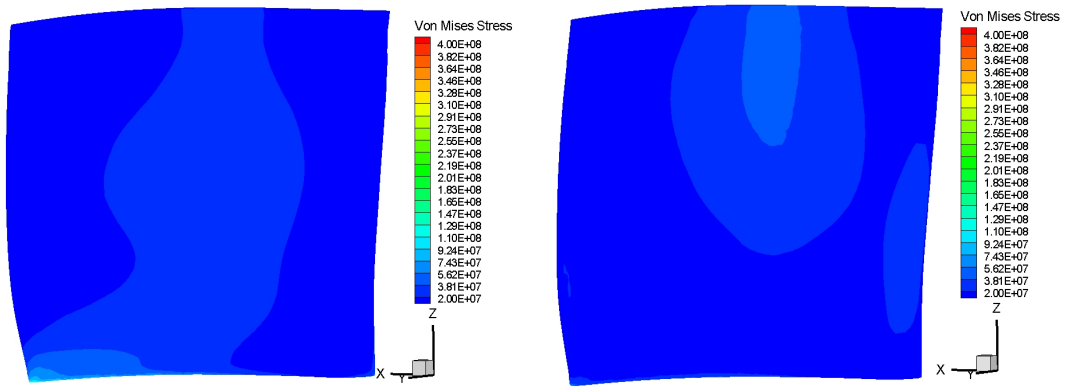


c.Lean $5^o$ d.Lean $10^o$

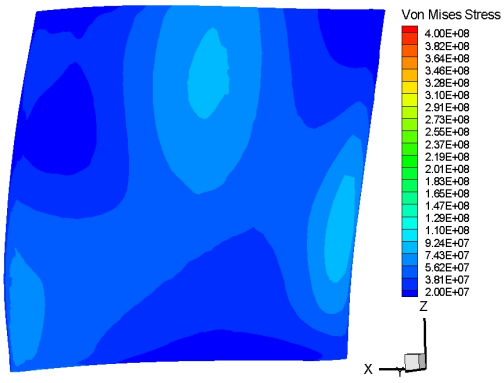


e.Lean $20^o$

Figure 4.5: Pressure side stress contours for different lean angles

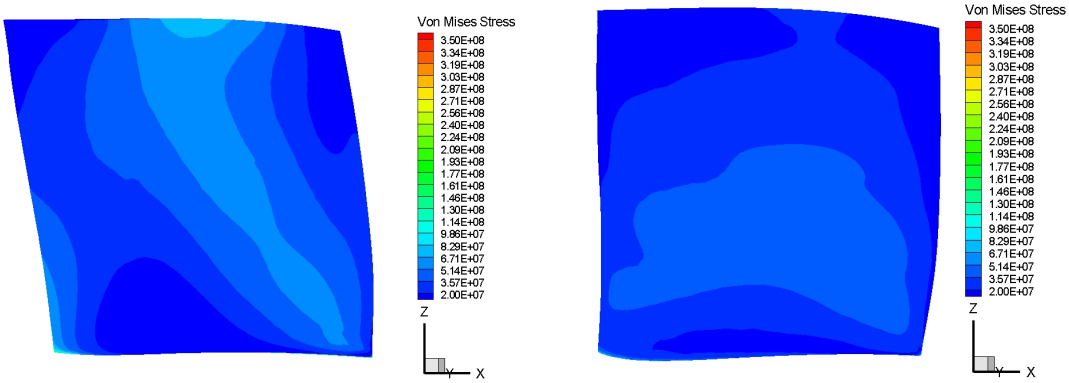


a.Sweep $-10^o$b.Sweep 0 (E/TU-3)

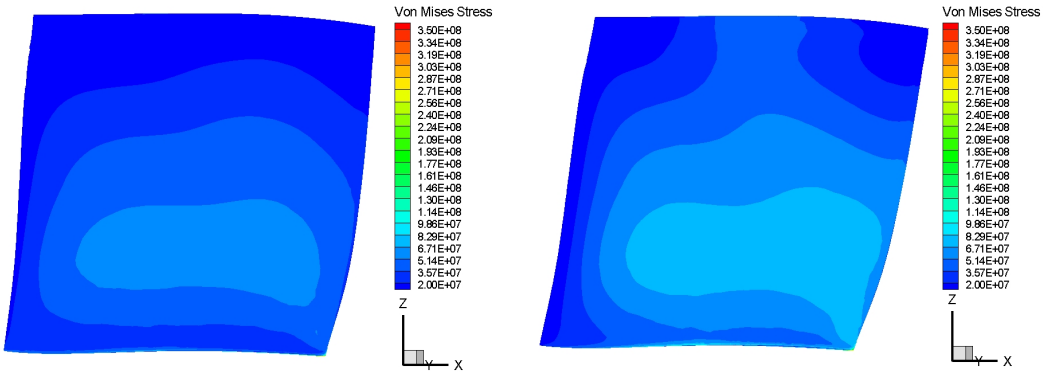


c.Sweep $5^o$ d.Sweep $10^o$

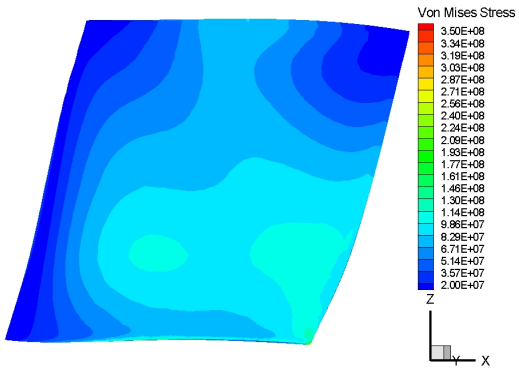


e.Sweep $15^o$

Figure 4.6: Suction side stress contours for different Sweep angles

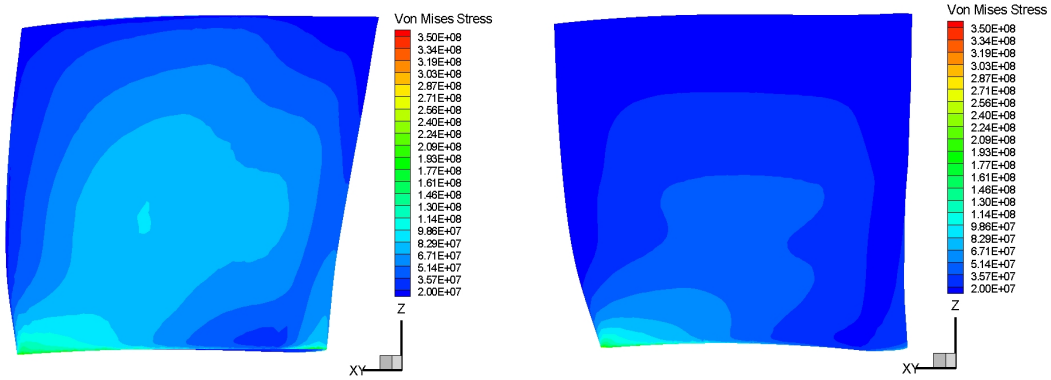


a.Sweep $-10^o$b.Sweep 0 (E/TU-3)

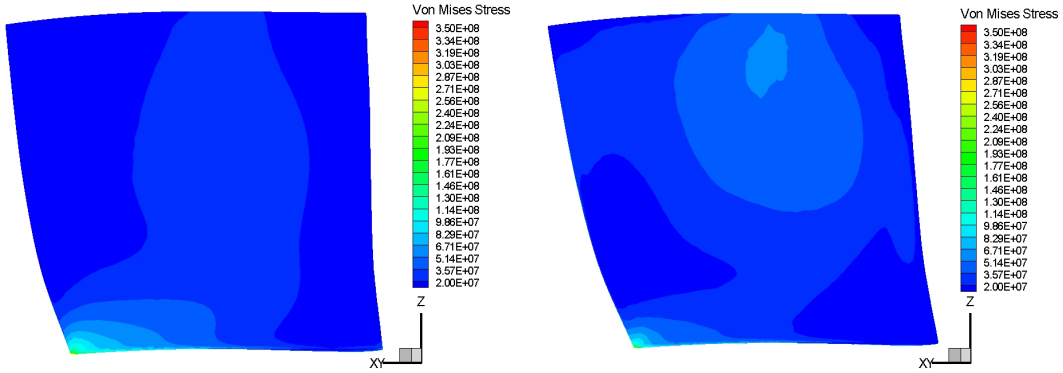


c.Sweep $5^o$ d.Sweep $10^o$

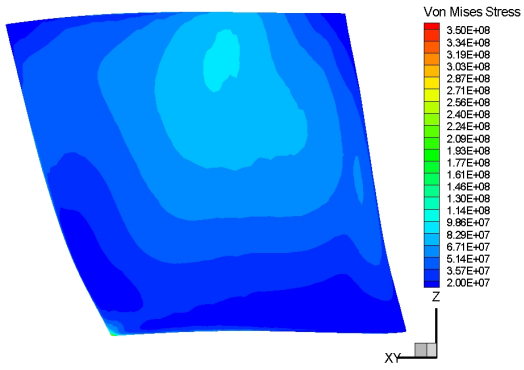


e.Sweep $15^o$

Figure 4.7: Pressure side stress contours for different sweep angles

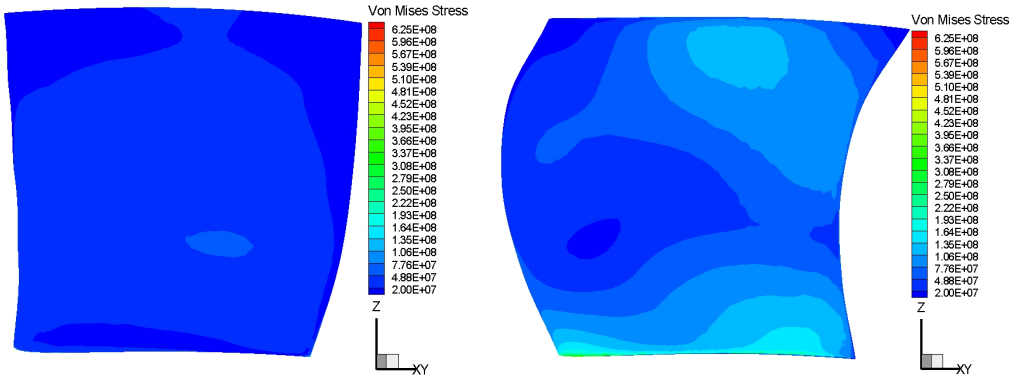


a.Bowing intensity 0 b.Bowing intensity 1

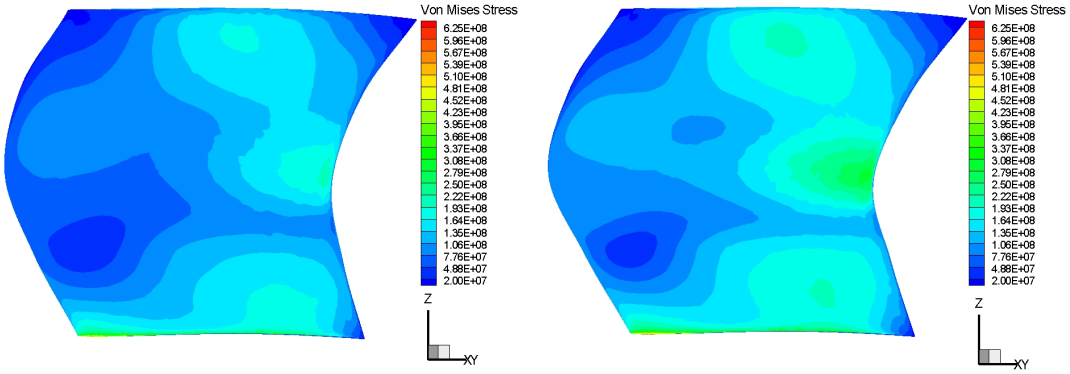


c.Bowing intensity 2 d.Bowing intensity 3

Figure 4.8: Suction side stress contours at different bowing intensity values

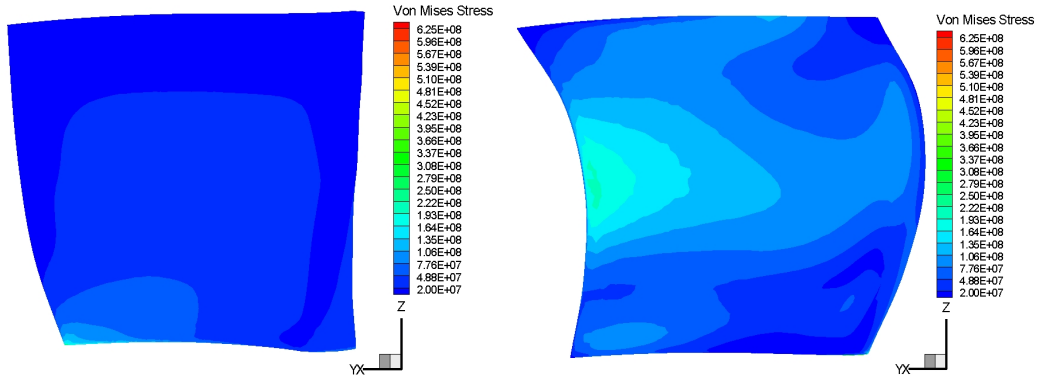


a.Bowing intensity 0 b.Bowing intensity 1

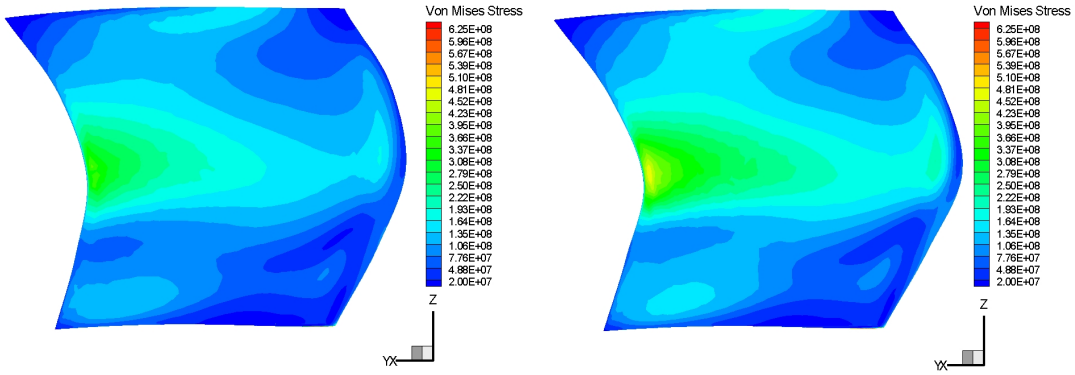


c.Bowing intensity 2 d.Bowing intensity 3

Figure 4.9: Pressure side stress contours at different bowing intensity values

| | $\sigma_{vm}$ | | $\omega_1$ | | $\omega_2$ | | $\omega_3$ | |
|---|---|---|---|---|---|---|---|---|
| | MISO | MIMO | MISO | MIMO | MISO | MIMO | MISO | MIMO |
| Epoch | 45000 | 55000 | 41000 | 55000 | 67400 | 55000 | 73800 | 55000 |
| Scaling | 0 to 1 | | | | | | | |
| Transfer Function | Sigmoid | | | | | | | |
| No of hidden nodes | 30 | | | | | | | |
| LR_IH | 0.67 | 0.83 | 0.5 | 0.83 | 0.23 | 0.83 | 0.75 | 0.83 |
| LR_HO | 0.07 | 0.07 | 0.07 | 0.07 | 0.065 | 0.07 | 0.07 | 0.07 |
| Errors | | | | | | | | |
| ARE | 7.5504 | 8.3351 | 1.0928 | 1.4907 | 0.6743 | 1.5180 | 1.0839 | 1.2983 |
| RMS | 56.6966 | 60.4724 | 27.4969 | 36.7636 | 25.5540 | 64.3925 | 67.1507 | 78.1204 |
| Max Error | 97.9028 | 129.2215 | 59.50148 | 61.8029 | 38.1838 | 133.1623 | 109.9396 | 155.5295 |
| Correlation | 0.9946 | 0.999759 | 0.9955 | 0.9998 | 0.9926 | 0.9998 | 0.9914 | 0.9998 |
| R Squared | 0.9663 | 0.9998 | 0.9835 | 0.9999 | 0.9812 | 0.9998 | 0.9611 | 0.9998 |
| RAAE | 0.1385 | 0.0146 | 0.0945 | 0.0121 | 0.1134 | 0.0115 | 0.1745 | 0.0114 |
| RMAE | 0.3168 | 0.0298 | 0.2781 | 0.0118 | 0.2048 | 0.0243 | 0.3230 | 0.02814 |

MISO - Multi Input Single Output, MIMO - Multi Input Multi Output

Figure 4.10: ANN training parameters and its performance variables (Errors)

| | Training | Testing |
|---|---|---|
| Epoch | 4200 | |
| Scaling | -1 to 1 | |
| Transfer Function | Tangent hyperbolic | |
| No of hidden nodes | 17 | |
| LR_IH | 0.3 | |
| LR_HO | 0.12 | |
| Errors | | |
| ARE | 4.9339 | 6.3833 |
| RMS | 24.92 | 32.754 |
| Max Error | 74.619 | 90.255 |
| Correlation | 0.9628 | 0.9207 |
| R Squared | 0.9227 | 0.8371 |
| RAAE | 0.2138 | 0.2831 |
| RMAE | 0.8323 | 1.1123 |

Figure 4.11: ANN training parameters and its performance variables (Updated errors with 100 sample points)

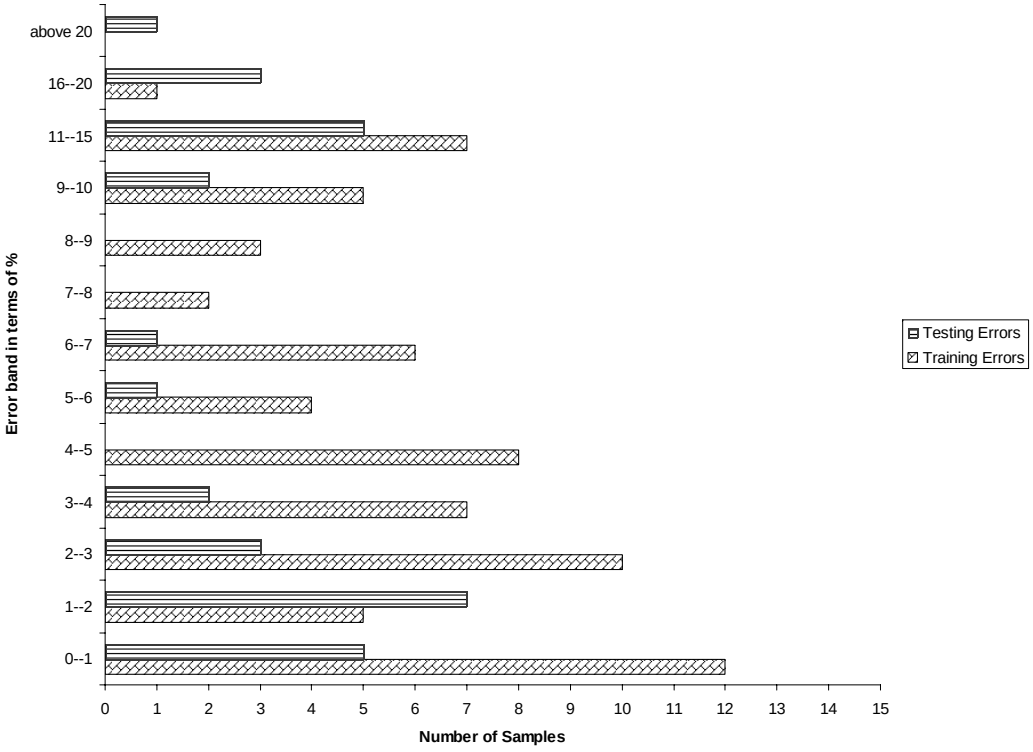


Figure 4.12: ANN training error bands (100 sample points)

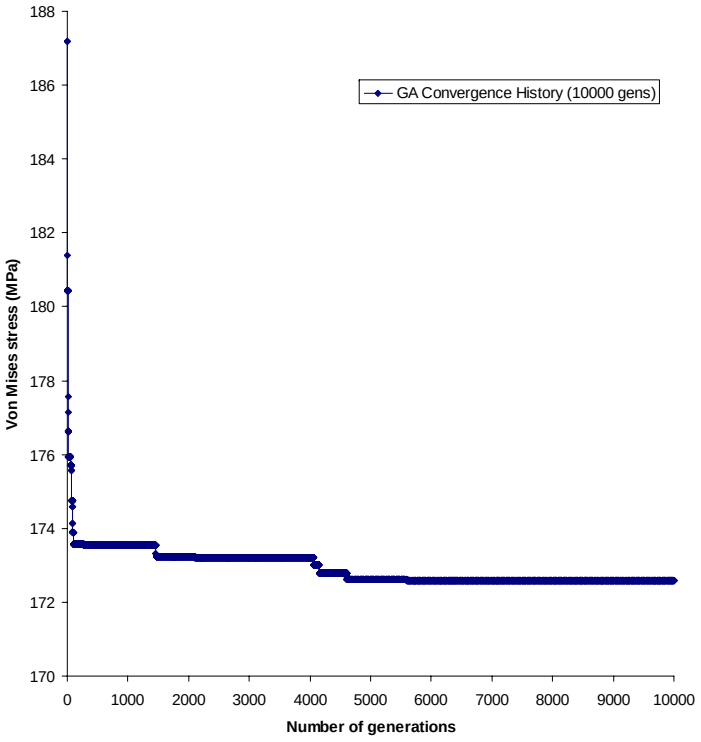


Figure 4.13: Genetic algorithm convergence history

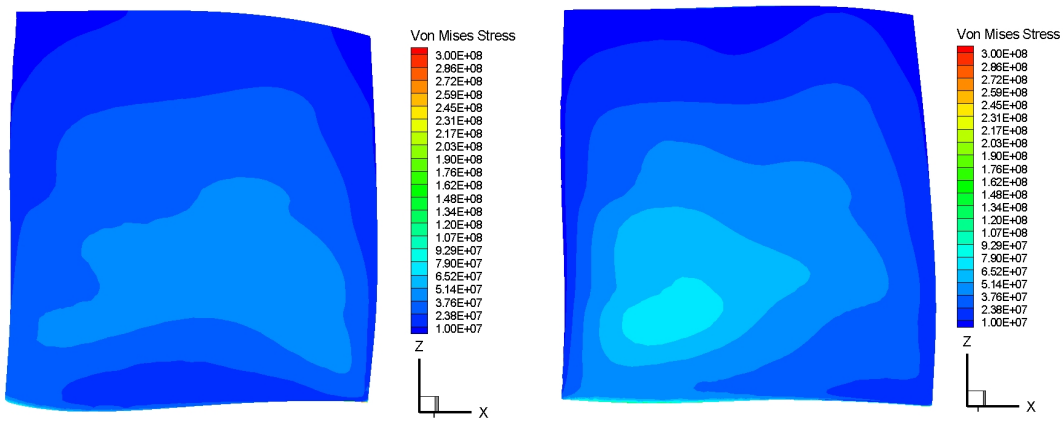


Suction side stress contours a.Initial E/TU-3 b. Optimum blade

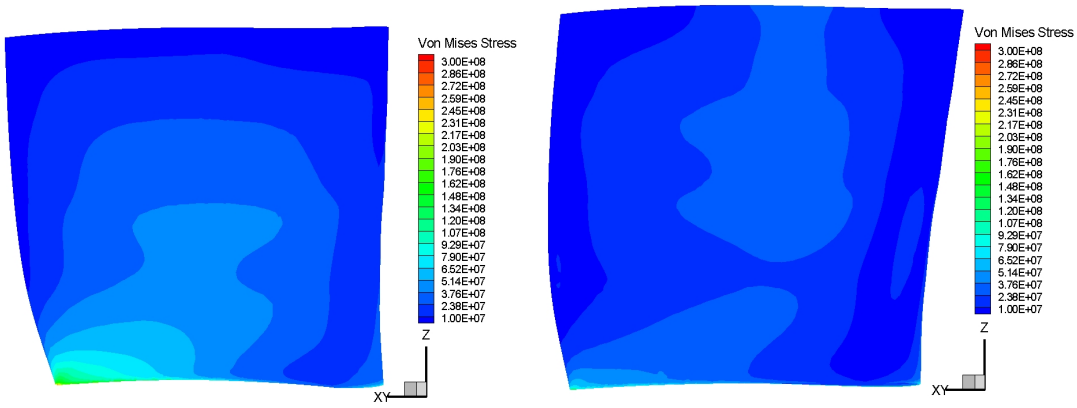


Pressure side stress contours a.Initial E/TU-3 b. Optimum blade

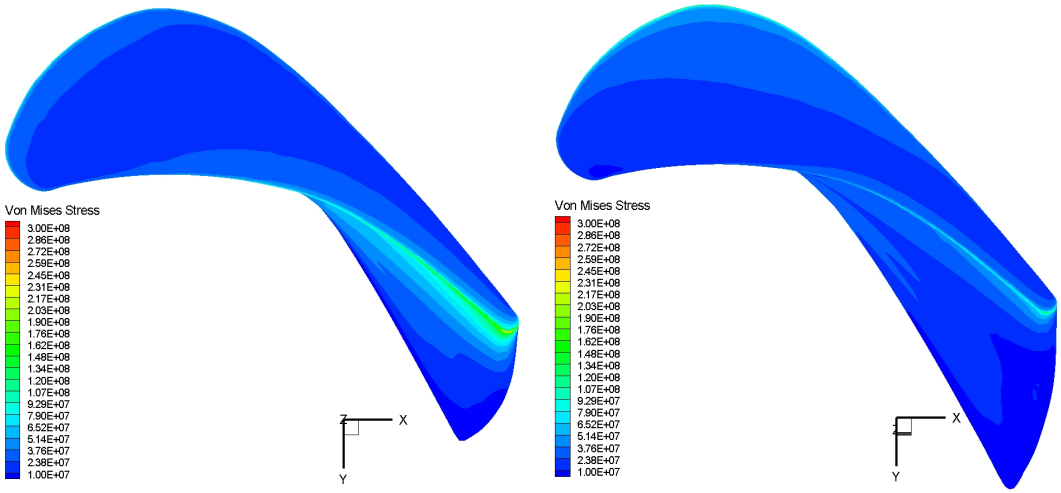


Hub stress contours a.Initial E/TU-3 b. Optimum blade

Figure 4.14: Suction side stress contours at different bowing intensity values

| | Training | Testing |
|---|---|---|
| Epoch | 2200 | |
| Scaling | -1 to 1 | |
| Transfer Function | Tangent hyperbolic | |
| No of hidden nodes | 10 | |
| LR_IH | 0.3 | |
| LR_HO | 0.12 | |
| Errors | | |
| ARE | 4.7648 | 7.7474 |
| RMS | 20.517 | 38.231 |
| Max Error | 49.177 | 85.774 |
| Correlation | 0.9752 | 0.9106 |
| R Squared | 0.9501 | 0.8136 |
| RAAE | 0.1755 | 0.3243 |
| RMAE | 0.5356 | 0.9686 |

Figure 4.15: ANN training parameters and its performance variables (Errors)(updated with 103 sample points)

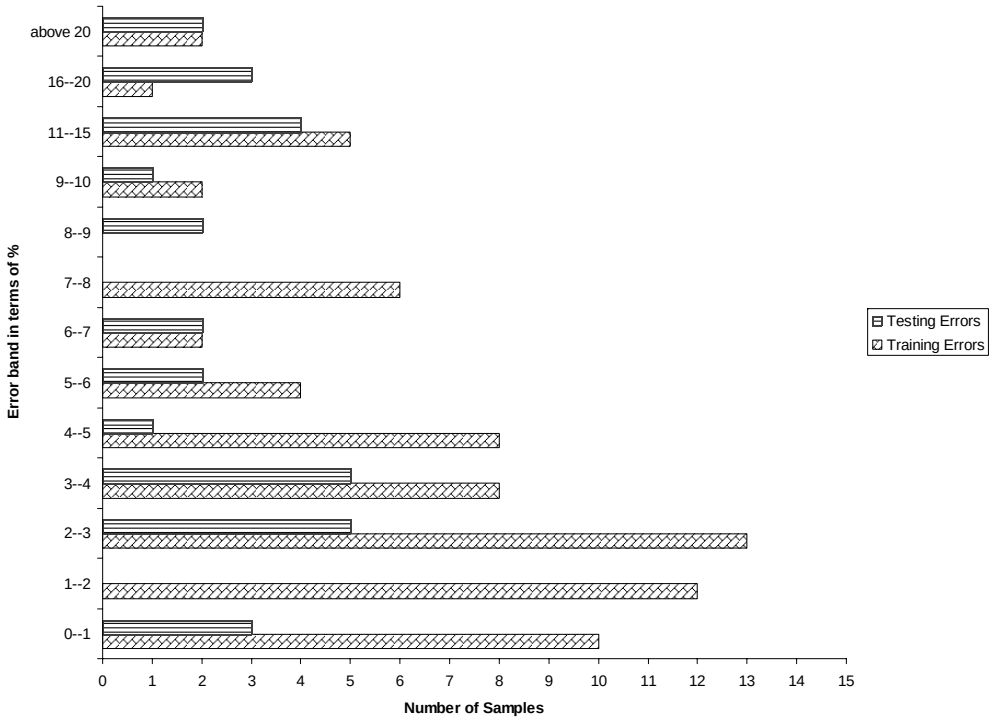


Figure 4.16: ANN training error bands (103 sample points)

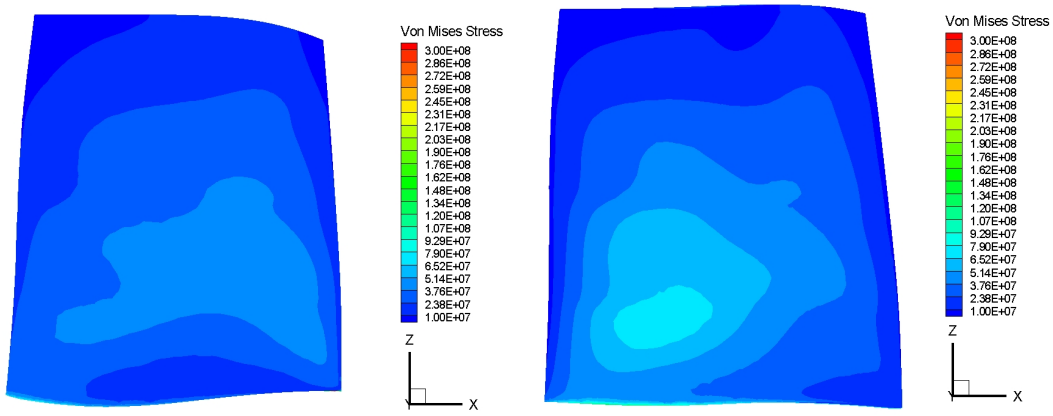


Suction side stress contours a.Initial E/TU-3 b. Optimum blade

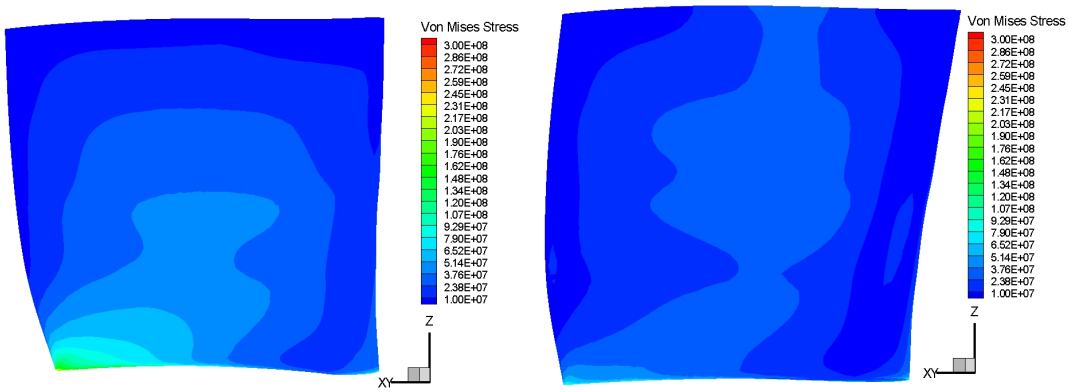


Pressure side stress contours a.Initial E/TU-3 b. Optimum blade

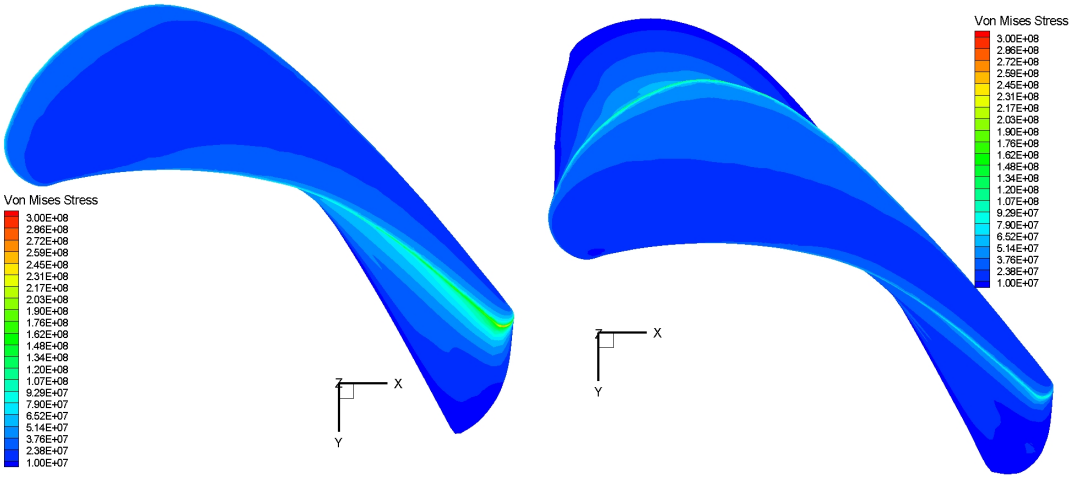


Hub stress contours a.Initial E/TU-3 b. Optimum blade

Figure 4.17: Suction side stress contours at different bowing intensity values

a.Stator view

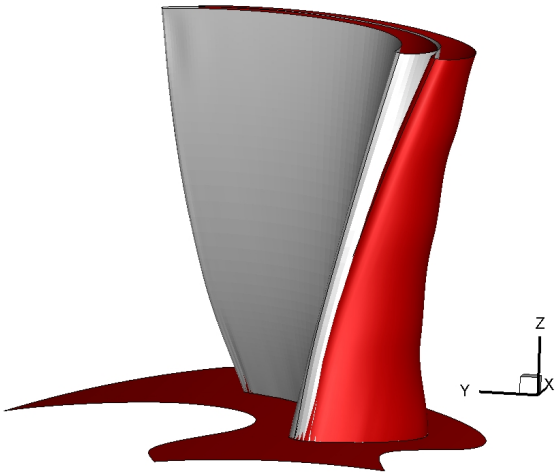


b.Rotor view

Figure 4.18: Stacking of the optimum blade (Initial E/TU-3 shown by wire frame)

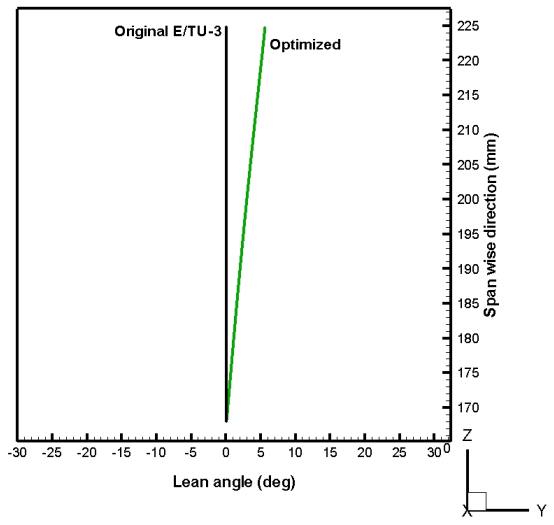


a.Lean angle (in the direction of rotation)

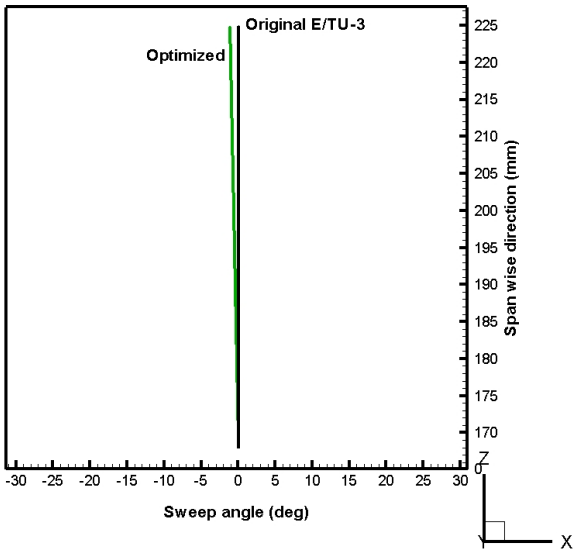


b.Sweep angle (in the axial direction)

Figure 4.19: Original and optimized stacking line representations

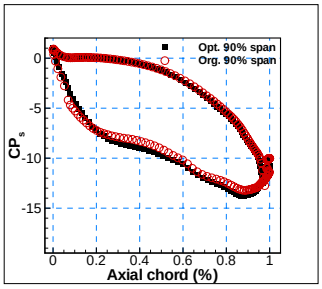


a.10 % span

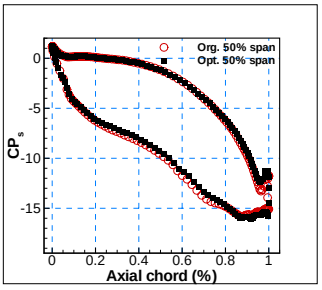


b.50 % span

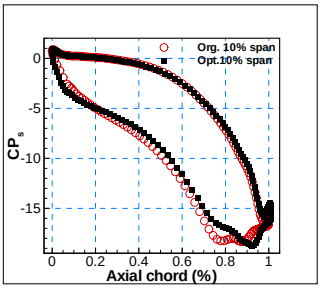


b.90 % span

Figure 4.20: Distribution of stator pressure coefficient at hub, mid-span and tip

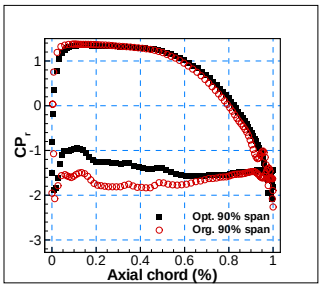


a.10 % span

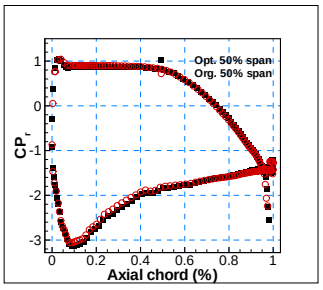


b.50 % span

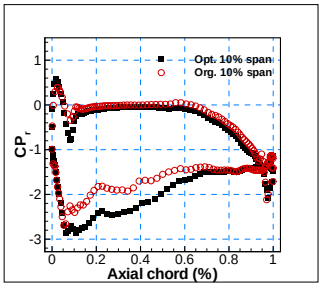


b.90 % span

Figure 4.21: Distribution of rotor pressure coefficient at hub, mid-span and tip

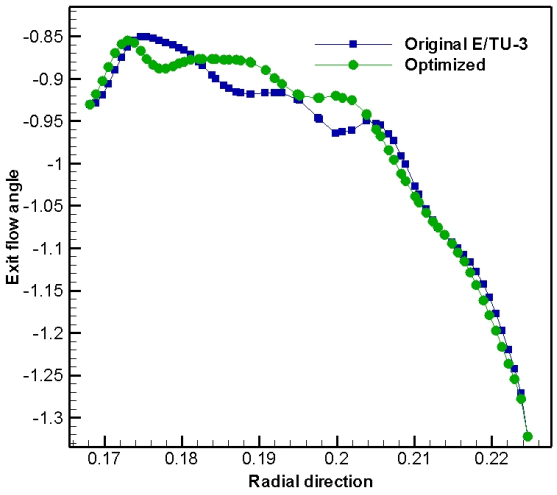


Figure 4.22: Exit flow angle comparison

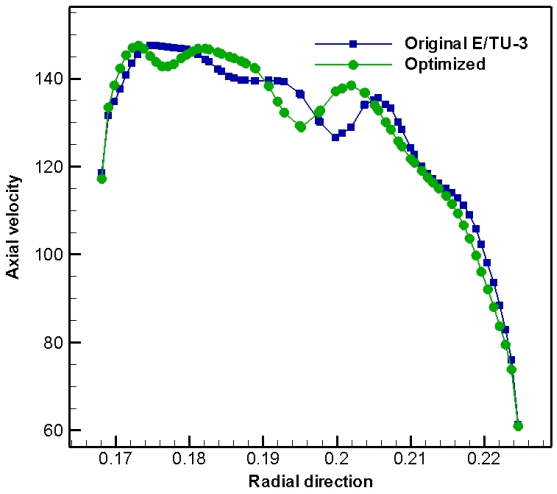


Figure 4.23: Axial velocity comparison

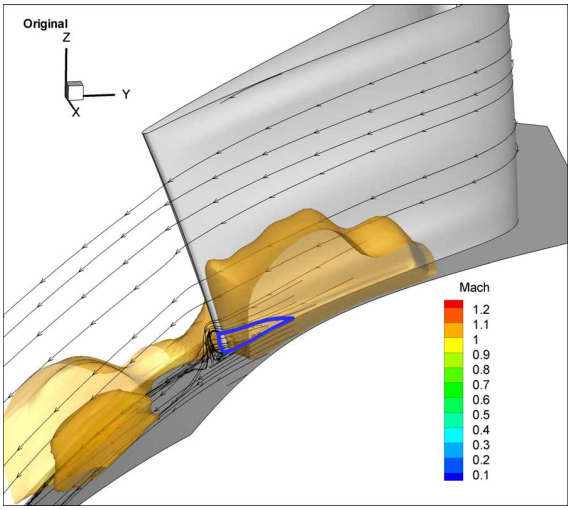


a. Original stator

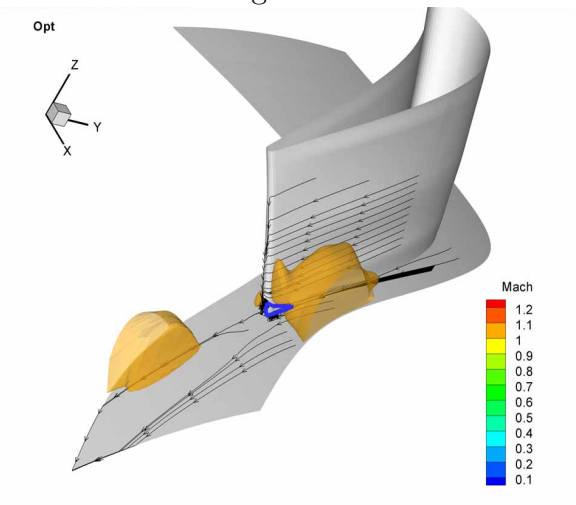


b. Optimum stator

Figure 4.24: SS flow separation and sonic surface for original & optimum stators [7]

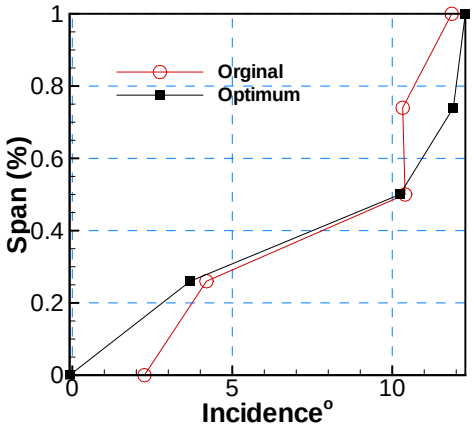


a. Incidence

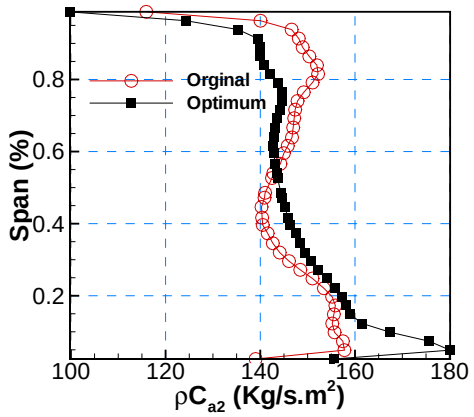


b. Mass flux

Figure 4.25: Spanwise distribution of original and optimum incidence and mass flux [7]

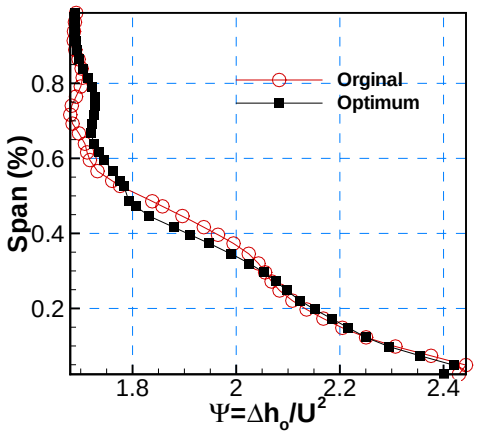


Figure 4.26: Spanwise distribution of stage loading [7]

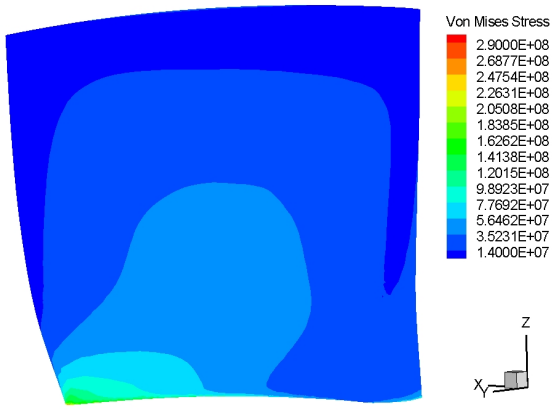


a. E/TU-3 (Original)

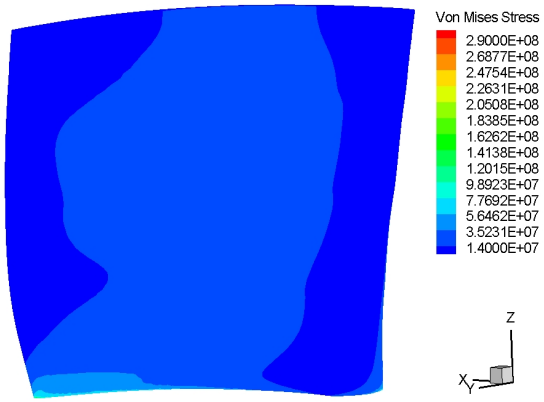


b. Optimized

Figure 4.27: Pressure side von Mises stress contour comparison

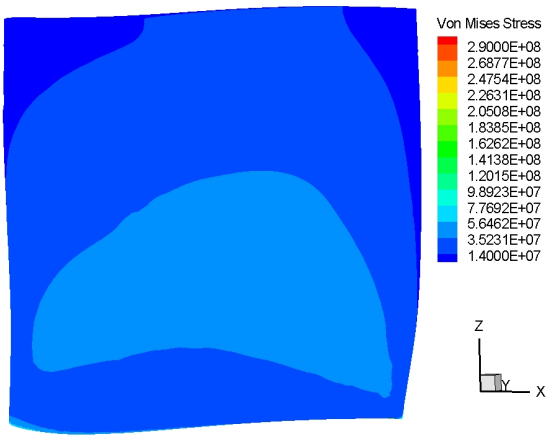


a. E/TU-3 (Original)

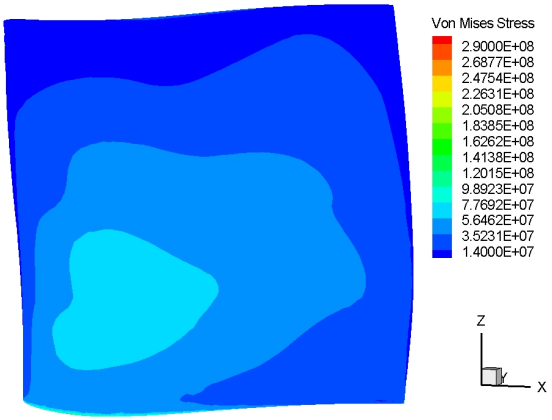


b. Optimized

Figure 4.28: Suction side von Mises stress contour comparison

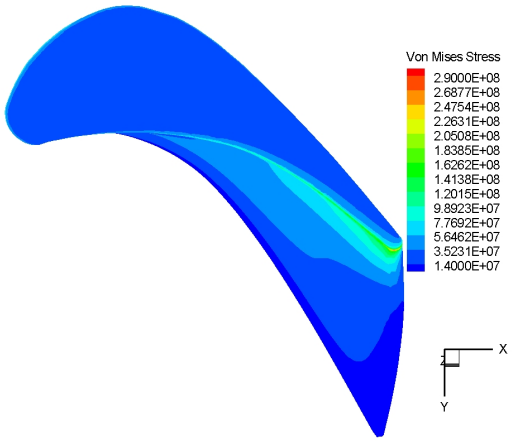


a. E/TU-3 (Original)

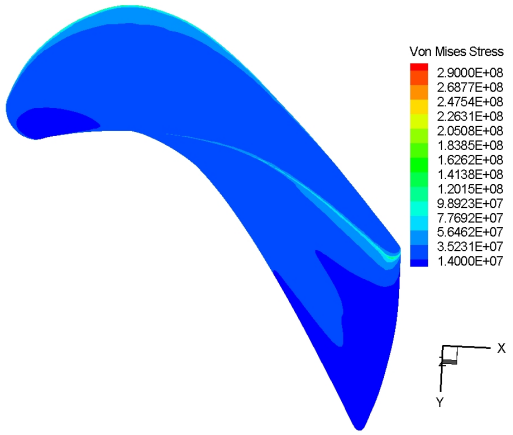


b. Optimized

Figure 4.29: Hub von Mises stress contour comparison

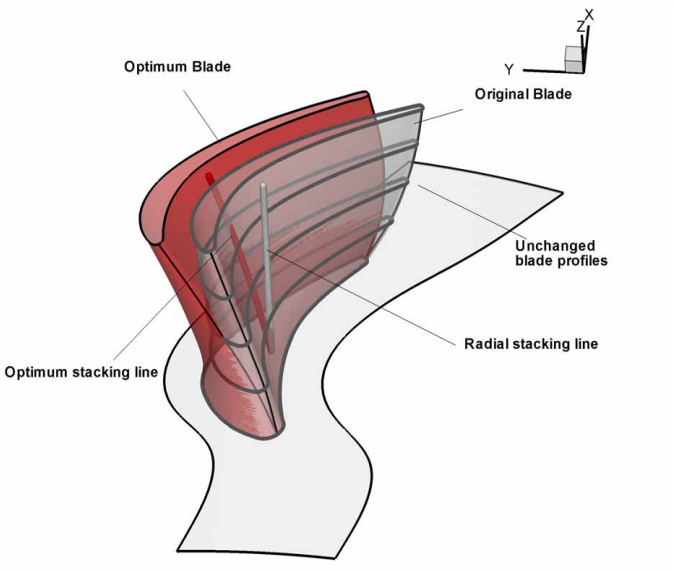


Figure 4.30: Original and optimum blade shapes

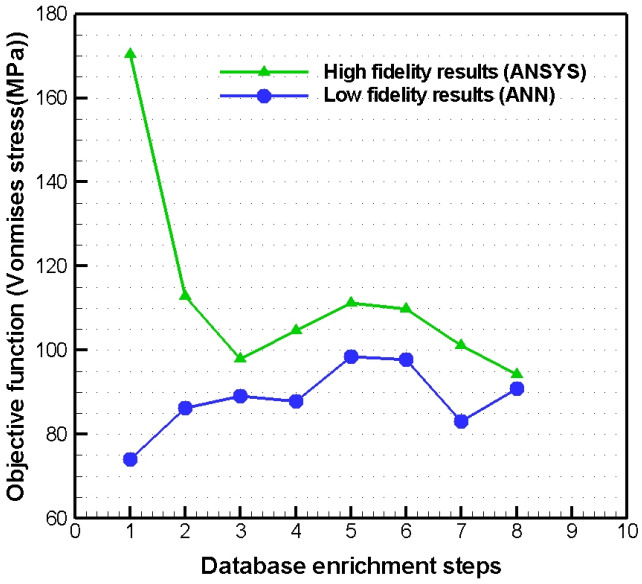


Figure 4.31: Database enrichment

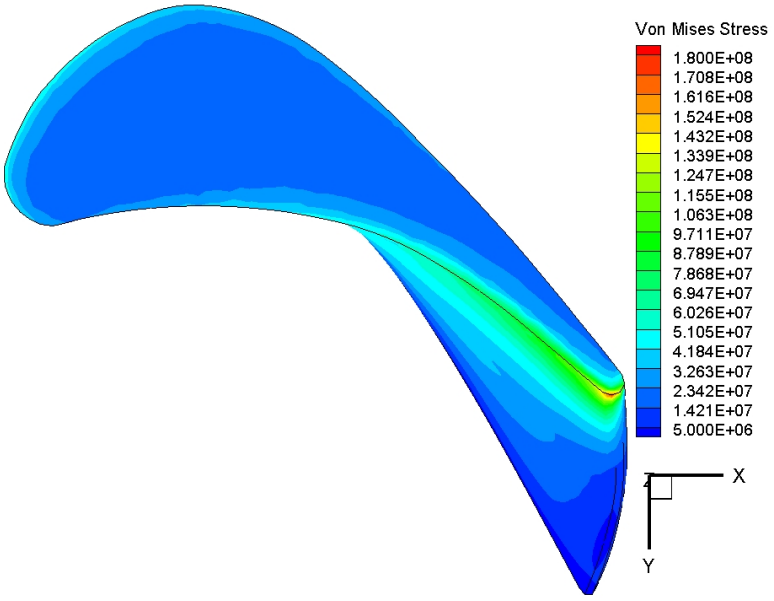


a. E/TU-3 (Original)

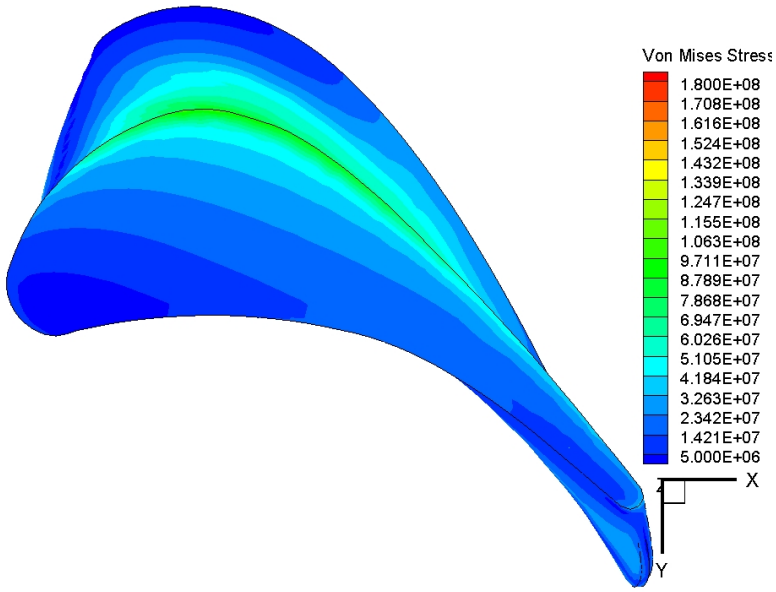


b. Optimized

Figure 4.32: Comparison of stress contours on the hub surface

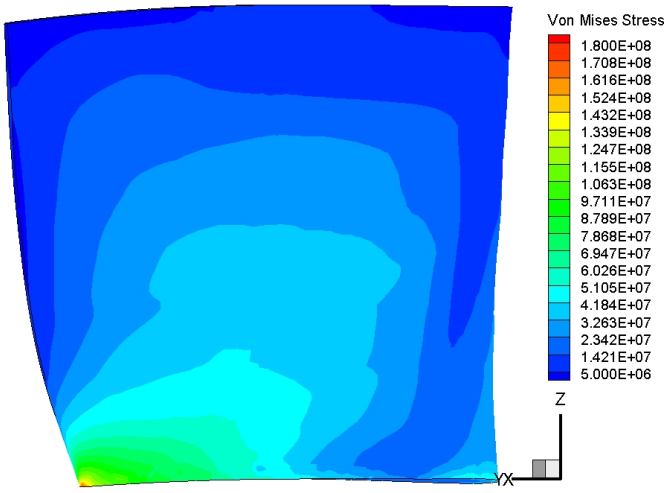


a. E/TU-3 (Original)

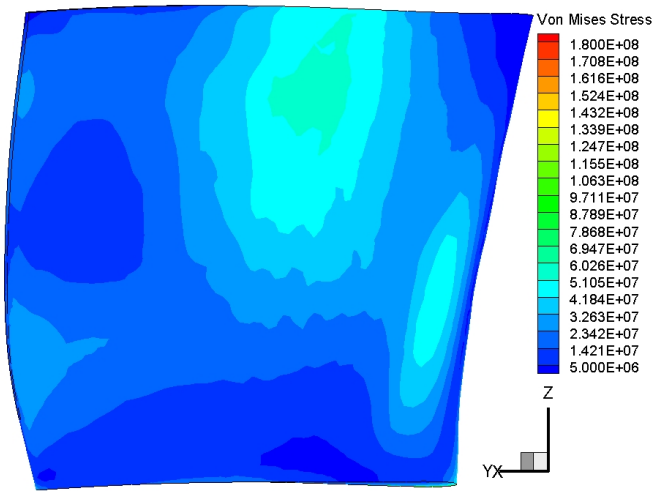


b. Optimized

Figure 4.33: Comparison of stress contours on the pressure surface

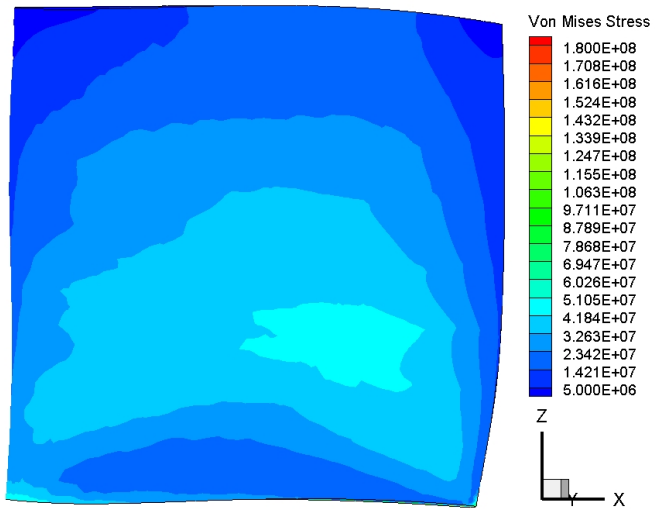


a. E/TU-3 (Original)

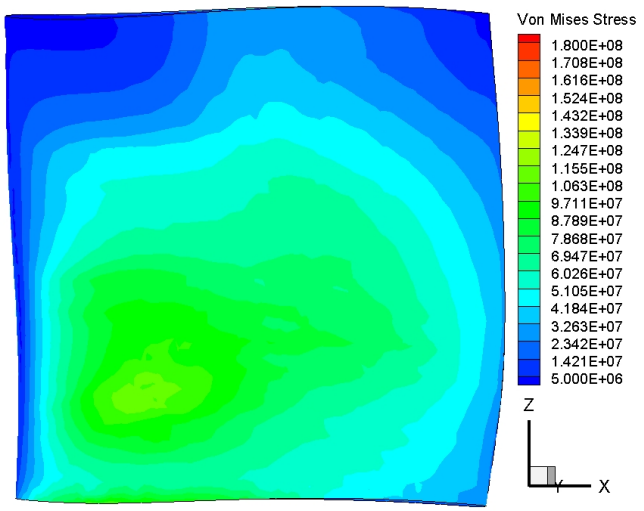


b. Optimized

Figure 4.34: Comparison of stress contours on the suction surface

# Chapter 5

# Conclusion

## 5.1. Summary

A structural shape optimization method was successfully developed, implemented and tested. Further, a multiobjective aero-structural optimization strategy has been developed by integrating the aerodynamic and structural disciplines. The aero-structural optimization methodology was successfully applied to redesign a turbine stage with the objective of improving the aerodynamic efficiency and minimizing the maximum operating stress. The optimizer is a combination of GA, multiple ANN, and have an option to include other response surface models such as RBF. In the process of approximating the design space by ANN (RSM), each output variable is approximated by an individual ANN. The addition of this technique to the optimizer greatly improved the accuracy of the response surface model in addition to giving complete control over the metamodel errors, handling different design variables and disciplines. The blade design variables are the blade lean and sweep and the bowing intensity, they are derived from QRBC parametrization scheme which helps to control and represent the stacking curve very effectively. The optimization of the E/TU-3

turbine stage is achieved with just 5 design variables controlling the shape of the stator and rotor blades. Finally, a highly flexible and robust optimization procedure was developed and tested. The notable improvements obtained from aerodynamic and structural performance demonstrates the robustness and accuracy of the optimizer as well as the developed methodology. The applicability and the way in which design variables are handled could be different for different problems, therefore care should be taken to fine tune the procedure according to the problem at hand.

## 5.2. Future work

- The current optimization procedure could be applied to optimize a compressor stage, which is probably more challenging and complex.

- In the current work, the turbine weight was not considered as an objective because the 2D airfoil profiles were fixed. A parameterization scheme such as the MRATD model [68] could be used in the optimization process, to include weight of the blade as an objective function. This will make the optimization space more complex but it may result in an innovative shape.

- Addition of manufacturing constraints to the optimization problem would add an interesting dimension to the optimization problem and would make the problem more attractive to the industries.

- The current optimization work is a combination of aerodynamic and structural disciplines however the methodology has the ability to handle other disciplines like heat transfer with cooling holes, blade life optimization, end wall contouring, and tip clearance could be added to the current aero-structural optimization process. This could result in a more comprehensive, a complete optimization tool which could be applied to many turbomachinery designs.

# Bibliography


[1] http://www.neuralpower.com/technology.htm.

[2] http://www.en.wikibooks.org.

[3] http://www.interwet.psu.edu/chapter4.htm.

[4] H. Adeli and M. Wu, "Regularization neural network for contruction cost estimation," *Journal of construction engineering and management*, 1998.

[5] M. Arabnia and W. Ghaly, "A strategy for multi-objective optimization of turbine stages in three-dimensional flow," *AIAA-2008-5808*, 2008.

[6] L. Fottner, *Test cases for computation of internal flows in aero engine components.* AGARD - AR - 275, Propulsion and Energetics Panel, 1990.

[7] V. K. Sivashanmugam, M. Arabnia, and W. Ghaly, "Aero-structural optimization of an axial turbine stage in three-dimensional flow," *Proceedings of ASME Turbo Expo 2010 Power for Land, Sea and Air, Glasgow*, 2010.

[8] I. Kroo, "Aeronautical applications of evolutionary design," *VKI Lecture series on Optimization methods & Tools for Multicriteria Multidisciplinary Design, Nov 15-19*, 2004.

[9] J. Sobieszczanski-Sobieski and R. T. Haftka, "Multidisciplinary aerospace design optimization: Survey and recent developments," *AIAA paper*, 2002.

[10] A. Oyama, M. S. Liou, and S. Obayashi, "Transonic axial flow blade shape optimization using evolutionary algorithm and three dimensional naviers-stokes solver," *AIAA Paper 2002-5642*, 2002.

[11] T. T. Mengistu and W. Ghaly, "Aerodynamic design of gas turbine cascades using global optimizers and artificial neural networks," *ICCFD3, Jul.*, 2004.

[12] Y. Lian and M. S. Liou, "Multiobjective optimization using coupled response surface model and evolutionary algorithm," *AIAA Journal, Vol.43, No.6, June 2005*, 2005.

[13] Y. Lian and M. S. Liou, "Aero-structural optimization of a transonic compressor rotor," *41st AIAA/ASME/SAE/ASEE Joint Propulsion Conference and Exhibit, AIAA 2005-3634*, 2005.

[14] S. Pierret, "Multi-objective and multi-disciplinary optimization of three-dimensional turbomachinery blades," *6th World Congress of Structural and Multidisciplinary optimization*, 2005.

[15] C. Vob, M. Aulich, B. Kaplan, and E. Nicke, "Automated multiobjective optimization in axial compressor blade design," *Proceedings of Turbo Expo 2006, GT2006-90420*, 2006.

[16] S. Pierret, R. F. Coelho, and H. Kato, "Multidisciplinary and multiple operating points shape optimization of three dimensional compressor blades," *Journal of Structure and Multidisciplary optimization*, 2007.

[17] T. T. Mengistu and W. Ghaly, "Gas turbine blade design using multi-objective optimization and dual geometry representation," *ISROMAC12-2008-20005, Feb.*, 2008.

[18] C. Luo, L. Song, J. Li, and J. Feng, "Multiobjective optimization approach to multidisciplinary design of a three dimensional transoni compressor blade," *Proceedings of Turbo Expo 2009, GT2009-59982*, 2009.

[19] M. Arabnia and W. Ghaly, "A strategy for multi-point shape optimization of turbine stages in three-dimensional flow," *Proceedings of Turbo Expo 2009, GT2009-59708*, 2009.

[20] R. T. Haftka and R. V. Grandhi, "Structural shape optimization - a survey," *Computer Methods in Applied mechanics and engineering 57, 91-106*, 1986.

[21] Y. Ding, "Shape optimization of structures - a literature survey," *Computers and Structures Vol.24, No.6, pp. 985-1004*, 1986.

[22] J. Frischbier, "Application of structural optimization in the design of jet engine turbine blades," *Transactions on the built Environment vol. 13, WIT Press, ISSN 1743-3509*, 1995.

[23] D. J. Doorly, J. Peiró, and J. P. Oesterle, "Optimization of aerosynamic and coupled aerodynamic-structural design using parallel genetic algorithms," *AIAA*, 1996.

[24] T. J. Martin and G. S. Dulikravich, "Aero-structural and optimization of internally cooled turbine airfoils," *ISABE 97-7165*, 1997.

[25] R. V. Tappetta, S. Nagendra, and J. E. Renaud, "A multidisciplinary design optimization approach for high temperature aircraft engine components," *Structural Optimization 18, 134-145, Springer - Verlag*, 1999.

[26] S. S. Talya, A. Chattopadhyay, and J. N. Rajadas, "Multidisciplinary analysis and design optimization procedure for cooled gas turbine blades," *AIAA - 2000 - 4877*, 2000.

[27] J. N. Rajadas and A. Chattopadhyay, "Application of design optimization to turbomachinery desgin," *AIAA - 2002 - 5662*, 2002.

[28] R. Dornberger, D. Buče, and P. Stoll, "Multidisciplinary optimization oin turbomachinery design," *ECCOMAS 2000, Barcelona, 11-14 Sept*, 2000.

[29] S. Pierret and C. Hirsch, "An integrated optimization system for turbomachinery blade shape design," *RTO AVT Symbosium on Reduction of Militaty vehicle acquisition time and cost through advanced modelling and virtual simulation, RTO-MP-089*, 2002.

[30] D. Buče, G. Guidati, and P. Stoll, "Automated design optimization of compressor blades for stationary, large-scale turbomachinery," *Proceedings of ICTI03, GT2003-38421*, 2003.

[31] C.-M. Jang, P. Li, and K.-Y. Kim, "Optimization of blade sweep in a transonic axial compressor rotor," *JSME, Series B, Vol.48, No.4*, 2005.

[32] C.-M. Jang and K.-Y. Kim, "Optimization of a stator blade using response surface method in a single stage transonic axial compressor," *J.Power and Energy, Proc.IMechE Vol.219 Part A*, 2005.

[33] C.-M. Jang, A. Samad, and K.-Y. Kim, "Optimal design of swept, leaned and skewed blades in a transonic axial compressor," *Proceedings of Turbo Expo 2006, GT2006-90384*, 2006.

[34] H.-D. Li, L. He, Y. S. Li, and R. Wells, "Blading aerodynamics design optimization with mechanical and aeromechanical constraints," *Proceedings of Turbo Expo 2006, GT2006-90503*, 2006.

[35] A. R. Rao, J. P. Scanlan, and A. J. Keane, "Applying multiobjective cost and weight optimization to the initial design of turbine disks," *Journal of Mechanical Design, Vol. 129, pp. 1302-1310*, 2007.

[36] S. Dominique and J. Y. Trépanier, "Automated preliminary structural rotor design using genetic algorithm and neural networks," *Proceedings of Turbo Expo 2008, GT2008-51181*, 2008.

[37] F. Pouzadaoux, G. Reydellet, E. Taillefer, and M. Masmoudi, "Introduction of multi-disciplinary optimization in compressor blade desig.," *12th AIAA/ISSMO Multidisciplinary Analysis and Optimization Conference, AIAA 2008-6018*, 2008.

[38] G. B. Ashakiran, A. Gogoi, and Q. H. Nagpurwala, "Multi-disciplinary design optimization of an axial turbine stage of aircraft auxilary power unit," *12th AIAA/ISSMO Multidisciplinary Analysis and Optimization Conference, AIAA 2008-6055*, 2008.

[39] Y. Panchenko, H. Moustapha, S. Mah, K. Patel, M. J. Dowhan, and D. Hall, "Preliminary multi-disciplinary optimization in turbomachinery design," *RTO AVT Symbosium on Reduction of Militaty vehicle acquisition time and cost through advanced modelling and virtual simulation, RTO-MP-089*, 2002.

[40] K. Deb, "Optimization for engineering design algorithms and examples," 2006.

[41] Y. Y. Lai and X. Yuan, "Blade design with three dimensional viscous analysis and hybrid optimization approach," *AIAA paper 2002-5658*, 2002.

[42] X. Xing and M. Damodaran, "Design of three dimensional nozzle shape using nurbs, cfd, and hybrid optimization strategies.," *AIAA paper 2004-4368*, 2004.

[43] T. T. Mengistu, *Aerodynamic Design and optimization of Turbomachinery Blading.* Concordia University Phd Thesis, 2005.

[44] A. Samad and K. Y. Kim, "Mulitple surrogate modeling for axial compressor shape optimization," *Journal of Propulsion and Power, Vol. 24, No. 2*, 2008.

[45] T. Verstraete, *Multidisciplinary Turbomachinery Component Optimization considering Performance, Stress, and Internal Heat Transfer*. Von Karman Institute for Fluid Dynamics, Turbomachinery and Propulsion Department, 2008.

[46] Haupt and Haupt, *Practical Genetic Algorithms*. Wiley International, 2004.

[47] J. Harinck, Z. Alsalihi, J. P. V. Buijtene, and R. A. V. den Braembussche, "Optimizaiton of a 3d radial turbine by means of an improved genetic algorithm," *Proceedings of the 6th European Conference on Turbomachinery, pp. 1033-1042*, 2005.

[48] Y. Y. Lai and X. Yuan, "Blade design with three-dimensional viscous analysis and hybrid optimization approach," *AIAA Paper 2002-5658*, 2002.

[49] N. U. Papila, *Neural Network and Polynomial - Based Response Surface Techniques for Supersonic Turbine Design Optimization*. PhD Thesis, The University of Florida, 2001.

[50] N. U. Papila, W. Shyy, N. Fitz-Coy, and R. T. Haftka, "Assesment of neural net and polynomial based techniques for aerodynamic applications," *AIAA Paper 1999-3167*, 1999.

[51] M. M. Rai and N. K. Madavan, "Improving the unsteady aerodynamic performance of transonic turbines using neural networks," *38th AIAA Aerospace Sciences Meeting and Exhibit, Reno, Nevada, AIAA 2000-0169*, 2000.

[52] S. Haykin, *Neural Networks: A Comprehensive Foundation*. 2nd Edition, Prentice-Hall, 1999.

[53] M. H. Hassoun, "Fundamentals of artificial neural networks," *MIT Press*, 1995.

[54] T. Masters, *Practical Neural Network Recipies in C++*.

[55] R. J. Schalkoff, *Artificial Neural Networks*. McGraw-Hill, 1997.

[56] S. P. Abhijit and B. M. Robert, *Pattern recoginition with Neural Networks in C++*. CRC Press, 1996.

[57] K. Swingler, *Applying Neural Networks:A Practical Guide*. Academic Press, 1996.

[58] R. Jin, W. Chen, and T. W. Simpson, "Comparative studies of metamodeling techniques under multiple modeling criteria," *8th AIAA/USAF/NASA/ISSMO Symbosium on Multidisciplinart Analysis and Optimization, AIAA 2000-4801*, 2000.

[59] L. Piegl and W. Tiller, *The NURBS Book*. Springer, 1995.

[60] K. Deb, *Multi-Objective Optimization using Evolutionary Algorithms*. John Wiley and Sons, 2001.

[61] M. Norgaard, C. C. Jorgenson, and J. C. Ross, "Neural network prediction of new aircraft design coefficients," *NASA TM-112197*, 1997.

[62] www.ansys.com, "Gambit user guide 2.3.16,"

[63] www.ansys.com, "Ansys icemcfd userguide,"

[64] M. P. Boyce, *Gas turbine engineering handbook*. 2nd Edn.,Boston,MA,Gulf Professional Pub., 2002.

[65] P. Hill and C. Peterson, *Mechanics and Thermodynamics of Propulsion*. 2nd Edition, Addison-Wesley Publishing Company, 1992.

[66] H. Moustapha, M. F. Zelesky, N. C. Baines, and D. Japikse, *Axial and Radial Turbines*. Concepts NREC, 2003.

[67] B. Lakshminarayana, *Fluid Dynamics and Heat Transfer of Turbomachinery*. John Wiley, 1996.

[68] T. Mansour, *Implicit geometric representation of gas turbine blades for optimal shape design.* M.A.Sc Thesis, Concordia University, 2005.

[69] S. Fazl, *High Fidelity Flow Simulation for Turbine Blade Shape Optimization.* CIADI Project Report, Concordia University, 2007.

# Appendix A

# ANN Error Measures

In this appendix different error measures used in this work to understand the generalization capability of the ANN explained in detail with their mathematical descriptions [69]. The details of these error terms are given explained below.

Notations used:

$y_i$ is the actual output

$\hat{y}_i$ is the neural net output

$\bar{y}_i$ is the mean of outputs

## A.1. Root mean squared Error (RMSE)

The root mean squared error is given by equation.

$$RMSE = \sqrt{\frac{\sum_{i=1}^{n_{error}} (y_i - \hat{y}_i)^2}{n_{error}}} \tag{A.1}$$

MSE which is the square of RMSE is also used for the BPNN to change the weights, as the weight change depends on the negative gradient of this error. Therefore it is used extensively in literature.

## A.2. Maximum Error

The maximum error is given by equation

$$MAX = max\{|y_i - \hat{y}_i|\}_{i=1,\ldots,n_{error}} \tag{A.2}$$

Maximum error will indicate only the maximum. This can be useful if there is a criterion for which a limit is set and anything above is considered unacceptable.

## A.3. R squared

The R squared error is defined by equation

$$R^2 = 1 - \frac{\sum_{i=1}^{n}(y_i - \hat{y}_i)^2}{\sum_{i=1}^{n}(y_i - \bar{y}_i)^2} = 1 - \frac{MSE}{Variance} \tag{A.3}$$

$R^2$ is more of a statistical measure for error. It is also known as the coefficient of determination and it gives information about the goodness of fit for the model. The value of MSE represents the departure of the metamodel from the real model, and the variance captures the irregularities of the problem. So the higher the value of $R^2$, the better is the approximation of the model. Range for R squared value is [-$\infty$, 1].

## A.4. Relative Average Absolute Error (RAAE)

The RAAE is defined by equation

$$RAAE = \frac{\sum_{i=1}^{n} |y_i - \hat{y}_i|}{n * STD} \tag{A.4}$$

RAAE takes the average of the errors and divides it by the standard deviation. Smaller the value for RAAE the better is the approximation.

## A.5. Relative Maximum Absolute Error (RMAE)

The RMAE is defined by equation

$$RMAE = \frac{max(|y_i - \hat{y}_1|, |y_i - \hat{y}_2|, ...|y_n - \hat{y}_n|)}{STD} \tag{A.5}$$

RMAE takes the maximum error and divides it by the standard deviation (spread of the output values about the mean measured in same units as the data). Large value of the RMAE indicates more error in one region of the error surface then others though the overall R square and RAAE values are really good. So a low value of RMAE will indicate good approximation for the ANN. But this metric is not as important as R square and RAAE due to its nature of not representing the whole error surface [58].

## A.6. Average Relative Error (ARE)

The average relative error is defined by equation

$$ARE = \frac{\frac{\sum_{i=1}^{i=n} |y_i - \hat{y}_i|}{y_i}}{n} \times 100 \tag{A.6}$$